博士論文

Discovery and Biosynthetic Investigation of Fungal Secondary Metabolites
(糸状菌由来二次代謝産物の探索と生合成研究)

全智揚
Quan, Zhiyang

Discovery and Biosynthetic Investigation of Fungal Secondary Metabolites

(糸状菌由来二次代謝産物の探索と生合成研究)

全　智揚

Quan, Zhiyang

Acknowledgement

对于本论文的完成，我首先要真挚的感谢我的博士课程指导教官，东京大学大学院药学系研究科天然物化学研究室 教授 阿部郁朗先生：没有您的热心指导和鞭策，就没有今天即将取得博士学位的我。在我最迷茫的时候，是您指引了我，让我找到方向；在我最困难的时候，是您激励了我，帮助我度过难关。是您对我的深厚信任和不断支持培养了我，造就了今天的我。我感谢您的指导，您的鞭策，您的激励，您的信任，您的支持，我由衷的感谢您！

其次，我还要感谢在学术上给与我巨大帮助的东京大学大学院药学系研究科天然物化学研究室 讲师 淡川孝义博士和在技术上给与我详尽指导的元东京大学大学院药学系研究科天然物化学研究室 助教 松田侑大博士。没有你们的无私帮助，完成我的博士研究是不可能的。希望今后也可以和你们继续合作。

当然，我更要感谢东京大学大学院天然物化学研究室的其他成员：元准教授 胁本敏幸博士，前准教授 冈田正宏博士，助教 森贵裕博士和元特任研究员 江上蓉子博士对我支持和鼓励。

研究室的历任秘书 马场友华子女士，尾崎日映女士，野口千花女士，堀野ともか女士，以及大塚奈央子女士，是你们的重要工作支持了实验室的日常运营。我感谢你们的辛苦工作。

在本文涉及的研究课题中，我的共同研究者，访问学者中山大学副教授 王冬梅博士做出了巨大的贡献，万分感谢您对我的指导。访问学者昆明植物研究所的副教授 汪光伟博士对我的研究提供了积极的建议。我的共同研究者，博士后研究员李畅博士也对本论文的完成贡献了力量。

研究室的其他访问学者暨南大学副教授 胡丹博士，沈阳药科大学副教授 秦斌博士，华南农业大学副教授 贺飞博士，富山大学助教 Chin Piow Wong 也分别和我进行了有益的学术探讨。

研究室的同学胁本行彦修士和岩渊大辉修士，是你们的友情点燃了我对研究的热情，中岛优博士，三桥隆章修士和星野翔太郎修士，和你们的讨论经常可以碰撞出智慧的火花，还有我的师弟和师妹齐藤有里修士，藤本贵之修士，藤冈拓真修士，衫田智惇修士，齐藤开同学和白桐暄同学，你们的青春活力让我对未来充满信心。

最后也要感谢研究室的师兄师弟们，你们的默默支持是我不断前进的力量。

在最后的最后，感谢东北大学的五味胜也教授和东京大学北本名誉教授为我们提供了菌种和载体。

January 2018

Chuan, Zhiyang

Abbreviation

AT	acetyltransferase
BGC	biosynthetic gene cluster
BLAST	Basic Local Alignment Search Tool
CD broth	Czapek-Dox broth
COSY	correlation spectroscopy
DMOA	3,5-dimethylorsellinic acid
DNA	deoxyribonucleic acid
FMO	flavin-dependent monooxygenase
FPP	farnesyl pyrophosphate
GO	galactose oxidase
HLG	halogenase
HMBC	hetero-nuclear multiple-bond connectivity
HMQC	hetero-nuclear multiple quantum coherence
HPLC	high-performance liquid chromatography
KBr	potassium bromide
KCl	potassium chloride
KF	potassium fluoride
KI	Potassium Iodide
KR	ketoreductase
LC-MS	liquid chromatography-mass spectrometry
NMR	nuclear magnetic resonance
NOESY	nuclear overhauser effect correlated spectroscopy
NPs	natural products
P450	cytochrome P450 monooxygenase
PCR	polymerase chain reaction
PEG	polyethylene glycol
pks	polyketide synthase
po	peroxidase
PT	prenyltransferase
SDR	short chain dehydrgenase
TM helix	transmembrane helix
UV	ultraviolet

Contents

1. Introduction 1

1.1. Natural Products and Drug Development 1

1.2. Fungal Meroterpenoids, a Class of Natural Products Rich in Structural Diversity 2

2. Methods 6

2.1. Introduction to Genome Mining 6

2.2. Heterologous Expression System in Aspergillus oryzae 6

3. Biosynthesis Research of Fungal Meroterpenoid Ascochlorin 8

3.1. Background 8

3.2. Previous Research 8

3.3. Purposes 8

3.4. Discovery of Biosynthetic Gene Cluster of Ascochlorin 9

3.5. Characterization of Genes Responsible for the Late-Stage of Ascochlorin Biosynthesis 10

3.6. Mutation Researches of AscF, a Unique Terpene Cyclase for Meroterpenoid 16

3.7. Discussion 18

3.8. Conclusion 20

4. Discovery of a Cytochrome P450 for Biosynthesis of Citreohybridonol 22

4.1. Background 22

4.2. Discovery of a New Potential BGC for Novel Meroterpenoids with Andrastin Scaffold 23

4.3. Purposes 25

4.4. Discovery of the Cytochrome P450 Responsible for the Citreohybridonol Biosynthesis 25

4.5. Details of Biosynthesis of Citreohybridonol 28

4.6. Isolation and Identification of Products Derived by the ctr Cluster in the Shunt Pathway 29

4.7. Discussion 31

4.8. 4.8 Conclusion 33

5. Summary and Prospect 36

6. Experiments 37

6.1. General 37

6.2. Experiments of Biosynthesis Research of Fungal Meroterpenoid Ascochlorin 40

6.3. Experiments of Discovery of a Cytochrome P450 for Biosynthesis of Citreohybridonol 44

7. Appendix 47

7.1. Appendix of Biosynthesis Research of Fungal Meroterpenoid Ascochlorin 47

7.2. Appendix of Discovery of a Cytochrome P450 for Biosynthesis of Citreohybridonol ... 65

1. Introduction

1.1. Natural Products and Drug Development

Nature provided a great molecule library exhibiting structural diversity and various bioactivities, composed the most important sources for drug development. In 1562 new approved drugs from 1981 to 2014, about 31% of them were discovered by random screening and manufactured by total synthesis. However, natural products and their derivatives occupied about 40% of the total number, and about 14% of all these drugs were synthetic mimic of natural products and drug with pharmacophore of natural products[1]. Furthermore, natural products and their derivatives contributed especially in anti-infective agents. Over 73% of anti-bacteria agents were derived from natural products, while only 22% of these new drugs were originated from total synthesis[1].

A very famous paradigm of natural products used as clinical drugs is artemisinin, a sesquiterpenoid known as the most important anti-malarial agent[2] [Figure 1-1]. This compound was isolated from higher plant *Artemisia annua* by Prof. Youyou Tu's group at 1972[2], and was widely applied in the combination therapy for severe malaria[3]. Her discovery saved many thousands of lives who suffered from malaria, a tropical disease caused by the parasites of *Plasmodium* species. This high value discovery also made Prof. Tu win half of the 2015 Nobel Prize in Physiology or Medicine[4] for her great contributions on the treatment of the tropical parasite disease.

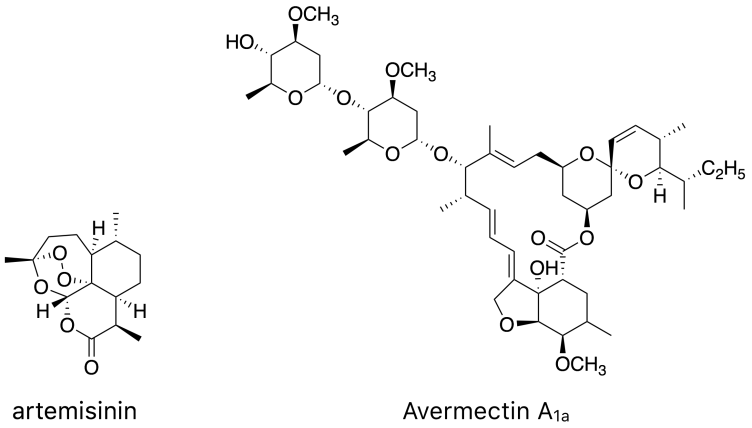

Figure 1-1. Artemisinin, an agent against Plasmodium falciparum malaria, and one of the avermectins, avermectin A1a, agent against parasitic worms.

Not only higher plants, but also microbes can produce secondary metabolites as seeds for drug development. Avermectins [Figure 1-1][5], isolated from *Streptomyces* species by Prof. Satoshi Ōmura in 1978[6], are a group of naturally occuring compounds considered as leads compounds with potent anti-parasitic activity. He shared one quarter of the 2015 Nobel Prize in Physiology or Medicine with Prof. Tu, for his contribution on anti-parasitic therapy development.

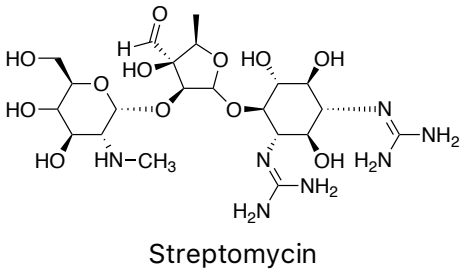

Figure 1-2. Streptomycin, an important antibiotic against tuberculosis.

Besides avermectins, the most widely used drug derived from the microbe is streptomycin [Figure 1-2]. Streptomycin, which was isolated from *Streptomyces griseus* by Prof. S. A. Waksman's group at 1944[7], was the first tuberculosis chemotherapeutic agent in history. Before the discovering of streptomycin, tuberculosis, which is an infection caused by *Mycobacterium tuberculosis*, was unable to be cured. However, due to the revolutionary discovery of streptomycin, many patients were saved by the antibiotic against *M. tuberculosis*. Thus, Prof. Waksman was also awarded the 1952 Nobel Prize in Physiology or Medicine for his discovery and investigation

on streptomycin.

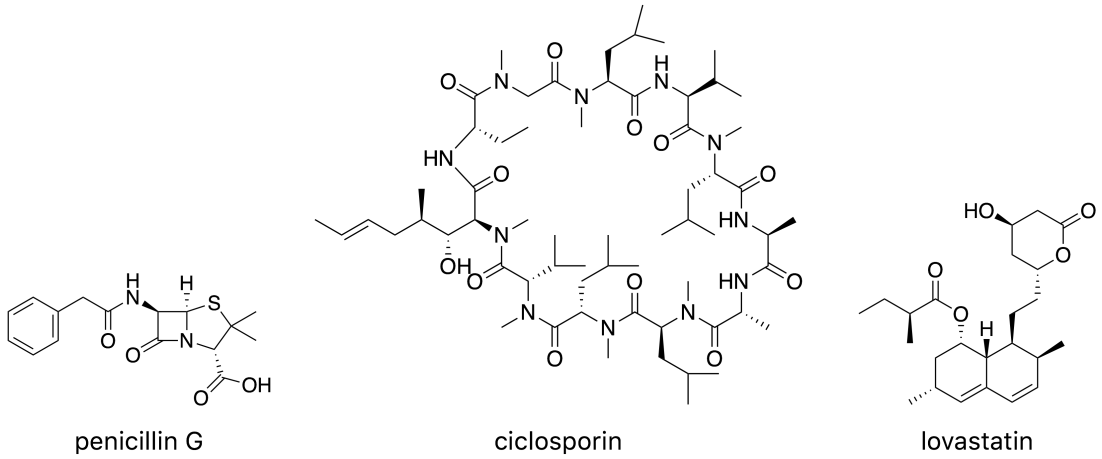

Figure 1-3. Bioactive metabolites produced by fungus.

As well as actinomycetes, fungi are also microbial producers of various natural products with bioactivities. Penicillin G [Figure 1-3], the first antibiotic against bacterial infection in history, produced by a very common fungus *Penicillium chrysogenum*[8], ciclosporin [Figure 1-3], an clinical widely used immunosuppressive agent[9], produced by an soil ascomycete fungus *Tolypocladium inflatum Gams*[10], and lovastatin [Figure 1-3], an antihyperlipidemic agent, produced by a saprotrophic fungus *Aspergillus terreus*[11], are good examples of valuable molecules isolated from fungi.

1.2. Fungal Meroterpenoids, a Class of Natural Products Rich in Structural Diversity

Fungi can also produce meroterpenoids, a class of naturally occurring compounds with unique structures partially derived from terpenes. Meroterpenoids are often classified into two groups, polyketide-terpenoids and non-polyketide-terpenoids[12], by the origins of their non-terpene parts.

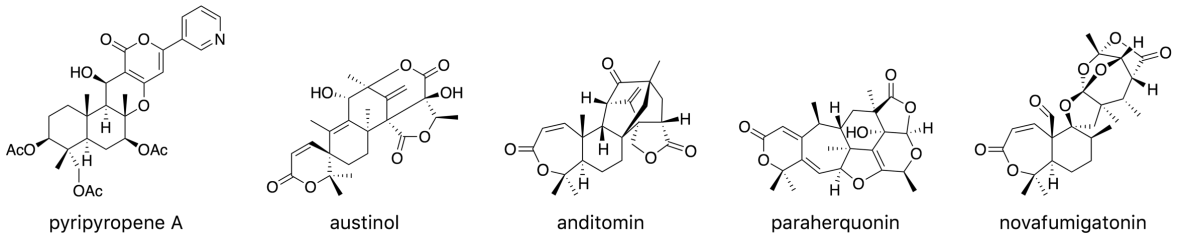

Figure 1-4. Structures of some polyketide-terpenoid type meroterpenoids.

Some examples of polyketide-terpenoids were given in Figure 1-4. It is noticed that all the structures of these meroterpenoids are very complex. These molecules were highly oxidized, and their carbon skeletons are very incredible. It is suggested that many oxidases involved in the meroterpenoids biosynthesis, and that some uncommon transitions also occurred in the biosynthetic reactions of meroterpenoids. Thus, it is very difficult to investigate the biosynthesis of meroterpenoids with complex structures.

However, to face these challenges, the detailed biosynthesis of the meroterpenoids in Figure 1-4 were successfully elucidated by my laboratory. Much knowledge about meroterpenoids biosynthesis was acquired through the experience of our investigation on this class of natural products. Next, I will take anditomin, which was isolated from *Emericella variecolor*[13], as an example to explain the biosynthesis of meroterpenoids.

Biosynthesis of Meroterpenoids

Anditomin is classified as polyketide-terpenoid, in other words, the biosynthetic origin of this meroterpenoid is polyketide. A farnesyl moiety originated from farnesyl pyrophosphate (FPP) composes the terpene part of anditomin. The polyketide part of anditomin, 3,5-dimethylorsellinic acid (DMOA), was produced by the catalysis of AndM, a polyketide synthase (PKS) [Figure 1-5][14]. After oxidation catalyzed by AndK, a cytochrome P450 (P450),

the polyketide part linked with FPP catalyzed by AndD, a prenyltransferase (PT) [Figure 1-5][14].

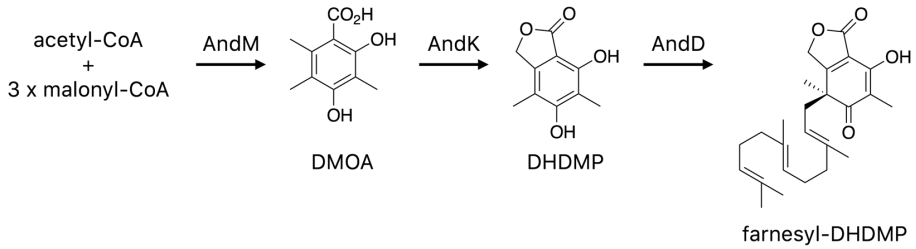

Figure 1-5. Early-stage biosynthesis of anditomin.

The cyclization reaction in anditomin biosynthesis was catalyzed by two enzymes, AndE, a flavin-dependent monooxygenase (FMO), and AndB, a meroterpenoid terpene cyclase (CYC)[14]. Farnesylated compound, farnesyl-5,7-dihydroxy-4,6-dimethylphthalide (DHDMP) was firstly epoxidized by AndE, then the product was cyclized by AndB to yield preandiloid A, a five-ring compound [Figure 1-6]. The oxidases involved in the epoxidation of farnesyl group are FMO in most cases.

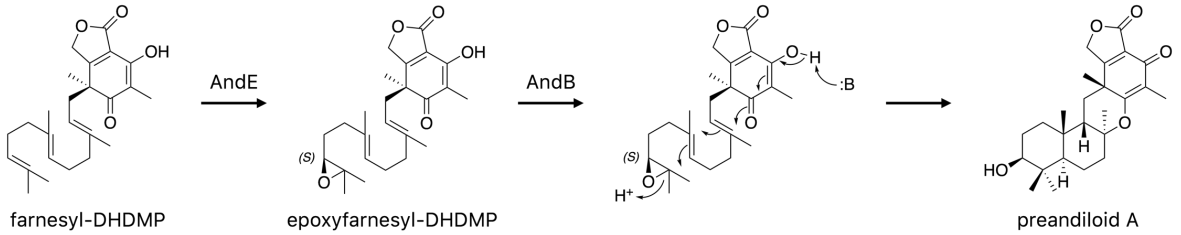

Figure 1-6. Cyclization in anditomin biosynthesis.

After the cyclization, preandiloid A was converted to the final product anditomin by the catalysis of tailoring enzymes group, AndC, A, J, I, G, H, and F [Figure 1-7][14]. This is the most complex procedure in the meroterpenoids biosynthesis. Tailoring enzymes, such as cytochrome P450, isomerases, dioxygenases, and acetyltransferase (AT), involved in this stage. Many interesting reactions also occurred in this stage, for example, AndA, a PhyH-like dioxygenase, catalyzed conversion from preandiloid B to andiconin [Figure 1-8][14].

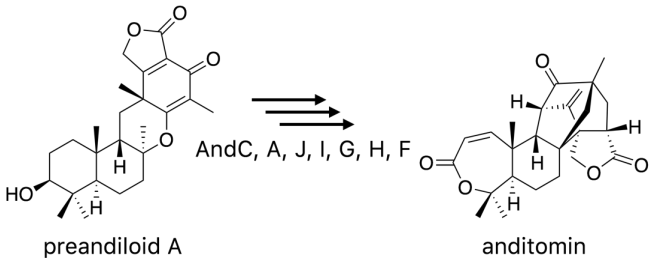

Figure 1-7. Late-stage biosynthesis of anditomin.

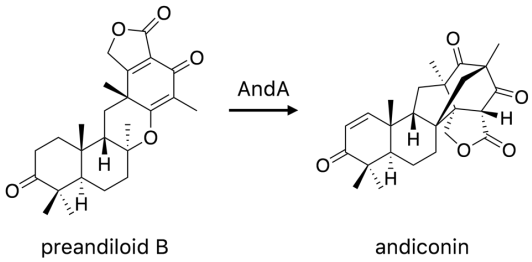

Figure 1-8. Conversion from preandiloid B to andiconin catalyzed by AndA.

Generally, the meroterpenoids biosynthesis can be clearly divided into three stages. I call the three stages the pre-cyclization stage, which equals the early-stage, cyclization stage, and post-cyclization stage, which equals the late-stage.

Two Main Contributors to the Diversity of Meroterpenoids

According to our biosynthetic investigations on fungal meroterpenoids, the diversity and complexity of structure are mainly contributed by (1) the diverse cyclization patterns in cyclization stages, and (2) the various tailoring reactions in post-cyclization stages. Meroterpenoids originated from DMOA and FPP provided the nice evidence to explain how they affect the diversity of meroterpenoids.

For example, austinol, andrastin A, and terretonin are meroterpenoids derived from DMOA and FPP[15]. As revealed in previous researches, epoxyfarnesyl-DMOA methyl ester is the common intermediate of all these three compounds [Figure 1-9]. The terpene cyclases catalyzing different cyclizations lead the biosynthesis to the completely different pathways [Figure 1-9][15]. Transmembrane terpene cyclases, AusL[16], the cyclase for biosynthesis of austinol, AdrI[17], the cyclase for biosynthesis of andrastin A, and Trt1[18], the cyclase for biosynthesis of terretonin, exhibit about 40 to 50% identity with each other, and these enzyme share the same substrate, but the different pattern of cyclization resulted in different product.

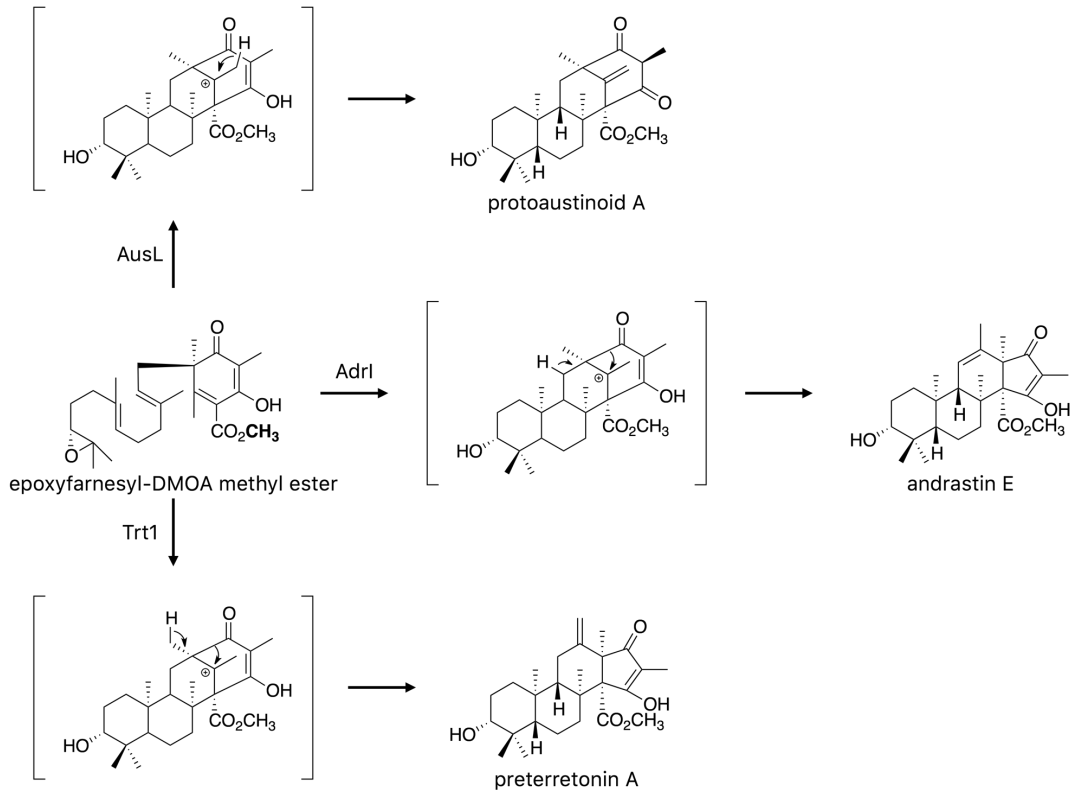

Figure 1-9. Different terpene cyclases catalyzed cyclizations in different patterns.

In further biosynthesis pathway of protoaustinoid A, different tailoring enzymes groups catalyzed various tailoring reactions, and lead to the final products, paraherquonin and austinol, whose carbon skeletons are completely different from each other [Figure 1-10]. Paraherquonin, whose biosynthetic gene cluster (BGC) is the *prh* cluster, and austinol, whose BGC is the *aus* cluster, have the same biosynthesis pathway in pre-cyclization stage, cyclization stage, and early part of post-cyclization stage. However, the different tailoring enzymes groups involved in the late part of post-cyclization stage made the carbon skeleton of final products so different with each other [Figure 1-10].

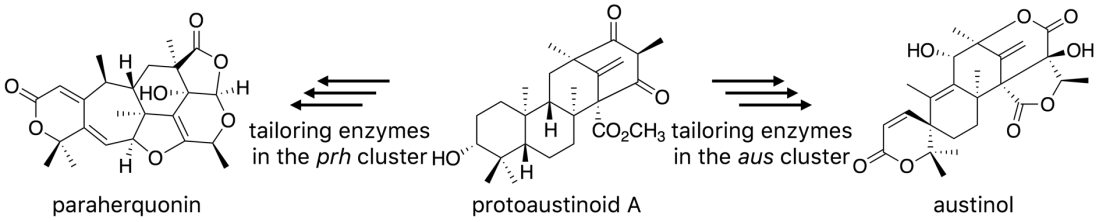

Figure 1-10. Paraherquonin and austinol have the same precursor, protoaustinoid A.

In next pages of this doctoral thesis, I will report the biosynthetic research of ascochlorin, who have a unique cyclization pattern in its biosynthesis, and the discovery of a cytochrome P450, which is also a unique tailoring enzyme for biosynthesis of citreohybridonol.

[References]

1. Newman, D. J.; Cragg, G. M., Natural products as sources of new drugs from 1981 to 2014. *Journal of Natural Products* **2016,** *79* (3), 629-661.

2. Tu, Y., Artemisinin—a gift from traditional chinese medicine to the world (Nobel Lecture). *Angewandte Chemie International Edition* **2016**.

3. Organization, W. H., *Guidelines for the treatment of malaria*. World Health Organization: 2015.

4. Davey, S., 2015 Nobel Prize in Physiology or Medicine: Punishing parasites. *Nature Chemistry* **2015,** *7* (12), 949-949.

5. Ōmura, S.; Shiomi, K., Discovery, chemistry, and chemical biology of microbial products. *Pure and Applied Chemistry* **2007,** *79* (4), 581-591.

6. Ōmura, S., A splendid gift from the earth: the origins and impact of the avermectins (Nobel Lecture). *Angewandte Chemie International Edition* **2016,** *55* (35), 10190-10209.

7. Waksman, S. A., Tenth anniversary of the discovery of streptomycin, the first chemotherapeutic agent found to be effective against tuberculosis in humans. *American Review of Tuberculosis* **1954,** *70* (1), 1.

8. Liras, P.; Martín, J., β-Lactam antibiotics. **2009**.

9. Stierle, A.; Strobe, G.; Stierle, D., Taxol and taxane production by *Taxomyces andreanae*, an endophytic fungus of pacific yew. *Science* **1993,** *260*, 214-216.

10. Alberts, A. W.; Chen, J.; Kuron, G.; Hunt, V.; Huff, J.; Hoffman, C.; Rothrock, J.; Lopez, M.; Joshua, H.; Harris, E., Mevinolin: a highly potent competitive inhibitor of hydroxymethylglutaryl-coenzyme A reductase and a cholesterol-lowering agent. *Proceedings of the National Academy of Sciences* **1980,** *77* (7), 3957-3961.

11. Geris, R.; Simpson, T. J., Meroterpenoids produced by fungi. *Natural Product Reports* **2009,** *26* (8), 1063-1094.

12. Simpson, T. J.; Walkinshaw, M. D., Anditomin, a new C 25 metabolite from *Aspergillus variecolor*. *Journal of the Chemical Society, Chemical Communications* **1981,** (17), 914-915.

13. Matsuda, Y.; Wakimoto, T.; Mori, T.; Awakawa, T.; Abe, I., Complete biosynthetic pathway of anditomin: nature's sophisticated synthetic route to a complex fungal meroterpenoid. *Journal of the American Chemical Society* **2014,** *136* (43), 15326-15336.

14. Matsuda, Y.; Abe, I., Biosynthesis of fungal meroterpenoids. *Natural Product Reports* **2016,** *33* (1), 26-53.

15. Matsuda, Y.; Awakawa, T.; Wakimoto, T.; Abe, I., Spiro-ring formation is catalyzed by a multifunctional dioxygenase in austinol biosynthesis. *Journal of the American Chemical Society* **2013,** *135* (30), 10962-10965.

16. Matsuda, Y.; Awakawa, T.; Abe, I., Reconstituted biosynthesis of fungal meroterpenoid andrastin A. *Tetrahedron* **2013,** *69* (38), 8199-8204.

17. Matsuda, Y.; Awakawa, T.; Itoh, T.; Wakimoto, T.; Kushiro, T.; Fujii, I.; Ebizuka, Y.; Abe, I., Terretonin biosynthesis requires methylation as essential step for cyclization. *ChemBioChem* **2012,** *13* (12), 1738-1741.

2. Methods

Before I elaborate my researches on fungal meroterpenoids in next several pages, I would like to slightly introduce the methods I used in all my investigations. I mainly utilized a genome mining approach to discover target BGC, coupled with a heterologous expression in *Aspergillus oryzae*, to investigate biosynthesis of known compounds as well as to search for and isolate novel compounds.

2.1. Introduction to Genome Mining

As has been described previously, fungi are prominent bio-resources that produce diverse natural products with a various bioactivities and structural complexity. They have been intensively investigated to obtain clinically valuable lead compounds.

As traditional method of natural products isolation from microbes, people usually cultivate collected microbes on different kinds of medium, then use spectroscopic analytical method to detect novel compounds. However, it became difficult to find novel natural products by using hitherto known methods to date. Thus, a new method which can discover novel molecules efficiently should be established to overcome this problem.

Genome mining is one of the most efficient methods for discovering and investigating natural products[19]. In fungal genomic DNA, the genes encoding enzymes that catalyze continuous reactions for the biosynthesis of a natural product are usually clustered. Such a group of biosynthetic genes is called biosynthetic gene cluster (BGC). Genome mining focuses on the sequenced genomic DNA of organisms to find out the potential BGC for novel compounds.

As sequencing technology improved, draft genome sequencing of fungi become easier to carry out. On the other hand, lower cost of genome sequencing makes small laboratories and institutions also be able to conduct such sequencings. Therefore, more and more genomic DNA data are available in open access database. On the basis of BGC predictions, it is efficient to explore novel natural products with potential bioactivities. These compounds could be obtained by heterologous expression and identified by spectroscopic analysis.

2.2. Heterologous Expression System in *Aspergillus oryzae*

A heterologous expression system in *Aspergillus oryzae* is utilized in my researches. *Aspergillus oryzae* NSAR1 strain[20], constructed based on a well investigated fungus *A. oryzae*, was used as the host for heterologous expression. As *A. oryzae* NSAR1 strain is a auxotrophic fungus, four fungal transformation vectors, pTAex3[21], pUSA[22], pUNA[23], and pAdeA[24], was developed for the fungal transformation. Another two antibiotics resistant vector, pPTRI[25], the pyrithiamine resistance, and pBARI[14], the glufosinate resistance, are also available. Hence, six fungal transformation vectors can be used in the transformation of *A. oryzae*. Using these six vectors, at most twelve genes was successfully introduced and expressed in *A. oryzae*[14].

The fermentation of *A. oryzae* transformants harboring biosynthetic genes ensures enough amount of product for compound isolation and characterization. The benefits of heterologous expression in *A. oryzae* are (1) a well-established transformation method, (2) its compatibility with other fungal genes to be expressed, (3) very low background production of own secondary metabolites, and (4) high production yields. The different combinations of genes for combinatorial biosynthesis were heterologous expressed in *A. oryzae*, and their metabolites were analyzed by HPLC and LC-MS. Specific compounds from these transformants will be isolated and identified.

[References]

1. Zerikly, M.; Challis, G. L., Strategies for the discovery of new natural products by genome mining. *ChemBioChem* **2009,** *10* (4), 625-633.

2. Jin, F. J.; Maruyama, J.-i.; Juvvadi, P. R.; Arioka, M.; Kitamoto, K., Development of a novel quadruple auxotrophic host transformation system by *argB* gene disruption using *adeA* gene and exploiting adenine auxotrophy in *Aspergillus oryzae*. *FEMS Microbiology Letters* **2004,** *239* (1), 79-85.

3. Fujii, T.; Yamaoka, H.; Gomi, K.; Kitamoto, K.; Kumaga, C., Cloning and nucleotide sequence of the ribonuclease T1 gene (*rntA*) from *Aspergillus oryzae* and its expression in *Saccharomyces cerevisiae* and *Aspergillus oryzae*. *Bioscience,*

Biotechnology, and Biochemistry **1995,** *59* (10), 1869-1874.

4. Yamada, O.; Nan, S. N.; Akao, T.; Tominaga, M.; Watanabe, H.; Satoh, T.; Enei, H.; Akita, O., *dffA* Gene from *Aspergillus oryzae* encodesl-ornithineN 5-oxygenase and is indispensable for deferriferrichrysin biosynthesis. *Journal of Bioscience and Bioengineering* **2003,** *95* (1), 82-88.

5. Yamada, O.; Lee, B. R.; Gomi, K.; Iimura, Y., Cloning and functional analysis of the *Aspergillus oryzae* conidiation regulator gene *brlA* by its disruption and misscheduled expression. *Journal of Bioscience and Bioengineering* **1999,** *87* (4), 424-429.

6. Jin, F. J.; Maruyama, J.-i.; Juvvadi, P. R.; Arioka, M.; Kitamoto, K., Adenine auxotrophic mutants of *Aspergillus oryzae*: development of a novel transformation system with triple auxotrophic hosts. *Bioscience, Biotechnology, and Biochemistry* **2004,** *68* (3), 656-662.

7. Kubodera, T.; Yamashita, N.; Nishimura, A., Pyrithiamine resistance gene (*ptrA*) of *Aspergillus oryzae*: cloning, characterization and application as a dominant selectable marker for transformation. *Bioscience, Biotechnology, and Biochemistry* **2000,** *64* (7), 1416-1421.

8. Matsuda, Y.; Wakimoto, T.; Mori, T.; Awakawa, T.; Abe, I., Complete biosynthetic pathway of anditomin: nature's sophisticated synthetic route to a complex fungal meroterpenoid. *Journal of the American Chemical Society* **2014,** *136* (43), 15326-15336.

3. Biosynthesis Research of Fungal Meroterpenoid Ascochlorin

3.1. Background

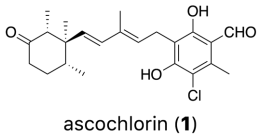

Figure 3-1. Structure of ascochlorin (**1**)

Ascochlorin (**1**) [Figure 3-1] is a fungal meroterpenoid isolated from fungus *Ascochyta viciae* by Dr. Tamura in 1968[26]. It is reported as an antiviral antibiotic and an antitumor agent[26] at first. Later researches reported that **1** and its derivatives exhibit anti-inflammatory activity[27], insulin resistance reducing activity[28], etc., and were considered as promising lead compounds. These compounds can be isolated from *Fusarium* sp.[29], *Microcera* sp.[30], *Nectria galligena*[31], and *Nectria coccinea*[32] beside *A. viciae*.

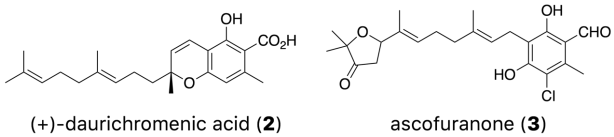

Figure 2. Structure of (+)-daurichromenic acid (**2**) and ascofuranone (**3**)

Compound **1** was identified as a polyketide-terpenoid, has a unique carbon skeleton composed with a cyclohexane ring at sesquiterpene part and a halogenized benzene ring at polyketide part. The terpene cyclases such as Pyr4[33], Trt1[18], AusL[16], and AndB[14], which are responsible for the cyclizations of meroterpenoids, always convert farnesyl moiety to a three rings system. This indicated that terpene cyclase responsible for the cyclization of **1** could be an enzyme with unique reaction mechanism. On the other hand, some bioactive compounds such as a potent anti-HIV agent (+)-daurichromenic acid[34] [Figure 3-2] and an anti-*Trypanosoma brucei brucei* agent ascofuranone[35] [Figure 3-2] exhibit similar structure to **1**. If we introduce or exchange the halogen atom at the benzene ring, an enhancement of the bioactivities provided by these compounds can be expected.

The research of terpene cyclase for biosynthesis of **1** can provide us the insight of unique cyclization reaction catalyzed by this enzyme, and investigation of tailoring enzymes of **1** can help us with the molecule engineering of similar compound with **1**. These are the reasons why I carried out the biosynthetic research of **1**.

3.2. Previous Research

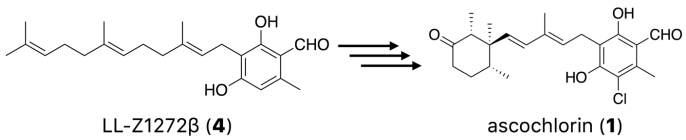

Figure 3-3. LL-Z1272β, a precursor of ascochlorin (**1**).

Previous research indicated that LL-Z1272β (**4**) is the precursor of **1**[36] [Figure 3-3]. Our previous work elucidated the biosynthetic pathway of **4**[37][Figure 3-4]. In the previous research, the biosynthetic gene cluster (BGC) for **4** was identified and named as the *stb* cluster. The three enzymes encoded in the *stb* cluster were functionally investigated [Figure 3-4].

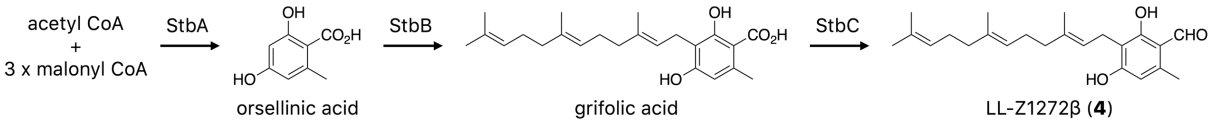

Figure 3-4. Biosynthesis pathway of LL-Z1272β (**4**), the precursor of ascochlorin (**1**).

3.3. Purposes

Although many previous researches isolated a lot of compounds predicted as precursors of ascochlorin (**1**)[36],

the BGC and detailed biosynthesis of **1** were still unknown. The purposes of this research are to identify the BGC responsible for ascochlorin, and to functionally analyze each enzyme in the biosynthetic pathway of **1**. The enzymes responsible for the cyclization and halogenation will also be discussed.

3.4. Discovery of Biosynthetic Gene Cluster of Ascochlorin

Identification of Metabolites from *Fusarium* sp. NBRC100844

Unidentified *Fusarium* sp. NBRC100844, the reported ascochlorin producer[29], was incubated in minimal medium Czapek-Dox broth (CD broth), and CD broth without potassium chloride (KCl), respectively. The mycelia of *Fusarium* sp. were separated from the medium after incubation. Ethyl acetate extracts from mycelia and medium of these two cultural conditions were subjected to a high-performance liquid chromatography (HPLC) analysis and a liquid chromatography-mass spectrometry (LC-MS) analysis.

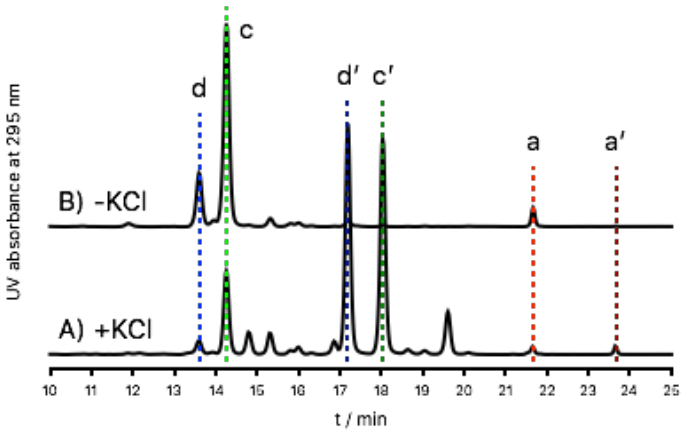

Figure 3-5. The HPLC profiles of extracts from mycelia of *Fusarium* sp. NBRC100844 cultivated in (A) CD broth, and (B) CD broth without KCl.

As the HPLC profiles of extracts from medium are almost the same with those from mycelia of *Fusarium*, only profiles of mycelia are showed. Several peaks were observed in the HPLC profiles of extracts from mycelia of *Fusarium* [Figure 3-5]. Peak **a'**, **c'** and **d'** are specific compounds isolated from CD broth (containing KCl) and cannot be isolated from CD broth without KCl. This suggested that these compounds are halogenated compounds.

The structures of these compounds were elucidated by LC-MS analysis and nuclear magnetic resonance (NMR) spectroscopy. As was expected, peak **a** is characterized as LL-Z1272β (**4**), and peak **d'** characterized as ascochlorin (**1**). The other compounds are also identified and considered as both derivatives of **a** and precursor of **d'** [Figure 3-6].

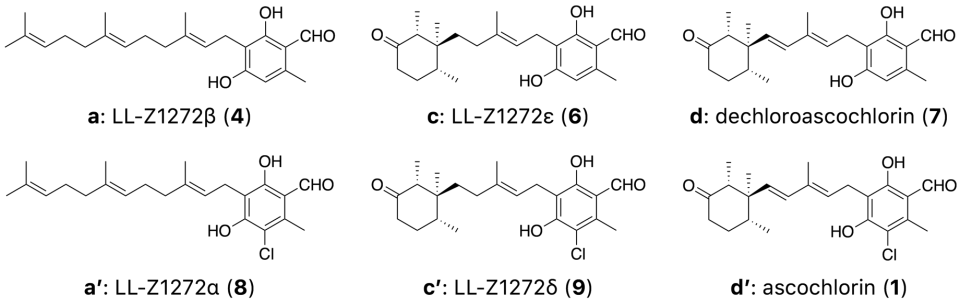

Figure 3-6. Structures of peaks isolated from *Fusarium* sp. NBRC100844.

Proposed Biosynthetic Pathway of Ascochlorin

On the basis of structures of these metabolites, the late biosynthetic steps of ascochlorin (**1**) started with LL-Z1272β (**4**) can be easily proposed [Figure 3-7]. In my proposed four steps pathway, two oxidases, one terpene cyclase, and one halogenase are predicted to be necessary. The four predicted biosynthetic enzymes plus three enzymes responsible for the early biosynthetic steps of **1**, which are revealed in our previous research[37], indicated that at most seven genes composed the biosynthetic gene cluster (BGC) for **1**.

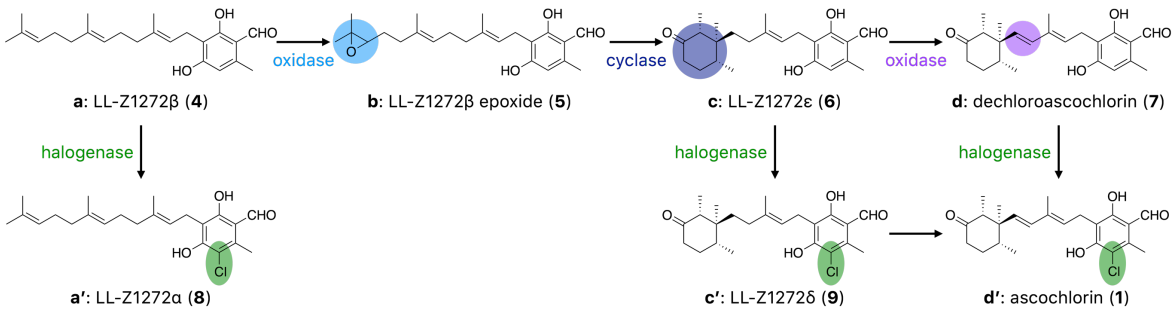

Figure 3-7. Proposed biosynthetic pathway from LL-Z1272β (**4**) to ascochlorin (**1**).

Identification of Biosynthetic Gene Cluster for Ascochlorin

Genomic DNA of *Fusarium* sp. NBRC100844 was isolated and purified. A draft genome sequencing analysis was performed on it. A protein Basic Local Alignment Search Tool (pBLAST) research was performed on the genomic database of *Fusarium* using StbB, the unique NRPS-like carboxylate reductase, as the query sequence. As a result, a protein exhibiting high similarity and identity (57/69%) with StbB was discovered. The gene for this protein clustered with six other genes encoding one polyketide synthase (PKS), one UbiA-type prenyltransferase (PT), one flavin-dependent halogenase (HLG), one cytochrome P450 monooxygenase/reductase (P450/CPR), one terpene cyclase (CYC), and one cytochrome P450 monooxygenase (P450) [Figure 3-8]. Besides NRPS-like carboxylate reductase, PKS and UbiA-type PT encoded by genes in this gene cluster also exhibit high similarity and identity with their homologues in the *stb* cluster [Table 3-1]. These three enzymes, which are homologues of StbA, StbB, and StbC, are predicted to be responsible for biosynthesis of **4**. The enzymes encoding by remaining four genes included all the necessary enzymes for the late stage of ascochlorin biosynthesis. It is suggested that this gene cluster is the BGC for ascochlorin, hence, the BGC is named as the *asc* cluster.

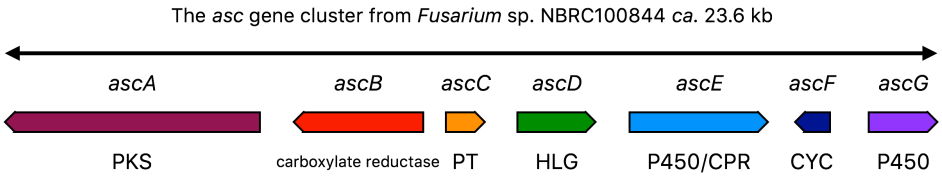

Figure 3-8. Candidate BGC for ascochlorin.

Table 3-1. Annotation of candidate BGC for ascochlorin.

Genes	Amino acids (base pairs)	Protein homologue, origin organism	Identities	Similarities	Predicted Function
ascA	2118 (6527)	StbA, *Stachybotrys bisbyi*	60%	76%	Polyketide synthase (PKS)
ascB	1064 (3316)	StbB, *Stachybotrys bisbyi*	61%	76%	NRPS-like carboxylate reductase
ascC	333 (1002)	StbC, *Stachybotrys bisbyi*	57%	69%	UbiA prenyltransferase (PT)
ascD	560 (1995)	AclH, *Aspergillus oryzae* RIB40	57%	72%	Flavin-dependent halogenase (HLG)
ascE	1069 (3535)	AoCYP505A3, *Aspergillus oryzae* RIB40	47%	64%	Cytochrome P450 monooxygenase / Cytochrome P450 reductase (P450/CPR)
ascF	267 (894)	AndB, *Emericella variecolor*	30%	49%	Terpene cyclase (CYC)
ascG	533 (1755)	AtaF, *Aspergillus terreus* NIH2624	33%	51%	Cytochrome P450 (P450)

3.5. Characterization of Genes Responsible for the Late-Stage of Ascochlorin Biosynthesis

The functional analysis of the *asc* cluster was carried out *in vivo* utilizing *Aspergillus oryzae* NSAR1 strain as a host organism.

Functional Confirmation of AscA, AscB, and AscC

Full length gene *ascA*, *ascC*, and cDNA of *ascB* were amplified by polymerase chain reaction (PCR), and subcloned to linear vector pAdeA and pTAex3 to yield fungal transformation plasmids pAdeA-AscA and pTAex3-AscB+AscC. *A. oryzae* transformant harboring *ascA* and transformant harboring *ascA*, *B*, and *C* was constructed by introducing pAdeA-AscA to *A. oryzae* NSAR1 strain and introducing pAdeA-AscA and pTAex3-AscB+AscC to the same strain utilizing polyethylene glycol (PEG)-mediated protoplast transformation method, respectively.

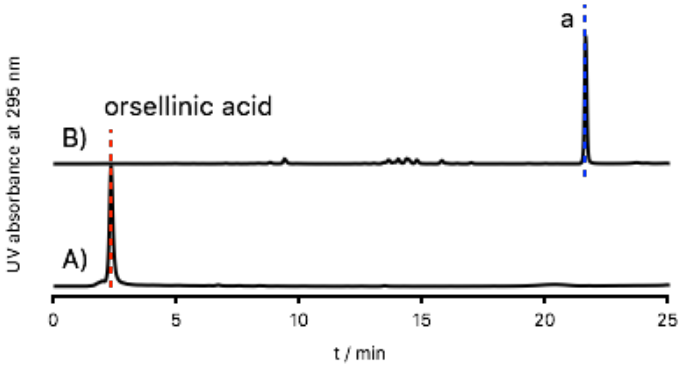

Figure 3-9. The HPLC profiles of extracts from mycelia of *A. oryzae* transformants harboring (A) *ascA*, and (B) *ascA*, *B* and *C*.

After induced incubation by CD-starch medium, the extracts from mycelia of these two *A. oryzae* transformants are subjected to the HPLC and LC-MS analysis. The significant peaks were identified by LC-MS and retention time comparison of HPLC profiles. As the results [Figure 3-9], the accumulation of orsellinic acid in mycelia of *A. oryzae* transformant harboring *ascA*, and the accumulation of peak **a** (compound **4**) in mycelia of *A. oryzae* transformant harboring *ascA*, *B*, and *C* were observed. This suggested that AscA, AscB, and AscC from the *asc* cluster have the same bioactivities with their homologues StbA, StbB, and StbC from the *stb* cluster, respectively. On the basis of the conclusion that **4** is the precursor of **1**, next research would investigate the functions of the remaining four enzymes encoded in the *asc* cluster, and elucidate the detailed biosynthetic pathway from **4** to **1**.

Characterizations of AscE and AscF

In our previous research on cyclized meroterpenoids, terminal of farnesyl moiety of prenylated polyketide was epoxidized by a flavin-dependent monooxygenase (FMO), then cyclized by a terpene cyclase (CYC). However, there is no gene for FMO in the *asc* cluster. Instead of FMO, two oxidases, a P450/CPR (AscE) and a P450 (AscG), were encoded in this BGC. Therefore, it is necessary to determine which oxidase is responsible for the epoxidation of **4**.

Full length gene *ascE*, *ascF*, and *ascG* were amplified by PCR and subcloned to linear vector pUSA to yield fungal transformation plasmids pUSA-AscE, pUSA-AscG, and pUSA-AscE+AscF. *A. oryzae* transformant harboring *ascA*, *B*, *C*, and *E* and transformant harboring *ascA*, *B*, *C*, and *G* were constructed by introducing plasmids pAdeA-AscA, pTAex3-AscB+AscC, and pUSA-AscE to *A. oryzae* NSAR1 strain and introducing pAdeA-AscA, pTAex3-AscB+AscC, and pUSA-AscE to the same strain using the same method as before, respectively. Results of analyzing metabolites extracted from mycelia of *A. oryzae* transformant harboring *ascA*, *B*, *C*, and *E*, and transformant harboring *ascA*, *B*, *C*, and *G* showed that only *ascE* harboring strain can produce different metabolite with *ascA*, *B*, and *C* harboring strain. It is suggested that AscE can recognize **4** as substrate. Instead of predicted intermediate LL-Z1272β epoxide (**5**), peak **b"** was observed in HPLC profile of extract from mycelia of transformant harboring *ascA*, *B*, *C*, and *E* [Figure 3-10 (B)].

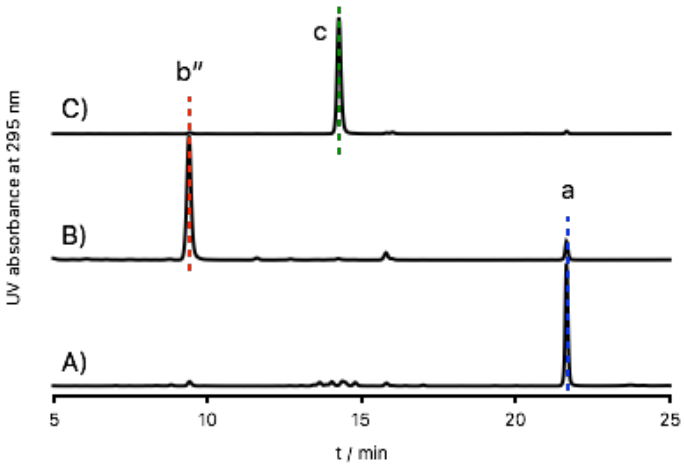

Figure 3-10. The HPLC profiles of extracts from mycelia of *A. oryzae* transformants harboring (A) *ascA*, *B* and *C*, (B) *ascA*, *B*, *C*, and *E*, and (C) *ascA*, *B*, *C*, *E*, and *F*.

Peak **b"** was isolated from metabolites from *A. oryzae* harboring *ascA*, *B*, *C*, and *E*, and identified as dihydroxy-LL-Z1272β (**10**) [Figure 3-11]by LC-MS and NMR spectra. Peak **b"** was considered as the product of a non-enzymatic reaction in acid condition from **5**. Thus, the true metabolite of AscE is **5**.

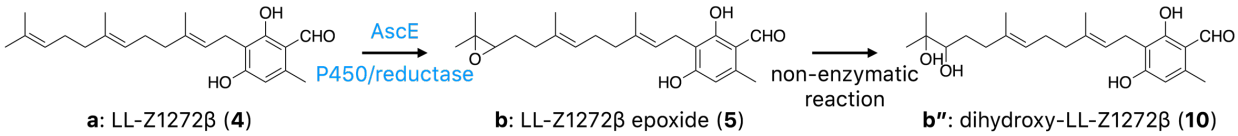

Figure 3-11. Peak **b"**: dihydroxy-LL-Z1272β is a product of peak **b**: LL-Z1272β epoxide from a non-enzymatic reaction.

A. oryzae transformant harboring *ascA*, *B*, *C*, *E*, and *F* was constructed by introducing plasmids pAdeA-AscA, pTAex3-AscB+AscC, and pUSA-AscE+ascF to *A. oryzae* NSAR1 strain. As the result of analysis of metabolites isolated from *A. oryzae* transformant harboring *ascA*, *B*, *C*, *E*, and *F*, peak **c** that is identified as LL-Z1272ε (**6**), was the only product of AscF [Figure 3-10 (C)]. It is suggested that AscF is the terpene cyclase responsible for the unique cyclization of **5** [Figure 3-12].

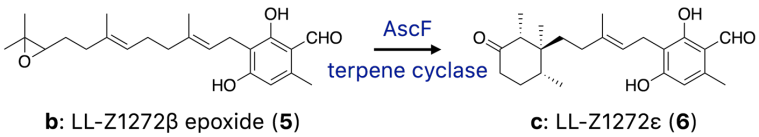

Figure 3-12. Peak **c**: LL-Z1272ε (**6**) is a cyclized product of LL-Z1272β epoxide (**5**) catalyzed by AscF.

Cyclization Mechanism of AscF and Stereochemistry Prediction of LL-Z1272β epoxide

AscF can be classified to be transmembrane Class II terpene synthase. The mechanism of the cyclization catalyzed by AscF will also be predicted based on the common mechanism of Class II terpene synthase. The cyclization of **5** started with the protonation of epoxide, followed with a series of transitions of hydrides and methyl [Figure 3-13 (A)]. The reaction finished after one cyclohexane ring cyclized.

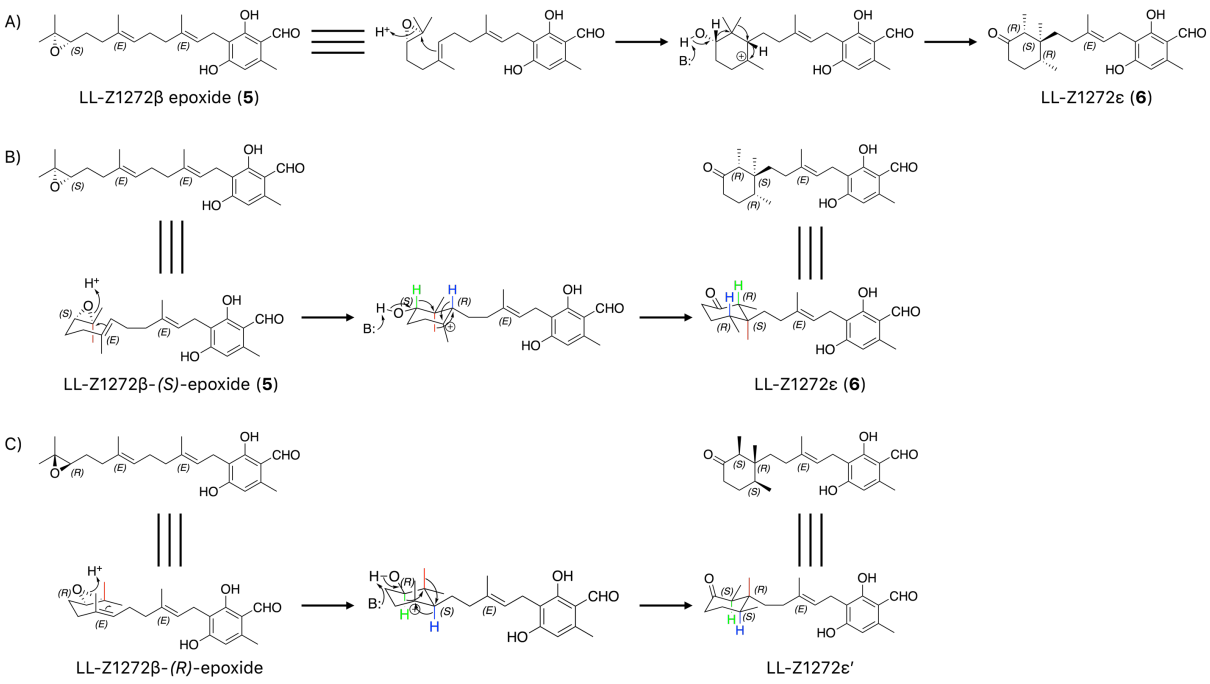

Figure 3-13. (A) Predicted cyclization mechanism of ascF. (B) LL-Z1272β-(*S*)-epoxide (**5**) is cyclized to LL-Z1272ε (**6**). (C) LL-Z1272β-(*R*)-epoxide is cyclized to a stereoisomer of LL-Z1272ε.

The configuration of **5** was predicted to be (*S*). LL-Z1272ε is a specific product of LL-Z1272β epoxide in (*S*) configuration, because of these unique transitions of hydrides and methyl occurred in cyclization reactions catalyzed by AscF [Figure 3-13 (B)]. On the other hand, epoxide in (*R*) configuration could be cyclized to a product with completely opposite stereochemistry in cyclohexane ring [Figure 3-13 (C)].

Characterizations of AscG

Full length gene *ascG* was subcloned to linear vector pPTRI to yield fungal transformation plasmid pPTRI-AscG. *A. oryzae* transformant harboring *ascA*, *B*, *C*, *E*, *F*, and *G* was constructed by introducing plasmids pAdeA-AscA, pTAex3-AscB+AscC, pUSA-AscE+AscF, and pPTRI-AscG to *A. oryzae* NSAR1 strain. Metabolites extracted from this strain were analyzed by HPLC and LC-MS. The result is compared with HPLC profiles of extract from mycelia of *A. oryzae* transformant harboring *ascA*, *B*, *C*, *E*, and *F*, and extract from mycelia of *Furasium* sp. NBRC100844 incubated without chloride. Peak **d** is identified as dechloroascochlorin (**7**), and is also a specific peak in HPLC profile of *A. oryzae* transformant harboring *ascA*, *B*, *C*, *E*, *F*, and *G* [Figure 3-14 (B), (C)]. The same peak cannot be observed in HPLC profile of *A. oryzae* transformant harboring *ascA*, *B*, *C*, *E*, and *F* [Figure 3-14 (A)], suggested that **7** was oxidized from **6** catalyzed by AscG.

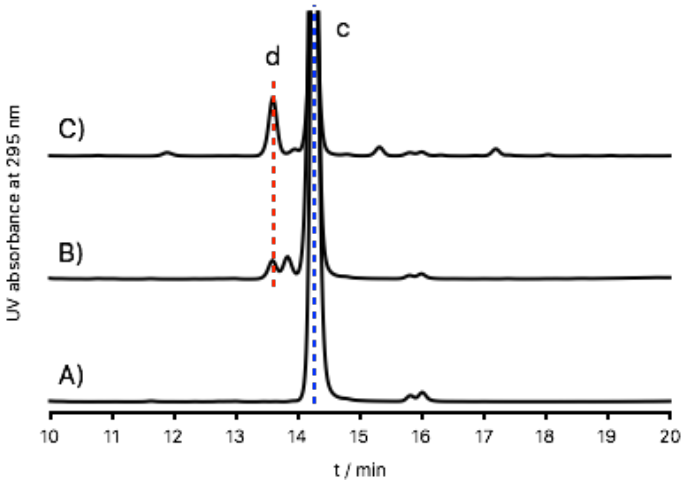

Figure 3-14. The HPLC profiles of extracts from mycelia of *A. oryzae* transformants harboring (A) *ascA*, *B*, *C*, *E*, and *F*, (B) *ascA*, *B*, *C*, *E*, *F*, and *G*, and (C) extracts from mycelia of *Fusarium* sp. NBRC100844 cultivated in CD-broth without chloride.

In detail, the methylene next to the quaternary carbon of double bond was firstly hydroxylated to an intermediate [Figure 3-15], because of the stabilizing effect of this double bond. After that, a dehydration reaction occurred spontaneously and formed a double bond to yield **7**.

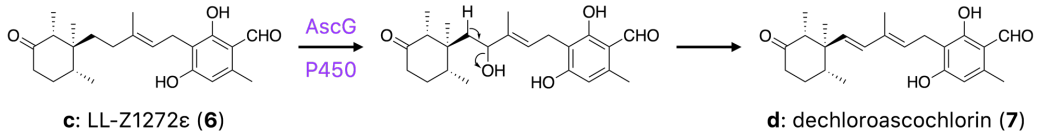

Figure 3-15. AscG catalyzed the oxidization of **6** to **7**.

Characterizations of AscD

Previous research reported that the benzene ring of ascochlorin can be halogenated by bromine instead of chlorine[32]. It is indicated that the enzyme for the halogenation of ascochlorin can accept various halogen as donor. Thus, *Fusarium* sp. NBRC100844 was separately cultivated in CD broth without chloride (KCl) plus fluoride (KF), CD broth, CD broth without chloride (KCl) plus bromide (KBr), and CD broth without chloride (KCl) plus iodide (KI) to verify if this fungus can also produce other halogenated compounds instead of chloride.

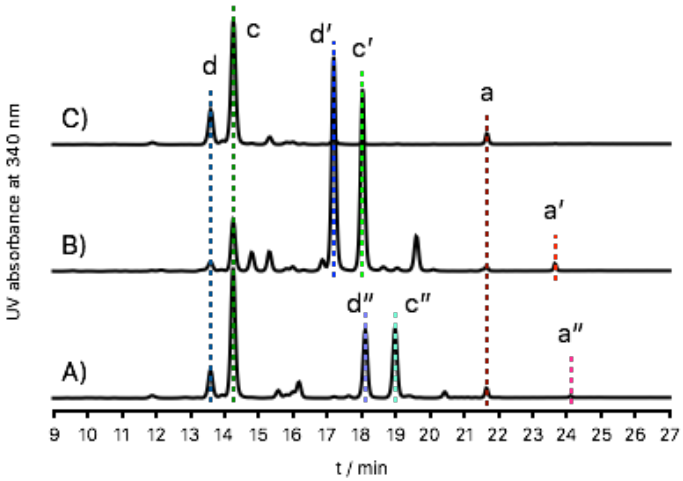

Figure 3-16. The HPLC profiles of extracts from mycelia of *Fusarium* sp. NBRC100844 cultivated in (A) CD broth without KCl plus KBr, (B) CD broth, (C) CD broth without KCl.

The extracts from mycelia of *Fusarium* sp. from these different broths were subjected to the HPLC and LC-MS analysis. As the results of analysis, *Fusarium* cannot grow well in medium plus KF, and cannot produce halogenated product in medium plus KI. Only fungus cultivated in medium with KBr produced different

metabolites from that of fungus cultivated in CD broth [Figure 3-16]. Specific metabolites isolated from *Fusarium* incubated in CD broth without KCl plus KBr were identified by LC-MS and NMR spectra. Peak **a"**, **c"** and **d"** were characterized as bromo analogue of LL-Z1272α (**11**), bromo analogue of LL-Z1272ε (**12**), and bromo analogue of ascochlorin (**13**), respectively [Figure 3-17]. These results confirmed the prediction that *Fusarium* sp. NBRC100844, the target organism in this research, can also produce bromo analogue of chloride compound, such as **11**, **12**, and **13**. Furthermore, it can also be proposed that the halogenation reactions with donors of chloride and bromide are catalyzed by AscD, the candidate flavin-dependent halogenase encoded in the *asc* cluster.

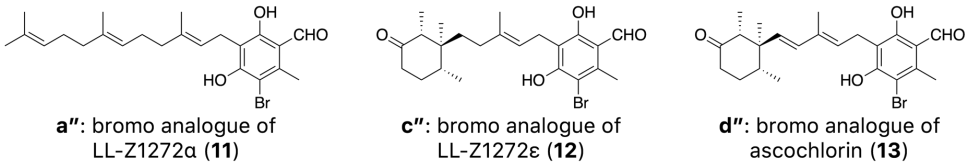

Figure 3-17. Structures of specific peaks isolated from *Fusarium* cultivated in CD-medium without KCl plus KBr.

cDNA of gene *ascD* was amplified and subcloned to vector pBARI to yield plasmid pBARI-AscD. *A. oryzae* transformant harboring *ascA*, *B*, *C*, *E*, *F*, and *D* was constructed by introducing fungal transformation plasmids pAdeA-AscA, pTAex3-AscB+AscC, pUSA-AscE+AscF, and pBARI-AscD to *A. oryzae* NSAR1 strain. The constructed *A. oryzae* transformant was cultivated in medium with high concentration of KCl or KBr after pre-incubated in complete medium. Extracts from mycelia of *A. oryzae* transformant were subjected to HPLC and LC-MS analysis. Specific peaks observed in *A. oryzae* transformant harboring *ascA*, *B*, *C*, *E*, *F*, and *D* were identified by comparing with HPLC and LC-MS profiles of metabolites isolated from wild type *Fusarium*.

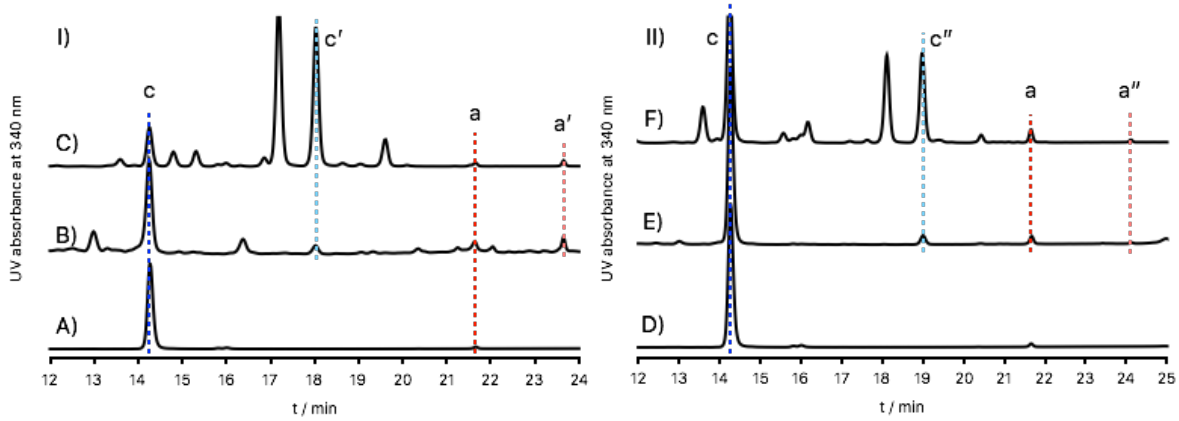

Figure 3-18. (I) The HPLC profiles of extracts from mycelia of (A) *A. oryzae* transformant harboring *ascA*, *B*, *C*, *E*, and *F* cultivated in medium with 5% KCl, (B) *A. oryzae* transformant harboring *ascA*, *B*, *C*, *E*, *F*, and *D* cultivated in medium with 5% KCl, and (C) *Fusarium* cultivated in medium with 5% KCl, (II) The HPLC profiles of extracts from mycelia of (D) *A. oryzae* transformant harboring *ascA*, *B*, *C*, *E*, and *F* cultivated in medium with 5% KBr, (E) *A. oryzae* transformant harboring *ascA*, *B*, *C*, *E*, *F*, and *D* cultivated in medium with 5% KBr, and (F) *Fusarium* cultivated in medium with 5% KBr.

As the results of HPLC analysis, chloride and bromide compounds produced by *Fusarium* [Figure 3-18 (C) and (F)] can also be observed in profile of *A. oryzae* transformant harboring *ascA*, *B*, *C*, *E*, *F*, and *D* [Figure 3-18 (B) and (E)], and cannot be observed in that of *A. oryzae* transformant harboring *ascA*, *B*, *C*, *E*, and *F*. This suggested that AscD is the halogenase responsible for the biosynthesis of ascochlorin (**1**). As predicted previously by the results of identification of metabolites isolated for wild type *Fusarium*, AscD can accept both chlorine and bromine as donor. The substrates of AscD can be **a**: LL-Z1272β (**4**), **c**: LL-Z1272ε (**6**), and **d**: dechloroascohlorin (**7**) [Figure 3-19].

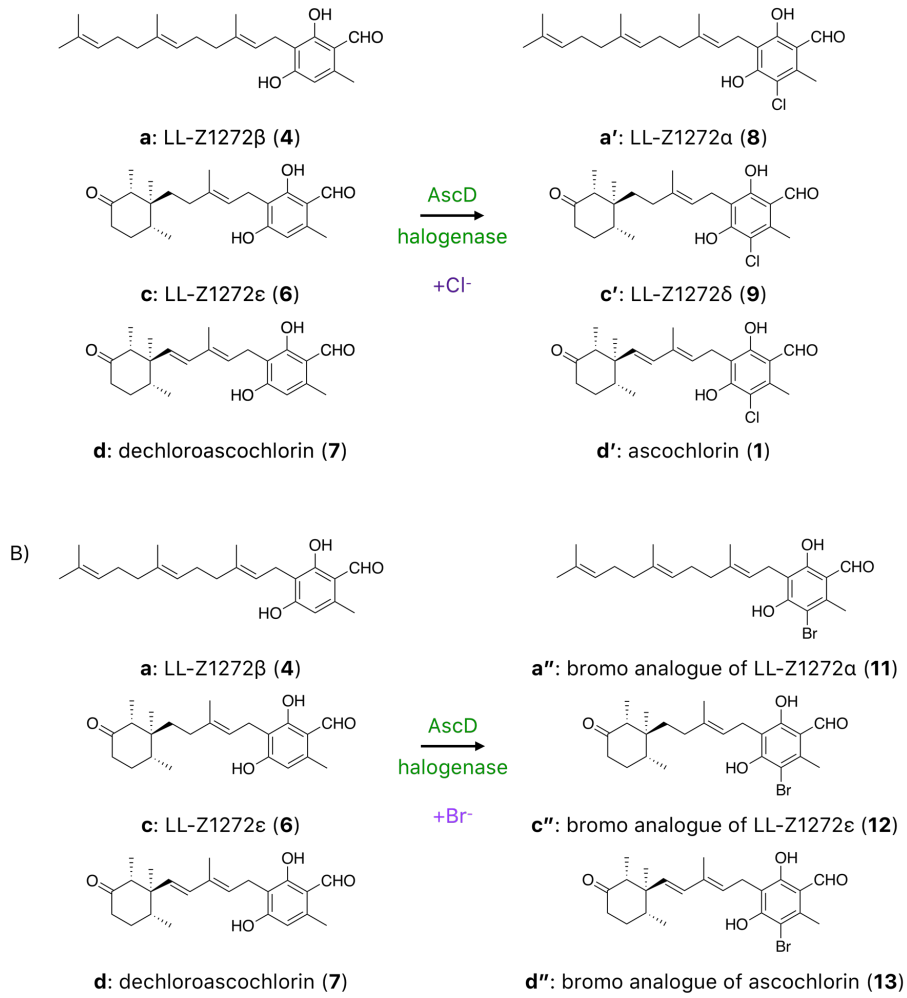

Figure 3-19. AscD is the halogenase that converts peak **a**, **b**, and **c** to (A) chlorides **a'**, **b'**, and **c'** or (B) bromide **a"**, **b"**, and **c"**.

3.6. Mutation Researches of AscF, a Unique Terpene Cyclase for Meroterpenoid

As mentioned previously, AscF is unique terpene cyclases that can cyclize a cyclohexane ring for ascochlorin (**1**). The others terpene cyclases for meroterpenoid investigated by our laboratory often construct a three rings system with farnesyl moity linked with polyketide part[33,18,16,14], while AscF only produced a single cyclohexane ring. Mutation researches would be carried out to study the relationship between the structure and enzymatic activity of AscF.

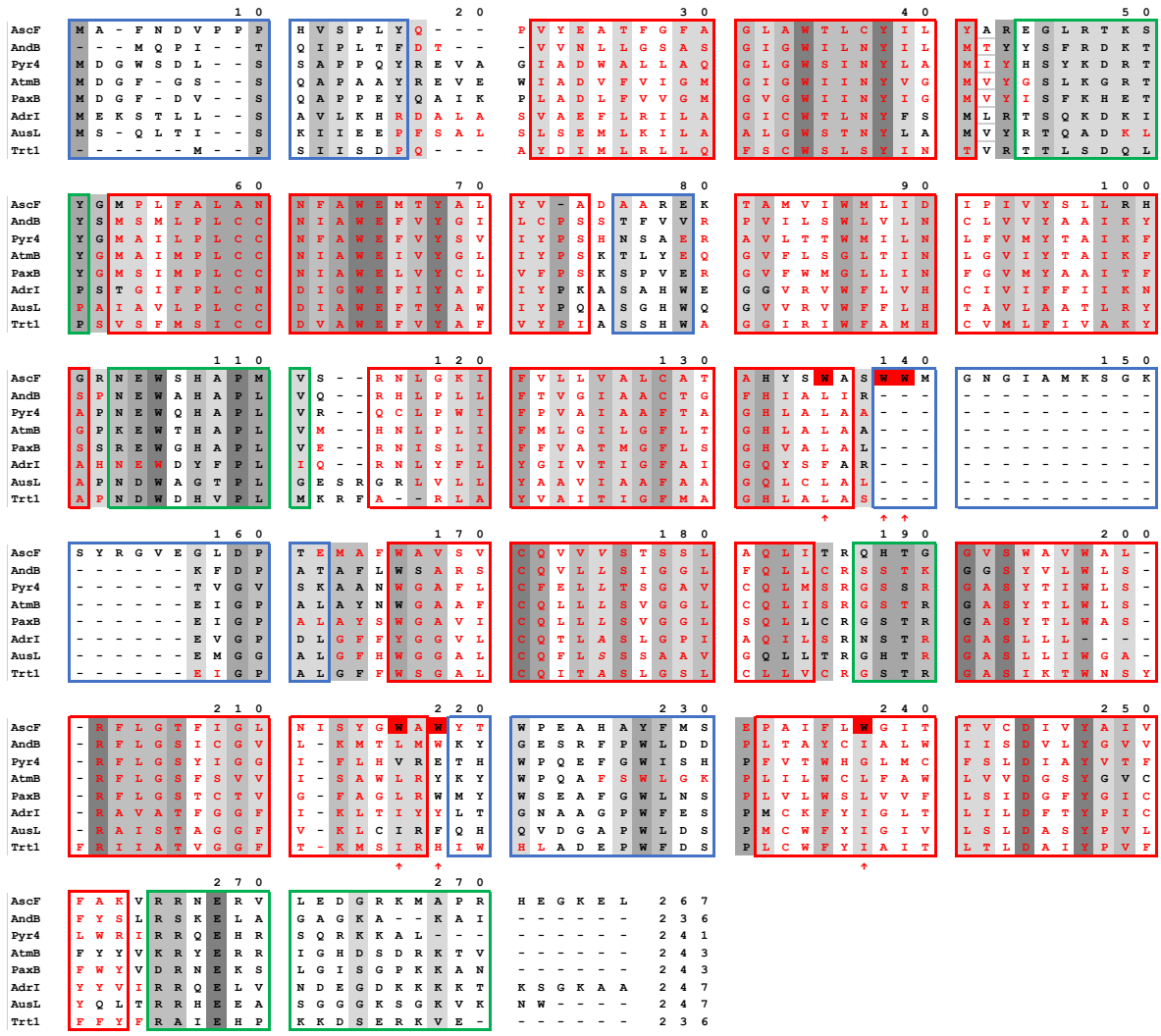

Figure 3-20. Alignment of terpene cyclases of meroterpenoids. Blue: outside of the membrane. Green: inside of the membrane. Red: transmembrane motifs.

Firstly, an alignment was created to compare AscF and seven functionally known meroterpenoid terpene cyclases. Amino acids sequences of these terpene cyclases were also processed by SOSUI and TMHMM to predict the membrane-binding domain [Figure 3-20]. Structures of all these cyclases can be classified as 7-transmembrane (7-TM) enzymes. The motifs located outside of the membrane (in the blue frames) are considered to be concerned with the enzymatic activity.

The most noticeable structural difference of AscF from other known cyclases is that AscF has a low similarity motif (WWMGNGIAMKSGKSYRGVE) located outside of the membrane. This motif was removed from AscF in order to make this cyclase to yield a more than one ring carbon skeleton. An *in vitro* assay was carried out, unfortunately, AscF completely lost its activity when this out-membrane motif was removed (unpublished data). This suggested that this motif is an essential motif that can hold the enzymatic activity of AscF.

Next, a point-mutation research was performed on AscF. Tryptophan, an aromatic residue that can stabilize the cation of intermediate, was chose as the mutation point. Previous research reported that mutations on aromatic residues of terpene cyclases changed the pattern of cyclization[38]. Four points of tryptophan, W127, W130W131, W207W209, and W228, which have low conservation with other known cyclases were mutated to alanine in order to get different compounds from mutant. An *in vivo* assay was carried out in *A. oryzae*, and four strains were constructed. Fungal transformation plasmids pUSA-AscE+AscF (W127A), pUSA-AscE+AscF (W130AW131A), pUSA-AscE+AscF (W207AW209A), and pUSA-AscE+AscF (W228A) were yielded based on pUSA-AscE+AscF. Gene *ascA*, *B*, *C*, and *E* were co-expressed with *ascF* (W127A), *ascF* (W130AW131A), *ascF* (W207AW209A), and *ascF* (W228A) to construct four *A. oryzae* transformants. Metabolites isolated from mycelia of these four transformant after incubation were subjected to HPLC analysis and LC-MS analysis.

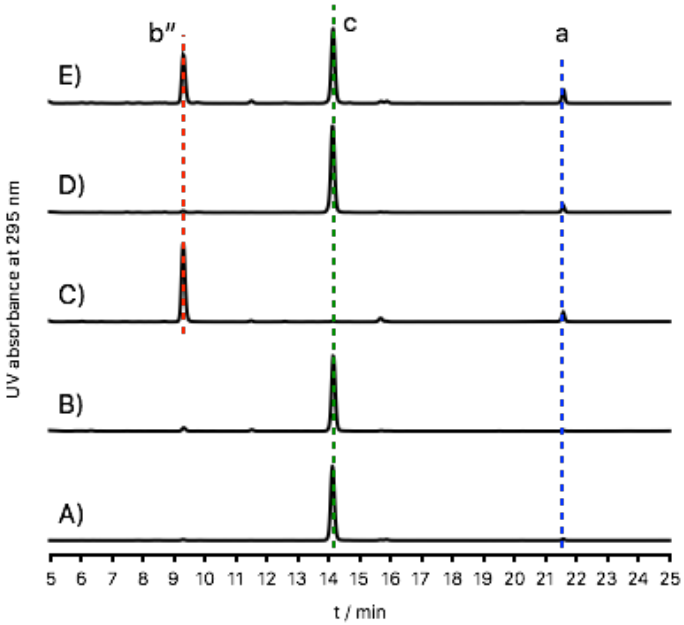

Figure 3-21. The HPLC profiles of extracts from mycelia of *A. oryzae* transformants harboring *ascA*, *B*, *C*, *E*, and (A) wild type asc*F*, (B) *ascF* (W127A), (C) *ascF* (W130AW131A), (D) ascF (W207AW209A), and (E) ascF (W228A).

The results of HPLC analysis suggested that activities of two mutants, AscF (W127A) and AscF (W207AW209A), are the same with wild type AscF, and peak **c**: LL-Z1272ε (**6**) was the only product of these three enzymes [Figure 3-21 (A), (B), and (D)]. Mutant AscF (W130AW131A) completely lost its enzymatic activity, instead of **c**, the spontaneous product **b"**: dihydroxy-LL-Z1272β (**10**) of **b**: LL-Z1272β epoxide (**5**) accumulated in mycelia of *ascF* (W130AW131A) co-expressed strain [Figure 3-21 (C)]. Not any peak **c** can be observed in the HPLC profile of this strain. Mutant AscF (W228A) still has its enzymatic activity as a cyclase, but the efficiency of this enzyme decreased according to the accumulation of peak **b"** [Figure 3-21(E)]. Unfortunately, no new compound was produced by these mutants.

3.7. Discussion

Reconstitution of Biosynthetic Pathway of Ascochlorin

An *A. oryzae* transformant harboring all seven genes from the *asc* cluster was constructed by introducing plasmids pAdeA-AscA, pTAex3-AscB+AscC, pUSA-AscE+AscF, pPTRI-AscG, and pBARI-AscD to *A. oryzae* NSAR1 strain. This transformant was separately cultivated in CD-starch medium with high concentration of KCl (5%) or KBr (5%) after pre-incubated in DPY medium. However, no significant final product **1** or its bromo analogue was detected in both HPLC and LC-MS analysis. Next, orsellinic acid was fed into the same medium in order to increase the production. As the result of LC-MS, bromo analogue of **1** (**13**) was detected at MS level, but the amount of this compound is very small (unpublished data).

It is noticed that **1** and its intermediates can be isolated in both broth and mycelia of *Fusarium*, while they only accumulated in mycelia of *A. oryzae* transformants harboring genes of the *asc* cluster. This indicted that a transporter that can recognize **1** and its intermediates as substrates exists in *Fusarium*. However, there is no candidate transporter encoded in the *asc* cluster. Thus, the gene encoding transporter for **1** must located in some other places on genomic DNA of *Fusarium*. It is estimated that the accumulation of intermediates of **1** in mycelia of *A. oryzae* transformants is because of the lack of specific transporter in these strains. As mentioned in background, **1** is isolated as an antibiotic and an antitumor agent[26]. Accumulations of **1** and its precursor in mycelia are harmful to their producer *A. oryzae* transformants. This is considered as one of the reasons why large amount of **1** and its bromo analogue (**13**) cannot be isolated from *A. oryzae* transformants.

On the other hand, it is observed that the amount of peak **d** (**7**), peak **c'** (**9**), and peak **c"** (**12**) in HPLC profiles is very small compared with these of wild type *Fusarium*. This indicated that enzymatic efficiency of AscD and AscG decreases in *A. oryzae* transformants for unknown reason. The reason can be predicted as the different pH conditions inside mycelia of two fungi, *Fusarium* and *A. oryzae*.

These are two main reasons why large amount of **1** and its bromo analogue (**13**) cannot be isolated in *A. oryzae* transformant. This also suggested that although *A. oryzae* is an excellent host organism for heterologous expression, it cannot heterologous express all the genes of other fungi perfectly.

Although, combinatorial biosynthesis utilizing *A. oryzae* as the host organism are proved to be a very suitable method for biosynthetic research of fungal metabolites, there are still some problems to solve. One of these problems is splicing. In this research, the expressing of AscB and AscD used their cDNAs instead of full length genes because of *A. oryzae* cannot correctly recognize introns and splice them. Our previous researches mainly focused on *Aspergillus* and *Penicillium*, which are very close to host organism on phylogenetic tree. This project whose investigating target is *Fusarium* is the first paradigm in our group to express gene from organism phylogenetically far from *Aspergillus*. We have evolved our technology of heterologous expression through this research.

Application of AscD, a Halogenase with Wide Substrate Specificity

AscD, the halogenase characterized in this research, was classified as the flavin-dependent halogenase, has a wide substrate specificity. As revealed in the *in vivo* experiments with *A. oryzae*, compound **4**, **6** and **7** can be recognized as its substrates, and both chlorine and bromine can be the halogen donors. As previously reported catalytic mechanism of flavin-dependent halogenase[39], firstly, donor anion chloride is oxidized to hypochlorous acid (HOCl) under the assistance of flavin in the pocket of enzyme, then, HOCl reacts with substrate to complete the chlorination [Figure 3-22]. The mechanism of bromination is similar with chlorination.

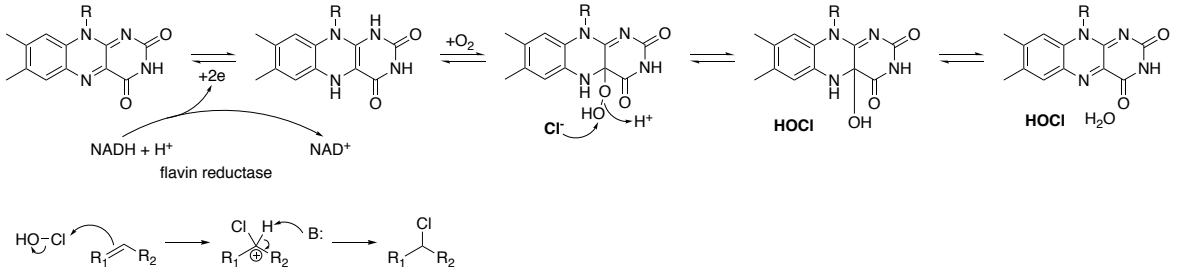

Figure 3-22. The mechanism of halogenation catalyzed by flavin-dependent halogenase.

No fluoride and iodide compound was detected in HPLC profiles of metabolites extracted from wild type *Fusarium* cultivated in medium containing fluoride or iodide. There are two reasons for fluorine. First reason is that fluoride is too toxic for fungi to live. The other reason is that hypofluorous acid (HOF) is too unstable to finish the fluorination reaction. The reason why iodide compound cannot be produced can be explained that the radius of iodine is too large to get into the pocket of the halogenase.

Two bromide compounds, compound **12** and **13**, were isolated from wild type *Fusarium* sp. NBRC100844. The cytotoxicity against MCF-7 breast cancer cell line of ascochlorin and its bromo analogues were measured. As the results of cytotoxicity assay, **6** exhibited IC_{50} value at 27 μM, **9** (chloride of **6**) exhibited IC_{50} value at 38 μM, **12** (bromide of **6**) exhibited IC_{50} value at 21 μM, **7** exhibited IC_{50} value at 15 μM, **1** (ascochlorin, chloride of **7**) exhibited IC_{50} value at 28 μM, and **13** (bromide of **7**) exhibited IC_{50} value at 18 μM. According to the IC_{50} values of these compounds, the bioactivities of both bromides and compounds without halogen are stronger than these of chlorides. This indicated that the chlorination of precursor of ascochlorin in *Fusarium* could be considered as a self-defense effect in organism. It is also noticed that in some case, bromide have stronger bioactivity than that of compound without halogen.

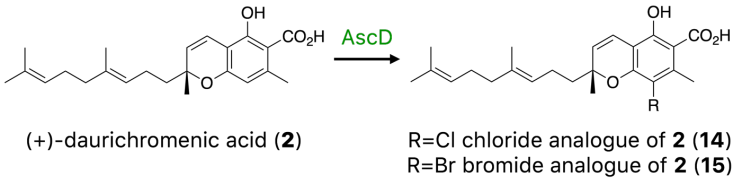

Figure 3-23. The conversion of (+)-daurichromenic acid to its chloride analogue and bromide analogue.

In our previous research[34], **2** was successfully converted to **14** by expressing AscD in its biosynthetic

pathway [Figure 3-23]. The bromide analogue of **2** (**15**) can be obtained with similar method. It is predicted that **15** may also be a potential bioactive compound stronger than **2**.

Mutation Researches of AscF

Unfortunately, no compound with novel cyclization pattern was isolated in our point mutation research on AscF. According to the results of in vivo assay of mutant of AscF, the unique motif of AscF (WWMGNGIAMKSGKSYRGVE) is very critical for the enzymatic activity. The exchange of residues on this motif could lead to completely losing of the enzymatic activity.

On the other hand, the exchange of residue on transmembrane (TM) helix also leads to the decreasing of enzymatic activity. This is indicated that the residue on TM helix may also involve in the catalysis.More investigation is necessary to elucidate the insight into cyclization mechanism of AscF.

3.8. Conclusion

In this research, the BGC for ascochlorin (**1**) was successfully identified by a genome mining approach [Figure 3-24]. The enzymes responsible for the biosynthesis of **1** were functionally analyzed. The activities of all these enzymes were characterized. The biosynthetic pathway of **1** was proposed on the basis of functional analysis of biosynthetic enzymes and identification of intermediates [Figure 3-25].

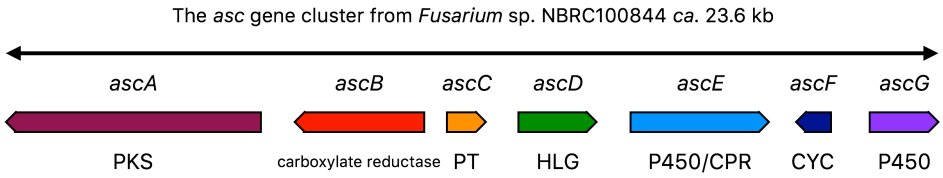

Figure 3-24. The *asc* cluster is the biosynthetic gene cluster for ascochlorin.

The key enzyme for carbon skeleton formation of **1**, AscF, was investigated by point-mutation. AscF, a terpene cyclase, was classified as a 7-TM enzyme. The importance of its unique motif, which has low conservation in other known cyclases, was elucidated. This motif located on the outside of the membrane was considered as a critical motif for the enzymatic activity of AscF.

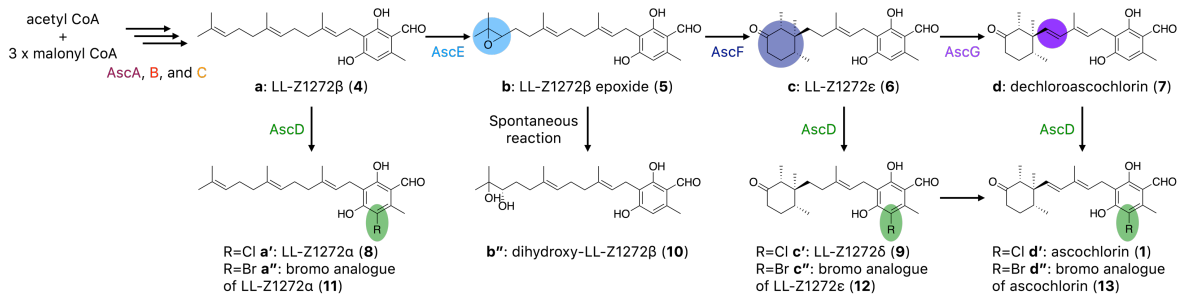

Figure 3-25. Biosynthetic pathway of ascochlorin and its bromo analogue.

[References]

1. Tamura, G.; Suzuki, S.; Takatsuki, A.; Ando, K.; Arima, K., Ascochlorin, a new antibiotic, found by paper-disc agar-diffusion method. I. *The Journal of Antibiotics* **1968,** *21* (9), 539-544.

2. Lee, S. H.; Kwak, C. H.; Lee, S. K.; Ha, S. H.; Park, J.; Chung, T. W.; Ha, K. T.; Suh, S. J.; Chang, Y. C.; Chang, H. W., Anti-inflammatory effect of ascochlorin in LPS-stimulated RAW 264.7 macrophage cells is accompanied with the down-regulation of iNOS, COX-2 and proinflammatory cytokines through NF-κB, ERK1/2, and p38 signaling pathway. *Journal of Cellular Biochemistry* **2016,** *117* (4), 978-987.

3. Hosokawa, T.; Ando, K.; Tamura, G., An ascochlorin derivative, AS-6, potentiates insulin action in streptozotocin diabetic mice and rats. *Agricultural and Biological Chemistry* **1982,** *46* (11), 2865-2869.

4. Hussain, H.; Drogies, K.-H.; Al-Harrasi, A.; Hassan, Z.; Shah, A.; Rana, U. A.; Green, I. R.; Draeger, S.; Schulz, B.; Krohn, K., Antimicrobial constituents from endophytic fungus *Fusarium* sp. *Asian Pacific Journal of Tropical Disease* **2015,** *5* (3), 186-189.

5. Isaka, M.; Yangchum, A.; Supothina, S.; Laksanacharoen, P.; Luangsa-ard, J. J.; Hywel-Jones, N. L., Ascochlorin derivatives from the leafhopper pathogenic fungus *Microcera* sp. BCC 17074. *The Journal of Antibiotics* **2015,** *68* (1), 47-51.

6. Gutiérrez, M.; Theoduloz, C.; Rodríguez, J.; Lolas, M.; Schmeda-Hirschmann, G., Bioactive metabolites from the fungus *Nectria galligena*, the main apple canker agent in Chile. *Journal of Agricultural and Food Chemistry* **2005,** *53* (20), 7701-7708.

7. Aldridge, D. C.; Borrow, A.; Foster, R. G.; Large, M. S.; Spencer, H.; Turner, W. B., Metabolites of *Nectria coccinea*. *Journal of the Chemical Society, Perkin Transactions 1* **1972**, 2136-2141.

8. Itoh, T.; Tokunaga, K.; Matsuda, Y.; Fujii, I.; Abe, I.; Ebizuka, Y.; Kushiro, T., Reconstitution of a fungal meroterpenoid biosynthesis reveals the involvement of a novel family of terpene cyclases. *Nature Chemistry* **2010,** *2* (10), 858-864.

9. Matsuda, Y.; Awakawa, T.; Itoh, T.; Wakimoto, T.; Kushiro, T.; Fujii, I.; Ebizuka, Y.; Abe, I., Terretonin biosynthesis requires methylation as essential step for cyclization. *ChemBioChem* **2012,** *13* (12), 1738-1741.

10. Matsuda, Y.; Awakawa, T.; Wakimoto, T.; Abe, I., Spiro-ring formation is catalyzed by a multifunctional dioxygenase in austinol biosynthesis. *Journal of the American Chemical Society* **2013,** *135* (30), 10962-10965.

11. Matsuda, Y.; Wakimoto, T.; Mori, T.; Awakawa, T.; Abe, I., Complete biosynthetic pathway of anditomin: nature's sophisticated synthetic route to a complex fungal meroterpenoid. *Journal of the American Chemical Society* **2014,** *136* (43), 15326-15336.

12. Okada, M.; Saito, K.; Wong, C. P.; Li, C.; Wang, D.; Iijima, M.; Taura, F.; Kurosaki, F.; Awakawa, T.; Abe, I., Combinatorial biosynthesis of (+)-daurichromenic acid and its halogenated analogue. *Organic Letters* **2017**.

13. Yabu, Y.; Yoshida, A.; Suzuki, T.; Nihei, C.-i.; Kawai, K.; Minagawa, N.; Hosokawa, T.; Nagai, K.; Kita, K.; Ohta, N., The efficacy of ascofuranone in a consecutive treatment on *Trypanosoma brucei brucei* in mice. *Parasitology International* **2003,** *52* (2), 155-164.

14. Hosono, K.; Ogihara, J.; Ohdake, T.; Masuda, S., LL-Z1272α epoxide, a precursor of ascochlorin produced by a mutant of *Ascochyta viciae*. *The Journal of Antibiotics* **2009,** *62* (10), 571-574.

15. Li, C.; Matsuda, Y.; Gao, H.; Hu, D.; Yao, X. S.; Abe, I., Biosynthesis of LL-Z1272β: discovery of a new member of NRPS-like enzymes for aryl-aldehyde formation. *ChemBioChem* **2016,** *17* (10), 904-907.

16. Tomita, T.; Kim, S.-Y.; Teramoto, K.; Meguro, A.; Ozaki, T.; Yoshida, A.; Motoyoshi, Y.; Mori, N.; Ishigami, K.; Watanabe, H.; Nishiyama, M.; Kuzuyama, T., Structural insights into the CotB2-catalyzed cyclization of geranylgeranyl diphosphate to the diterpene cyclooctat-9-en-7-ol. *ACS Chemical Biology* **2017,** *12* (6), 1621-1628.

17. Dong, C.; Flecks, S.; Unversucht, S.; Haupt, C.; Van Pee, K.-H.; Naismith, J. H., Tryptophan 7-halogenase (PrnA) structure suggests a mechanism for regioselective chlorination. *Science* **2005,** *309* (5744), 2216-2219.

4. Discovery of a Cytochrome P450 for Biosynthesis of Citreohybridonol

4.1. Background

Introduction for Andrastin A

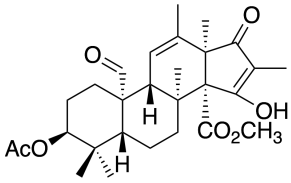

andrastin A (**1**)

Figure 4-1. Structure of andrastin A (**1**)

Andrastin A [Figure 4-1], isolated as an inhibitor of protein farnesyltransferase[40], is a meroterpenoid widely distributed in *Penicillium* sp.[40-41], and was considered as a promising lead compound with antitumor activity for its enhancement effect of drug accumulation in vincristine-resistant KB cells[42].

Biosynthetic Research of Andrastin A

Meroterpenoid andrastin A was considered to be derived from 3,5-dimethylorsellinic acid (DMOA) and farnesyl pyrophosphate (FPP)[40], and the late steps in the biosynthesis of andrastin A were successfully revealed by my laboratory[17]. In our previous research, the BGC for andrastin A was discovered [Figure 4-2, Table 4-1], and genes responsible for the late steps of andrastin A biosynthesis were functionally analyzed *in vivo*.

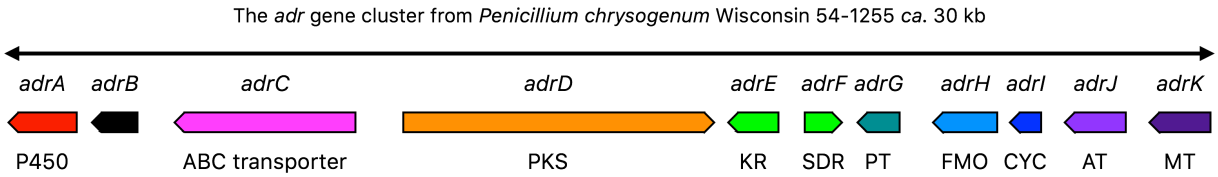

Figure 4-2. BGC for andrastin A: the *adr* cluster.

Table 4-1. Annotation of the *adr* cluster.

Genes	Amino acids (base pairs)	Protein homologue, origin organism	Identities	Similarities	Predicted Function
adrA	512 (1744)	BDBG_03859, *Ajellomyces dermatitidis*	58%	77%	Cytochrome P450 (P450)
adrB	1213 (1162)	-	-	-	Hypothetical protein
adrC	1442 (4613)	ANI_1_1494064, *Aspergillus niger*	58%	73%	ABC transporter
adrD	2496 (7930)	AusA, *Aspergillus nidulans*	54%	69%	Polyketaide synthase (PKS)
adrE	336 (1280)	PMAA_102060, *Talaromyces marneffei*	48%	64%	Ketoreductase (KR)
adrF	255 (949)	Trt9, *Aspergillus terreus*	67%	81%	Short chain dehydrgenase (SDR)
adrG	325 (1073)	AusN, *Aspergillus nidulans*	56%	74%	UbiA-like prenyltransferase (PT)
adrH	451 (1643)	AusM, *Aspergillus nidulans*	55%	68%	FAD-dependent monooxygenase (FMO)
adrI	248 (803)	Trt1, *Aspergillus terreus*	45%	66%	Terpene cyclase (CYC)
adrJ	498 (1556)	AOR_1_310024, *Aspergillus oryzae*	42%	60%	Acetyltransferase (AT)
adrK	277 (1060)	AusD, *Aspergillus nidulans*	67%	80%	Methyltransferase (MT)

In detail, the function of AdrI, the putative meroterpenoid terpene cyclase, was characterized firstly, and andrastin E (**2**) was confirmed as the product of the cyclization catalyzed by AdrI. Andrastin E is a stable compound, have high permeability of cell wall of *A. oryzae*. Thus, andrastin E feeding experiments were performed to investigate the conversions of compounds occurred in late steps of andrastin A biosynthesis. *In vivo* assays were utilized to study the functions of the enzymes catalyzing the reactions in andrastin A biosynthetic pathway. Genes in *adr* cluster were heterologously expressed in *A. oryzae*, and the transformants harboring different combinations of these genes were inoculated in medium containing andrastin E. Identification of specific metabolites of each *A.*

oryzae transformant elucidated the reactions occurred in andrastin A biosynthetic pathway and the function of each enzyme.

Andrastin E, the product of the cyclization catalyzed by AdrI, a terpene cyclase (CYC), is converted to andrastin F by the catalysis of AdrF, a short chain dehydrogenase (SDR) and AdrE, a ketoreductase (KR). Then, andrastin F is converted to andrastin C through an additional reaction catalyzed by AdrJ, an acetyltransferase (AT). Finally, andrastin C was oxidized twice to the final product andrastin A under the catalysis of AdrA, a cytochrome P450 monooxygenase (P450) [Figure 4-3].

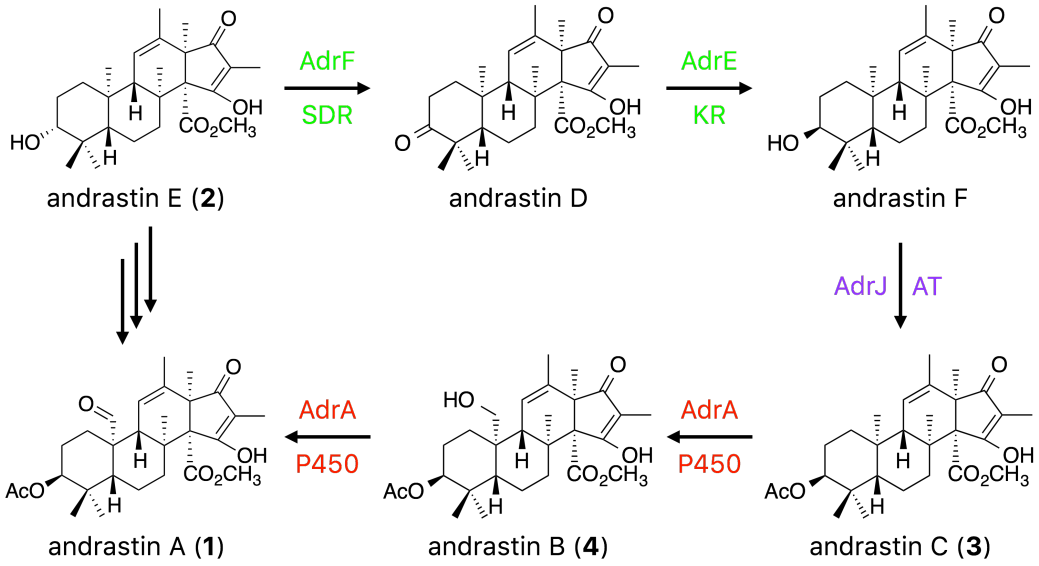

Figure 4-3. The late steps of andrastin A biosynthesis.

4.2. Discovery of a New Potential BGC for Novel Meroterpenoids with Andrastin Scaffold

Emericella variecolor is a filamentous fungus, which is reported as a producer of many bioactive secondary metabolites[43-46]. Draft genome sequencing analysis of *Emericella variecolor* NBRC32302 was performed in order to elucidate the complete biosynthesis of anditomin[14], a unique meroterpenoid isolated from this fungus. A new biosynthetic gene cluster, which exhibited high similarity with andrastin A biosynthetic gene cluster (the *adr* cluster), was discovered in the genome of *E. variecolor* [Figure 4-4], when we searched for the biosynthesis gene cluster for anditomin.

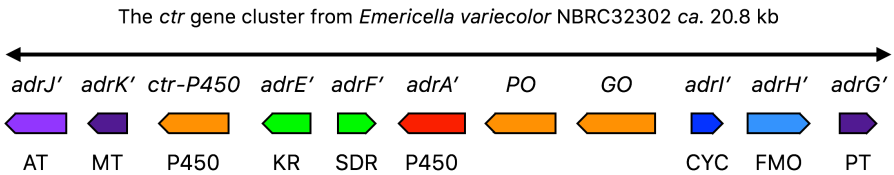

Figure 4-4. A potential BGC for meroterpenoids of andrastin scaffold.

Table 4-2. Detailed annotation of the *ctr* cluster.

Genes	Amino acids (base pairs)	Protein homologue, origin organism	Identities	Similarities	Predicted Function
adrJ'	494 (1553)	AdrJ, *Penicillium chrysogenum*	54%	71%	Acetyltransferase (AT)
adrK'	278 (990)	AdrK, *Penicillium chrysogenum*	69%	82%	Methyltransferase (MT)
ctr-P450	518 (1771)	Pc16g00090, *Penicillium chrysogenum*	65%	74%	Cytochrome P450 (P450)
adrE'	292 (1220)	AdrE, *Penicillium chrysogenum*	43%	58%	Ketoreductase (KR)
adrF'	258 (964)	AdrF, *Penicillium chrysogenum*	62%	79%	Short chain dehydrgenase (SDR)
adrA'	502 (1685)	AdrA, *Penicillium chrysogenum*	61%	75%	Cytochrome P450 (P450)
PO	465 (1783)	PEX2_109150, *Penicillium chrysogenum*	51%	70%	Dyp-type peroxidase
GO	658 (1977)	Pc21g18600, *Penicillium chrysogenum*	41%	61%	Galactose oxidase
adrI'	243 (785)	AdrI, *Penicillium chrysogenum*	68%	82%	Terpene cyclase (CYC)
adrH'	473 (1581)	AdrH, *Penicillium chrysogenum*	59%	71%	FAD-dependent monooxygenase (FMO)
adrG'	310 (933)	AdrG, *Penicillium chrysogenum*	66%	80%	UbiA prenyltransferase (PT)

The final product of this new biosynthetic gene cluster was unknown when I started this research. My later research revealed that this BGC is for citreohybridonol (**5**) [Figure 4-6] biosynthesis, thus, the BGC was designated as the *ctr* cluster. Eleven genes are contained in the *ctr* cluster, and eight of them encode proteins that exhibit high similarity with their homologues encoded in the *adr* cluster [Table 4-2]. However, the rest of the genes in the *ctr* cluster encoding a putative cytochrome P450 (*ctr-P450*), a putative Dyp-type peroxidase (*PO*), and a putative galactose oxidase (*GO*), respectively, do not exhibit high similarity to proteins encoded by genes in the *adr* cluster. Compared with the *adr* cluster, it is noticed that gene encoding PKS, which is for biosynthesis of DMOA, does not exist in the *ctr* cluster. However, the BGC for anditomin, which is also located in genomic DNA of *E. variecolor*, contains a PKS exhibiting the same function with the PKS encoded in the *adr* cluster. This indicated that co-expression of these three additional genes with andrastin biosynthetic genes may derive new products of andrastin scaffold.

Functional Analysis of AdrI′, a Predicted Terpene Cyclase

In order to elucidate the products derived by the *ctr* cluster, the function of AdrI', the homologue of terpene cyclase AdrI, was investigated, because terpene cyclase is one of the most essential enzyme for carbon skeleton construction and mainly contributes to the diversity of meroterpenoids. An alignment of AdrI' and AdrI was created, and AdrI' showed 68% identity and 82% similarity with AdrI as the result of analysis [Figure 4-5].

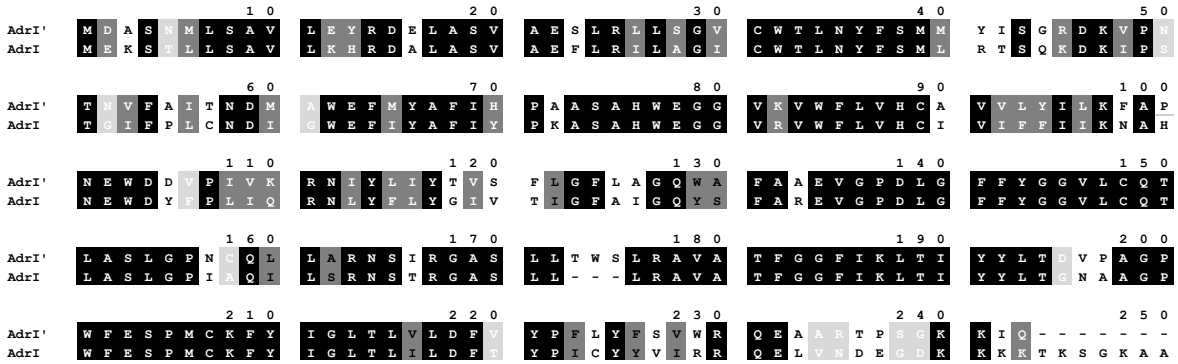

Figure 4-5. Alignment of AdrI' and AdrI.

The *adrI'* was heterologously expressed in *A. oryzae* transformant harboring *trt4*, *2*, *5*, and *8*[18]. The extract isolated form this transformant was analyzed by compared the HPLC and LC-MS profile with andrastin E standard. The main specific metabolite of *adrI'* expressing strain was identified as andrastin E. It is suggested that AdrI' have the same function as that of AdrI as predicted. This strongly indicated the potential that the *ctr* cluster is a BGC for meroterpenoid of andrastin scaffold.

Furthermore, many meroterpenoids with the same carton skeleton as that of andrastin, such as citreohybridonol (**5**)[47], citreohybridones[48-50], isocitreohybridones[49-52], citreohybriddiones[51, 53], and atlantinones[54-55], have been reported [Figure 4-6], however, the detailed biosynthesis of these natural products is still unknown. All

of these compounds are oxidized products based of andrastin A. Therefore, it is expected that the *ctr* cluster may derive new compounds on the scaffold of andrastin A for the three additional oxidases encoded in this BGC.

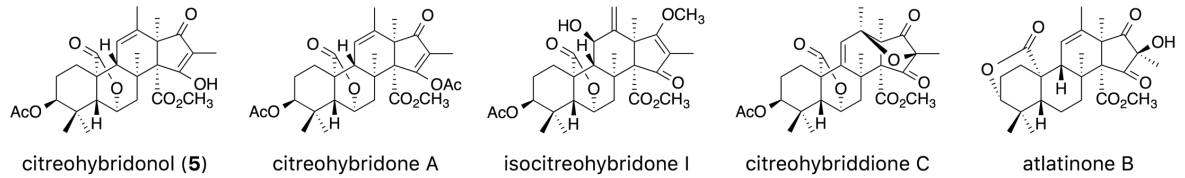

Figure 4-6. Oxidized analogues of andrastin A.

4.3. Purposes

As has been previously described, the *ctr* cluster was a potential BGC for natural product with andrastin A scaffold. The purposes of this research are to identify the final product and its intermediates derived by the *ctr* cluster and reveal the functions of three additional cryptic genes, *ctr-P450*, *PO*, and *GO*, in this gene cluster.

4.4. Discovery of the Cytochrome P450 Responsible for the Citreohybridonol Biosynthesis

Construction and Metabolites Identification of a Seven-Gene Co-Expression Transformant

In order to elucidate the product of the *ctr* cluster, which was hypothesized to be a BGC for oxidized product of andrastin A, an *A*. oryzae transformant harboring three additional genes in the *ctr* cluster, *ctr-P450*, *PO*, and *GO*, with andrastin A biosynthetic genes *adrF*, *E*, *J*, and *A* was constructed. Full length genes *ctr-P450*, *PO*, and *GO* were amplified and subcloned to vector pBARI to yield fungal transformation plasmid pBARI-CtrP450+PO+GO. Then, this plasmid was introduced to *A*. *oryzae* transformant harboring *adrF*, *E*, *J*, and *A*[17] to construct the seven-gene expressing system. An andrastin E bio-conversion experiment was conducted utilizing this strain to elucidate the product of the *ctr* cluster.

A. *oryzae* transformant harboring *adrF*, *E*, *J*, *A*, *ctr-P450*, *PO*, and *GO* was inoculated in medium with andrastin E (**2**), and *A*. *oryzae* harboring *adrF*, *E*, *J* and *A* introduced with empty vector pBARI cultivated in the same condition was used as a negative control. The broth of these two strains were extracted after incubation. The extracts were subjected to HPLC and LC-MS analysis. As the results of analysis, the main peak around 21 min in profile of negative control was identified as andrastin A (**1**) [Figure 4-7 (A)], and the significant peak around 19 min in profile of *A*. *oryzae* transformant co-expressing seven genes was detected and considered as the final product of the *ctr* cluster [Figure 4-7 (B)]. The specific product converted from andrastin E by the seven-gene co-expressing strain was isolated and structurally investigated using NMR spectroscopy and LC-MS analysis. This compound was identified as citreohybridonol (**5**) [Figure 4-8].

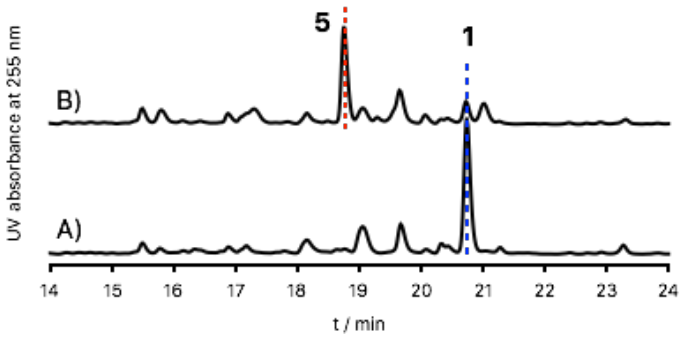

Figure 4-7. HPLC profiles of extracts from broth of *A*. *oryzae* transformants harboring (A) *adrF*, *E*, *J*, and *A*, and (B) *adrF*, *E*, *J*, *A*, *ctr-P450*, *PO*, and *GO* cultivated with andrastin E.

Compound **5** was a highly oxidized meroterpenoid with the same skeleton as that of andrastins. The structure of **5** verified the hypothesis that the *ctr* cluster is for biosynthesis of a natural product of andrastin A scaffold. This compound was isolated from a hybrid *Penicillium* strain[47], and has never been isolated from *Emericella* species.

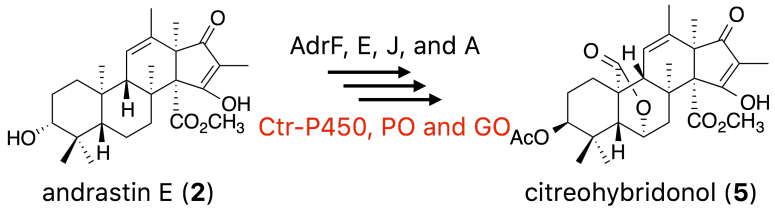

Figure 4-8. Citreohybridonol (**5**) was converted from andrastin E (**2**) by *A. oryzae* transformant harboring *adrF*, *E*, *J*, *A*, *ctr-P450*, *PO*, and *GO*.

Construction and Metabolites Identification of Six-Gene Co-Expression Transformants

Next, the functions of the three additional genes, *ctr-P450*, *PO*, and *GO*, was investigated to reveal how they involved in the reaction from **2** to **5**. *A. oryzae* co-expressing six genes, *adrF*, *E*, *J*, and *A* from the *adr* cluster, and combinations of two genes of *ctr-P450*, *PO*, and *GO*. Fungal transformation plamsids pBARI-CtrP450+PO, pBARI-CtrP450+GO and pBARI-PO+GO were yielded in the similar method as plasmid pBARI-CtrP450+PO+GO. *A. oryzae* transformants harboring six genes are constructed by introducing these three plasmids separately to *A. oryzae* harboring *adrF*, *E*, *J*, and *A*.

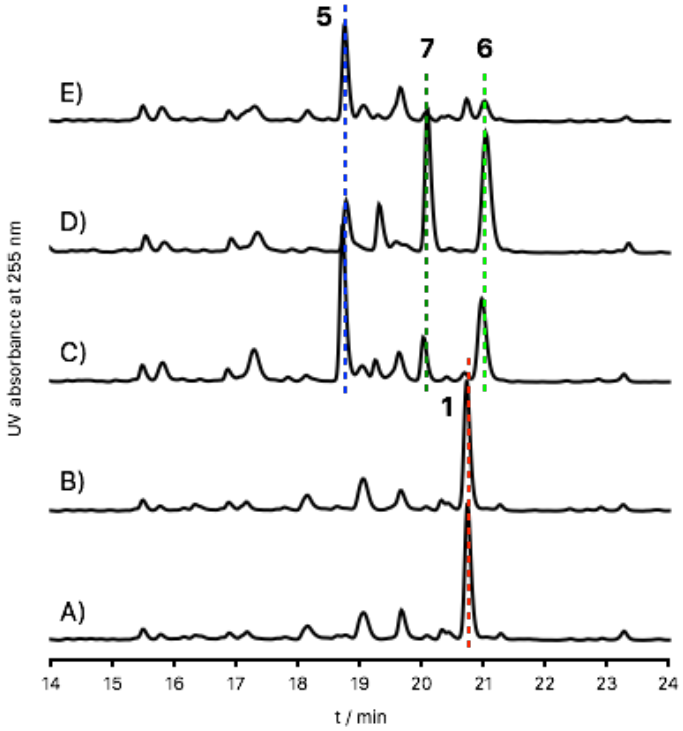

Figure 4-9. HPLC profiles of extracts from broth of *A. oryzae* transformants harboring (A) *adrF*, *E*, *J*, and *A*, (B) *adrF*, *E*, *J*, *A*, *PO*, and *GO*, (C) *adrF*, *E*, *J*, *A*, *ctr-P450*, and *PO*, (D) *adrF*, *E*, *J*, *A*, *ctr-P450*, and *PO*, (E) *adrF*, *E*, *J*, *A*, *ctr-P450*, *PO*, and *GO* cultivated with **2**

Three *A. oryzae* transformants harboring six genes were inoculated in medium containing **2**. The extracts from broth of these transformants were subjected to HPLC and LC-MS analysis. *A. oryzae* transformant harboring *adrF*, *E*, *J*, and *A* introduced empty vector and transformant harboring seven genes were used as negative control strain and positive control strain, respectively. Observed from the results of HPLC analysis, the profile of extract from broth of *A. oryzae* transformant harboring *adrF*, *E*, *J*, *A*, *PO*, and *GO* is similar to that of negative control, and **1** is the major product converted from **2** by these two strains [Figure 4-9 (A) and (B)]. On the other hand, **5** was detected from profiles of all the transformants harboring *ctr-P450*, which is similar with positive control [Figure 4-9 (C), (D), and (E)]. This indicated that CtrP-450 is the only enzyme of these three enzymes encoded in the *ctr* cluster oxidizing **2** to **5** coupled with AdrF, E, J and A. Proteins PO and GO are not concerned with the biosynthesis of **5**.

Two new peaks, **6** around 21 min and **7** around 20 min, were also detected in profiles of *A. oryzae* transformants harboring *ctr-P450*. These two compounds were isolated and structurally elucidated as 6α-hydroxyandrastin C (**6**) and deoxocitreohybridonol (**7**) [Figure 4-10]. Both compounds were identified as novel

compounds.

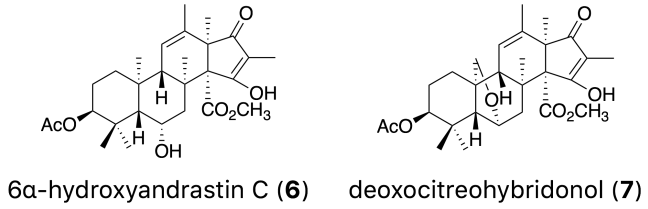

Figure 4-10. Structures of 6α-hydroxyandrastin C (**6**) and deoxocitreohybridonol (**7**), oxidized product from andrastin E.

Ctr-P450, the Cytochrome P450 Monooxygenase Responsible for Citreohybridonol Biosynthesis

To verify the hypothesis that only Ctr-P450 out of these three enzymes is active in citreohybridonol biosynthesis, *ctr-P450* was co-expressed with *adrF*, *E*, *J*, and *A* in *A. oryzae*. Fungal transformation plasmid pBARI-CtrP450 was constructed by subcloning full length gene *ctr-P450* to vector pBARI. This plasmid was introduced to *A. oryzae* transformant harboring *adrF*, *E*, *J*, and *A* to yield a five-gene co-expressing system. The five-gene co-expressing transformant was incubated in medium with **2**, and the extract from the broth was analyzed by HPLC and LC-MS.

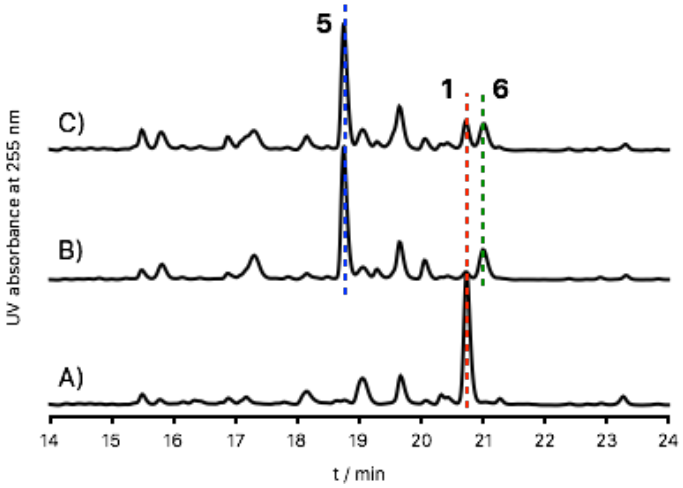

Figure 4-11. HPLC profiles of extracts from broth of *A. oryzae* transformants harboring (A) *adrF*, *E*, *J*, and *A* (negative control), (B) *adrF*, *E*, *J*, *A*, and *ctr-P450*, (C) *adrF*, *E*, *J*, *A*, *ctr-P450*, *PO*, and *GO* (positive control) cultivated with **2**.

As expected, the HPLC profile of *A. oryzae* transformant harboring *adrF*, *E*, *J*, *A*, and *ctr-P450* was almost the same as that of *A. oryzae* harboring all seven genes. The main product citreohybridonol (**5**) and small amount of **6** can be detected in both profiles at similar heights, respectively [Figure 4-11]. This strongly proved my hypothesis that only Ctr-P450 in three enzymes of Ctr-P450, PO, and GO is activated in the biosynthetic pathway of citreohybridonol.

Considering the structures of **5**, **6**, and **7**, it is indicated that the substrates of Ctr-P450 cannot be andrastin D, E, and F, because no oxidized intermediate of such substrates was isolated. Thus, it is suggested that andrastin C (**3**), is oxidized for several times to citreohybridonol (**5**), the final product of the *ctr* cluster, and that these reactions are catalyzed by two cytochrome P450s, AdrA and CtrP450 [Figure 4-12].

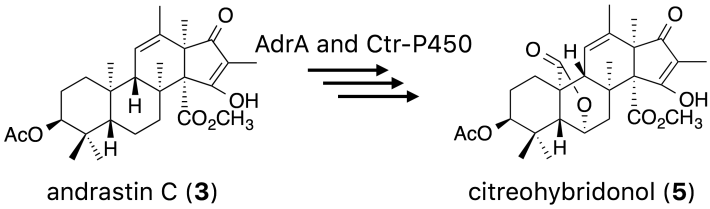

Figure 4-12. Citreohybridonol (**5**) was oxidized from andrastin C (**3**) by AdrA and Ctr-P450.

4.5. Details of Biosynthesis of Citreohybridonol

Andrastins feeding experiments were conducted in order to investigate the details of conversion from andrastin C (**3**) to citreohybridonol (**5**). Firstly, full length gene *adrA* from the *adr* cluster and *ctr-P450* from the *ctr* cluster were amplified and subcloned to vector pTAex3 to yield fungal transformation plasmids pTAex3-AdrA and pTAex3-CtrP450, respectively. Then, *A. oryzae* transformant harboring *ctr-P450* was constructed by introducing plasmid pTAex3-CtrP450 to *A. oryzae* NSAR1 strain. The same *A. oryzae* strain with empty vector pTAex3 was used as negative control. Purified andrastin C, B, and A were used respectively as the substrate in bio-conversion experiments utilizing *A. oryzae* transformants harboring *ctr-P450*. The extracts isolated from broth were subjected to HPLC and LC-MS analysis.

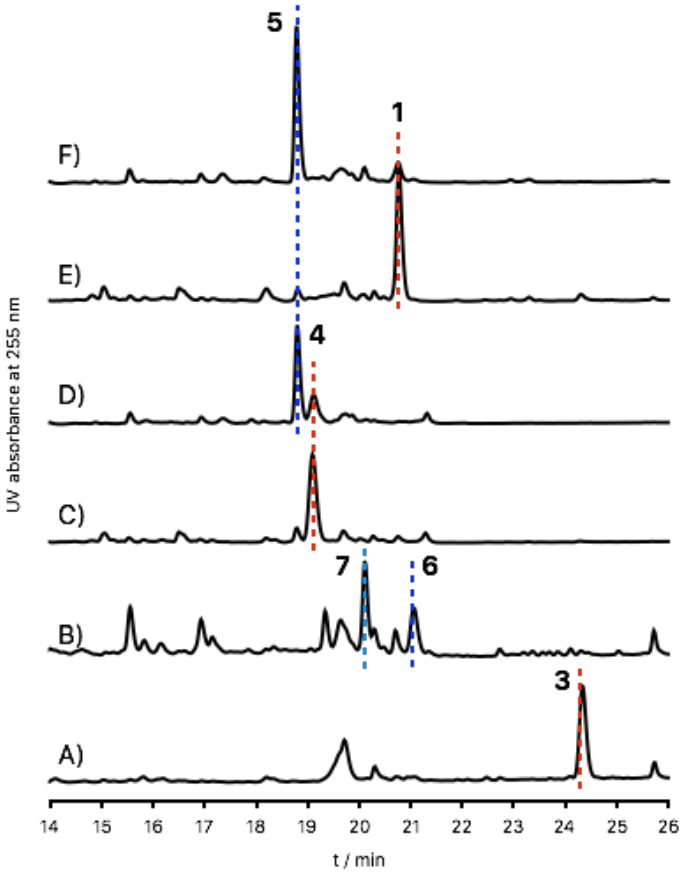

Figure 4-13. HPLC profiles of extracts from broth of *A. oryzae* transformants harboring (A) empty plasmid pTAex3 (negative control) cultivated with andrastin C (**3**), (B) *ctr-P450* cultivated with andrastin C (**3**), (C) empty plasmid pTAex3 (negative control) incubated with andrastin B (**4**), (D) *ctr-P450* cultivated with andrastin B (**4**), (E) empty plasmid pTAex3 (negative control) cultivated with andrastin A (**1**), (F) *ctr-P450* cultivated with andrastin A (**1**).

As the results of HPLC analysis, both andrastin B (**4**) and andrastin A (**1**) are oxidized to citreohybridonol (**5**) only by Ctr-P450, while andrastin C (**3**) was converted to **6** and **7**, instead of **5** [Figure 4-13]. As proved previously, andrastin C (**3**) is oxidized twice to **1** via **4** catalyzed by a single cytochrome P450 AdrA [Figure 4-3]. Similar with AdrA, Ctr-P450 is also considered to be a cytochrome P450 that can consecutively catalyze oxidation reactions for twice. The conversion of **3** to **7** is a good example [Figure 4-13 (A) and (B)]. Another bio-conversion experiment that cultivate *A. oryzae* transformant harboring *ctr-P450* with **6** was also performed, and it is proved that the oxidation reaction converting **6** to **7** is catalyzed by Ctr-P450 [Figure 4-14]. Firstly, Ctr-P450 catalyzes the reaction in which **3** was oxidized to **6**, then catalyzes the next reaction in which **6**, the oxidized product, is converted to **7**, the final product [Figure 4-15].

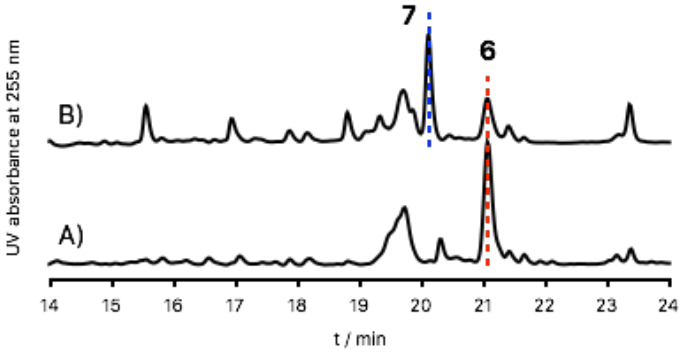

Figure 4-14. HPLC profiles of extracts from broth of *A. oryzae* transformants harboring (A) empty plasmid pTAex3 (negative control) cultivated with 6α-hydroxyandrastin C (**6**), and (B) *ctr-P450* cultivated with 6α-hydroxyandrastin C (**6**).

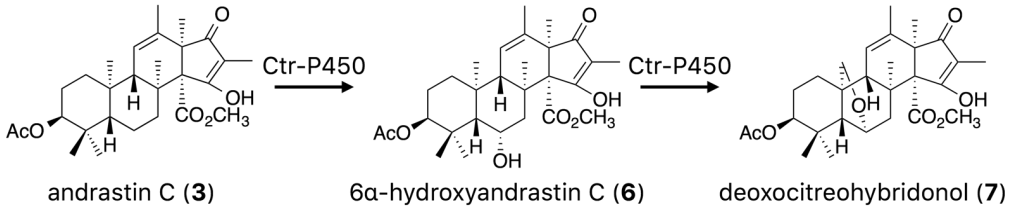

Figure 4-15. Andrastin C (**3**) was oxidized twice via **6** to **7** by the catalysis of Ctr-P450.

Similar two-step oxidation is proposed to be catalyzed by Ctr-P450 when substrate is andrastin B (**4**). It is difficult to hypothesize that **4** is directly oxidized to citreohybridonol (**5**), but **4** can be oxidized to andrastin A (**1**) by the catalysis of a cytochrome P450, AdrA, as proved previously[17]. Thus, it is suggested that **4** was firstly oxidized by CtrP450 to **1**, just like catalyzed by AdrA, then **1** was oxidized to **5** by the same enzyme [Figure 4-16], although **1** cannot be detected by HPLC or LC-MS analysis as the intermediate.

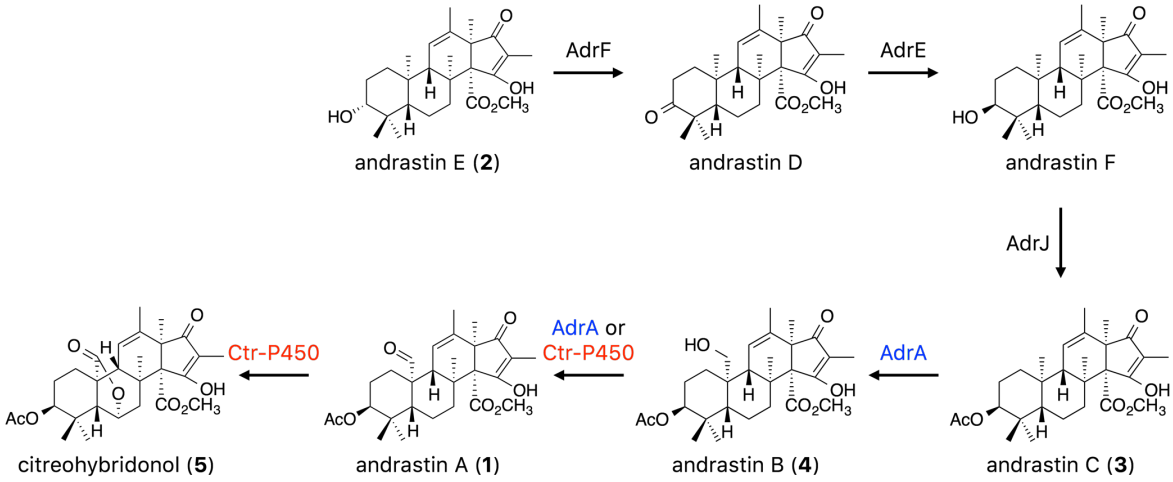

Figure 4-16. Biosynthesis of citreohybridonol (**5**) started from andrastin E (**2**).

4.6. Isolation and Identification of Products Derived by the *ctr* Cluster in the Shunt Pathway

The insight into citreohybridonol (**5**) biosynthesis from andrastin B (**4**) was provided by bio-conversion experiments utilizing **4** and andrastin A (**1**) as substrates. The biosynthetic pathway from andrastin E (**2**) to citreohybridonol (**5**), final product of the *ctr* cluster, was also proposed on the basis of the feeding experiments [Figure 4-16]. According to this scheme, andrastin C (**3**) was firstly oxidized by the catalysis of AdrA, then, the product was oxidized by the catalysis of Ctr-P450 to yield **5**.

However, 6α-hydroxyandrastin C (**6**) and deoxocitreohybridonol (**7**), which are directly oxidized products of **3** [Figure 4-15], can also be isolated from broth of *A. oryzae* transformants, which are able to convert **2** to **5** [Figure

4-9 (C) and (D)]. This indicated another possibility that there existed a different citreohybridonol biosynthetic pathway. In this pathway, andrastin C (**3**) was firstly oxidized by Ctr-P450 rather than AdrA, and then the products of the oxidation catalyzed by Ctr-P450, such as **6** and **7**, were further oxidized to **5** by the catalysis of AdrA [Figure 4-17].

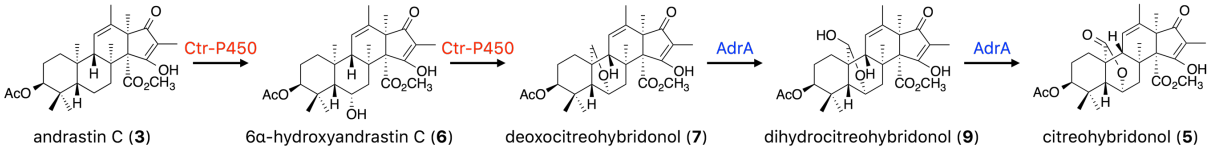

Figure 4-17. Another possibility: a putative alternative citreohybridonol (**5**) biosynthetic pathway.

In order to verify this hypothesis, *A. oryzae* transformant harboring *adrA* was constructed by introducing fungal transformation plasmid pTAex3-AdrA to *A. oryzae* NSAR1 strain. Utilizing the same method, cultivations of *A. oryzae* transformant harboring empty plasmid pTAex3 were negative control groups. Possible substrates of AdrA, andrastin C (**3**), 6α-hydroxyandrastin C (**6**), and deoxocitreohybridonol (**7**), were cultivated with *A. oryzae* transformant harboring *adrA*, and the extracts of their broth were subjected to the HPLC and LC-MS analysis.

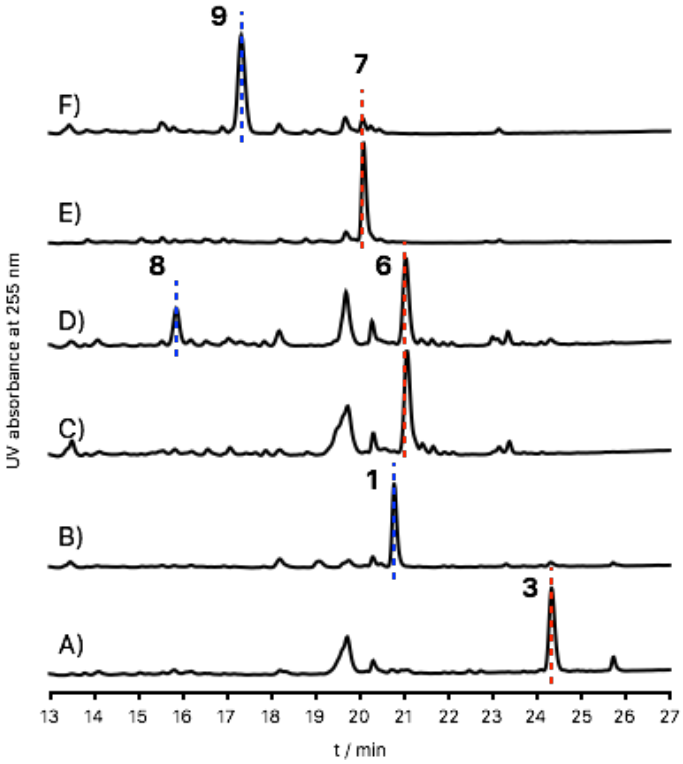

Figure 4-18. HPLC profiles of extracts from broth of *A. oryzae* transformants harboring (A) empty plasmid pTAex3 (negative control) cultivated with andrastin C (**3**), (B) *adrA* cultivated with andrastin C (**3**), (C) empty plasmid pTAex3 (negative control) incubated with 6α-hydroxyandrastin C (**6**), (D) *adrA* cultivated with 6α-hydroxyandrastin C (**6**), (E) empty plasmid pTAex3 (negative control) cultivated with deoxocitreohybridonol (**7**), (F) *ctr-P450* cultivated with deoxocitreohybridonol (**7**).

As expected, andrastin C (**3**) was converted to andrastin A (**1**) by catalysis of AdrA [Figure 4-18 (B)]. Two significant peaks, peak **8** around 16 min and peak **9** around 17 min detected in HPLC profiles of *A. oryzae* transformant harboring *adrA* were oxidized from 6α-hydroxyandrastin C (**6**) and deoxocitreohybridonol (**7**), respectively [Figure 4-18 (D) and (F)]. Structural investigation using LC-MS and NMR spectra of isolated **8** and **9** gave the structures of these two compounds [Figure 4-19]. The two compounds were identified as novel compounds.

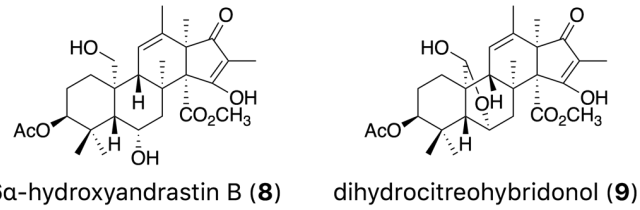

Figure 4-19. Structures of two novel meroterpenoids, 6α-hydroxyandrastin B (**8**) and dihydrocitreohybridonol (**9**).

At last, **8** and **9** were incubated with *A. oryzae* transformants harboring cytochrome P450 to verify if these compounds can be oxidized to citreohybridonol (**5**). Utilizing *A. oryzae* transformant harboring *adrA*, transformant harboring *ctr-P450* and transformant harboring empty vector pTAex3 as negative control, which are constructed previously, compounds feeding experiments were carried out. The extract isolate from each broth was subjected to a HPLC and LC-MS analysis. However, contrary to the hypothesis that there is another biosynthetic pathway of citreohybridonol (**5**), **8** and **9** cannot be further oxidized to **5** by the catalysis of CtrP450 or AdrA. Therefore, these compounds, 6α-hydroxyandrastin C (**6**), deoxocitreohybridonol (**7**), 6α-hydroxyandrastin B (**8**), and dihydrocitreohybridonol (**9**) were considered as shunt products of the *ctr* cluster [Figure 4-20].

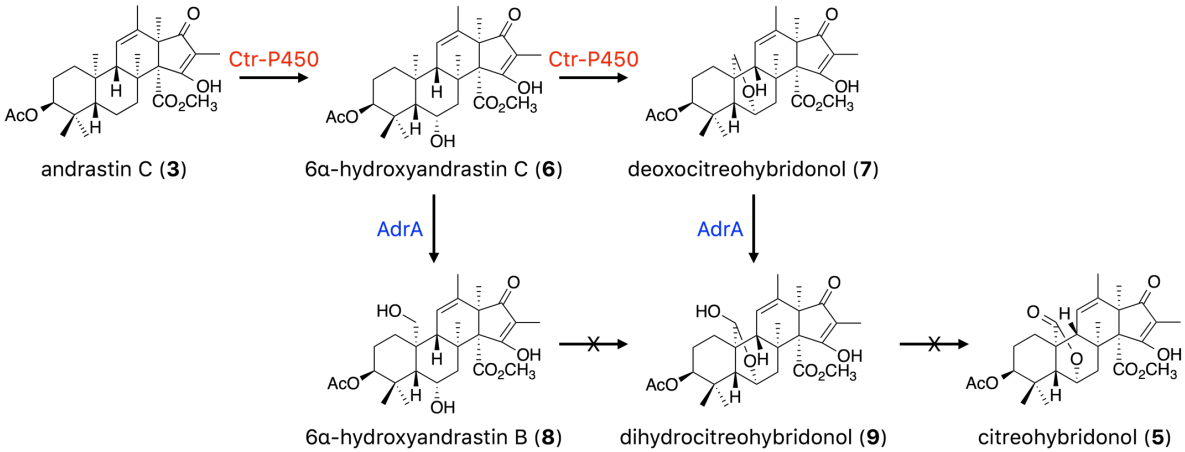

Figure 4-20. Shunt pathway started from andrastin C (**3**).

4.7. Discussion

Pathway Selection in the Conversion of Andrastin C

The most amazing point in this research is that different products can be isolated just because of the different orders of the catalysis of the same enzymes. As elucidated in this research, the common precursor, andrastin C (**3**), is converted to the major product, citreohybridonol (**5**), when it is firstly oxidized by the catalysis of AdrA, then oxidized by the catalysis of CtrP450. On the other hand, the same precursor **5**, would convert to the shunt products, 6α-hydroxyandrastin B (**8**) and dihydrocitreohybridonol (**9**), when the order of the catalysis is reversed [Figure 4-21]. In conclusion, the pathway is determined by the order of catalysis. It is because Ctr-P450 cannot catalyze the oxidation at C-23 on its substrates after C-6 is oxidized. I will give a detailed description about this later.

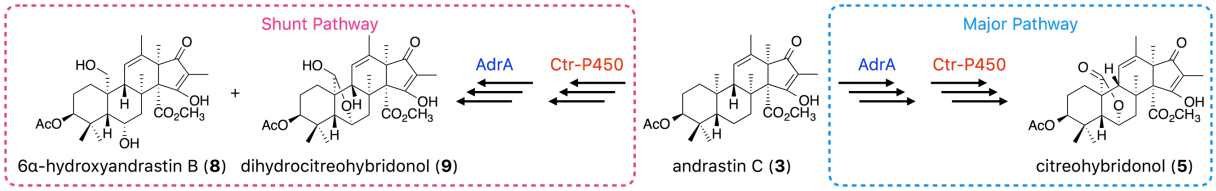

Figure 4-21. Two pathways shared same starting substrate, andrastin C (**3**).

Oxidation Sites on Substrates of AdrA and Ctr-P450

Both AdrA and Ctr-P450 are classified to be cytochrome P450 monooxygenases. AdrA catalyzes the reactions of oxidation from andrastin C (**3**) to andrastin A (**1**) [Figure 4-22]. The only oxidation site of AdrA is C-23 of its substrates, which is suggested by the reaction catalyzed by AdrA. The oxidation of 6α-hydroxyandrastin C

(**6**) to 6α-hydroxyandrastin B (**8**) and the oxidation of deoxocitreohybridonol (**7**) to dihydrocitreohybridonol (**9**) on the C-23 on the substrates are good evidences for my proposed behavior of AdrA.

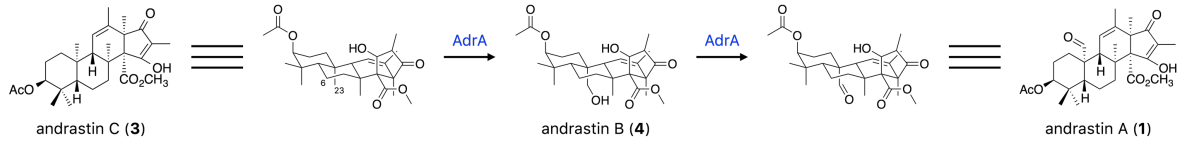

Figure 4-22. The oxidations from andrastin C (**3**) to andrastin A (**1**) catalyzed by AdrA. The oxidation site of AdrA is C-23 of substrates.

Different from AdrA, Ctr-P450 have two oxidation sites at C-6 and C-23 on its substrates. The oxidation reaction of andrastin C (**3**) to 6α-hydroxyandrastin C (**6**) have proved that C-6 is the oxidation site of Ctr-P450 [Figure 4-23 (A)], and the oxidation reaction of andrastin B (**4**) to citreohybridonol (**5**) indicated that C-23 is also one of the oxidation sites of Ctr-P450 [Figure 4-23 (B)].

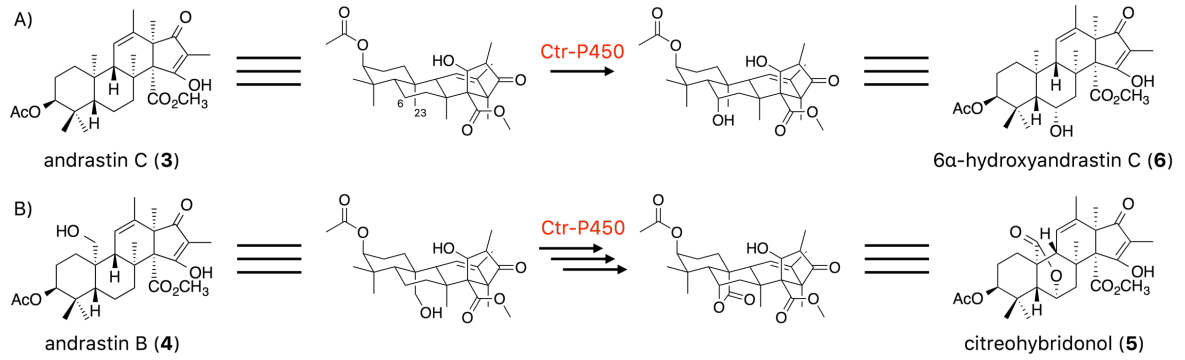

Figure 4-23. The oxidation reactions catalyzed by Ctr-P450. Ctr-P450 can oxidize (A) C-6 as well as (B) C-23 as its oxidation site.

C-22, 23, and 24 on andrastin C (**3**), which is a substrate of Ctr-P450 are in the same surface, which is observed in 3D configuration. The distance between all these three carbons and C-6 is predicted to be about 3.2 Å [Figure 4-24]. The other substrates of Ctr-P450 are similar with **3**. However, only C-23 and 6 can be the oxidation sites of Ctr-P450. The active site of Ctr-P450 should not be too far from C-6 and 23. Thus, this indicates that the active site of this cytochrome P450 is located between these two carbons. The oxidation reaction of **3** catalyzed by Ctr-P450 suggested that Ctr-P450 prefers to catalyze the hydroxylation of C-6 on **3**, although this enzyme can catalyze the oxidation on both C-6 and 23.

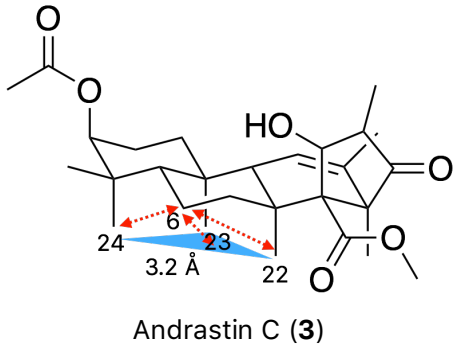

Figure 4-24. The configurations of C-22, 23, and 24 of andrastin C.

Substrate Specificity of Ctr-P450

From the in vivo assay of Ctr-P450, andrastin C (**3**), andrastin B (**4**), andrastin A (**1**), and 6α-hydroxyandrastin C (**6**) were considered as substrates of Ctr-P450 [Figure 4-25 (A)]. On the other hand, other analogues of these compound, 6α-hydroxyandrastin B (**8**) and dihydrocitreohybridonol (**9**), cannot be accepted by Ctr-P450 as substrates [Figure 4-25 (B)]. This indicates that Ctr-P450 can hardly accept substrates whose C-6 is oxidized.

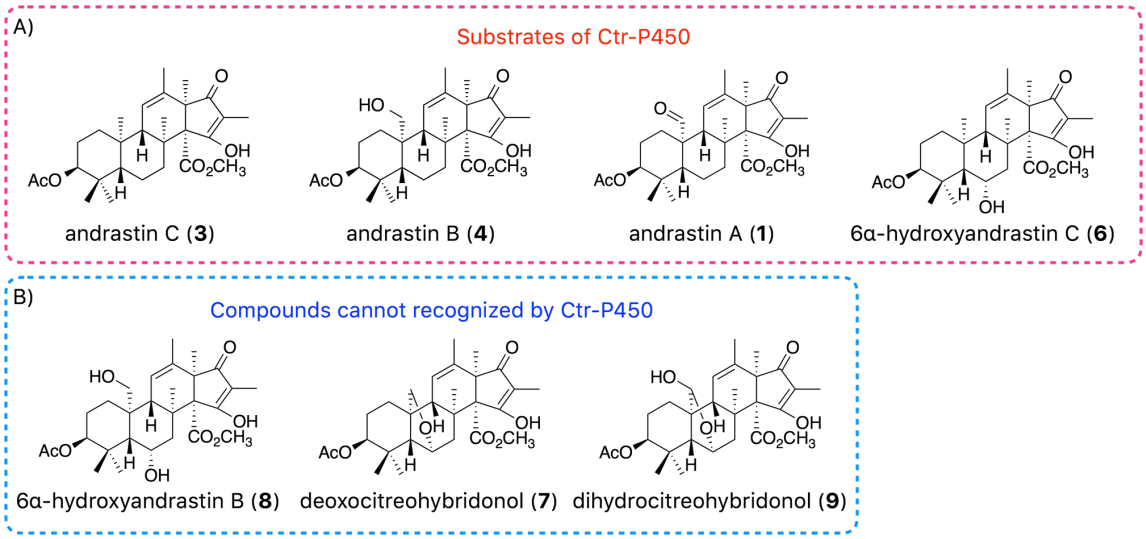

Figure 4-25. (A) The substrates of Ctr-P450. (B) Compounds cannot be accepted by Ctr-P450 as substrates.

The oxidation preference on andrastin C (3) and the substrate specificity of Ctr-P450 are considered as the main reason affect the pathway selection on **3**.

Proposed Biosynthetic Mechanism of Andrastin A (1) to Citreohybridonol (5)

After my detailed discussion on Ctr-P450, it is reveal that both C-6 and 23 on the substrates of Ctr-P450 can be oxidation sites of this P450, and Ctr-P450 hardly accept substrates whose C-6 is hydroxylated. If C-6 of andrastin A (**1**) is firstly hydroxylated, the second oxidation cannot occur catalyzed by Ctr-P450. On the basis of this, the detailed biosynthetic mechanism of citreohybridonol (**5**) can be proposed. The aldehyde group on C-23 of andrastin A (**1**) was firstly oxidized to carboxylic acid by the catalysis of Ctr-P450. Then the intermediate 1 was hydroxylated on C-6 to intermediate 2. Finally, **5** was produced from intermediate 2 in a spontaneous esterification reaction [Figure 4-26].

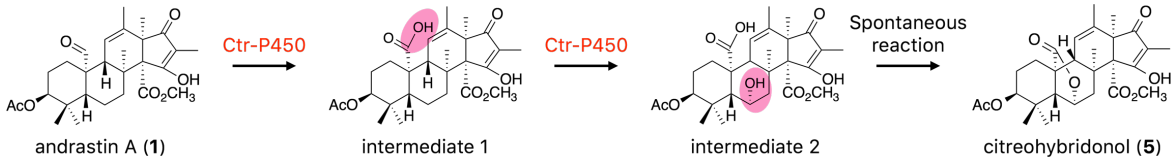

Figure 4-26. Proposed biosynthesis of citreohybridonol (**5**) from andrastin A (**1**).

In vivo Assays of tailoring enzymes, AdrF′, AdrE′, AdrJ′, and AdrA′

AdrF', AdrE', AdrJ', and AdrA' encoded in the *ctr* cluster are homologues of AdrF, AdrE, AdrJ, and AdrA encoded in the *adr* cluster. The similarity between tailoring enzymes of the *ctr* cluster and their homologues of the *adr* cluster is about 60% to 80%. The co-expression system in order to functionally investigate Ctr-P450 are expressing gene *adrF*, *E*, *J* and *A* in the *adr* cluster. The function of AdrF', E', J', and A' was still unknown.

Several combinations of these four genes, *adrF'*, *E'*, *J'*, and *A'* were expressed in *A. oryzae*. As the results (unpublished data), AdrF' and AdrJ' exhibited the same enzymatic activity with their homologues, AdrF and AdrJ in the *adr* cluster. However, AdrE' and AdrA' completely lost their enzymatic activities compared with AdrE and AdrA.

4.8. 4.8 Conclusion

In this research, a cryptic biosynthetic gene cluster, the *ctr* cluster, was discovered. The major product derived from this BGC was isolated and identified as citreohybridonol (**5**) [Figure 4-27], a meroterpenoid of andrastin A scaffold, as predicted previously.

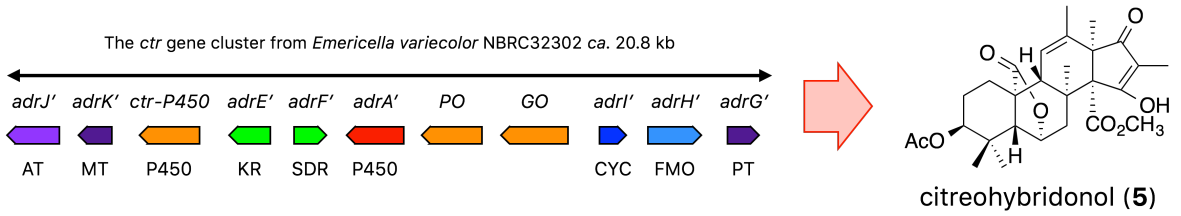

Figure 4-27. The *ctr* cluster, a BGC for biosynthesis of citreohybridonol.

The detailed biosynthetic pathway of citreohybridonol was investigated, and as the result, only Ctr-P450, a cytochrome P450 enzyme encoded in the *ctr* cluster, is responsible for the biosynthesis of this meroterpenoid.

Another four novel meroterpenoids, 6α-hydroxyandrastin C (**6**), deoxocitreohybridonol (**7**), 6α-hydroxyandrastin B (**8**), and dihydrocitreohybridonol (**9**), are also isolated and structurally elucidated as the shunt products of the *ctr* cluster [Figure 4-28].

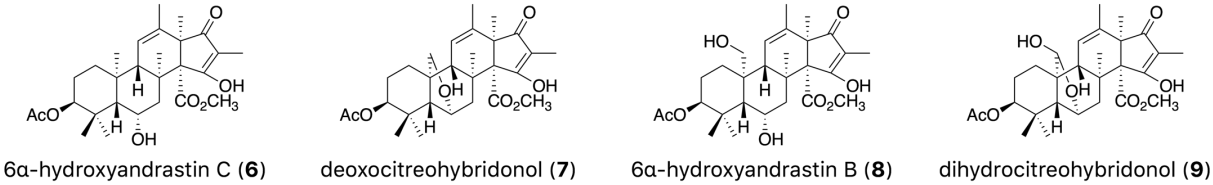

Figure 4-28. Structures of 6α-hydroxyandrastin C, 6α-hydroxyandrastin B, deoxocitreohybridonol, and dihydrocitreohybridonol.

[References]

1. Uchida, R.; Shiomi, K.; Inokoshi, J.; Tanaka, H.; Iwai, Y.; Ōmura, S., Andrastin D, novel protein farnesyltransferase inhibitor produced by *Penidllium* sp. FO-3929. *The Journal of Antibiotics* **1996,** *49* (12), 1278-1280.

2. Fernández-Bodega, M. A.; Mauriz, E.; Gómez, A.; Martín, J. F., Proteolytic activity, mycotoxins and andrastin A in *Penicillium roqueforti* strains isolated from Cabrales, Valdeón and Bejes–Tresviso local varieties of blue-veined cheeses. *International Journal of Food Microbiology* **2009,** *136* (1), 18-25.

3. Rho, M.-C.; Toyoshima, M.; Hayashi, M.; Uchida, R.; Shiomi, K.; Komiyama, K.; Ōmura, S., Enhancement of drug accumulation by andrastin A produced by *Penicillium* sp. FO-3929 in vincristine-resistant KB cells. *The Journal of Antibiotics* **1998,** *51* (1), 68-72.

4. Matsuda, Y.; Awakawa, T.; Abe, I., Reconstituted biosynthesis of fungal meroterpenoid andrastin A. *Tetrahedron* **2013,** *69* (38), 8199-8204.

5. Malmstrøm, J.; Christophersen, C.; Barrero, A. F.; Oltra, J. E.; Justicia, J.; Rosales, A., Bioactive metabolites from a marine-derived strain of the fungus *Emericella variecolor*. *Journal of Natural Products* **2002,** *65* (3), 364-367.

6. Bringmann, G.; Lang, G.; Steffens, S.; Günther, E.; Schaumann, K., Evariquinone, isoemericellin, and stromemycin from a sponge derived strain of the fungus *Emericella variecolor*. *Phytochemistry* **2003,** *63* (4), 437-443.

7. Wei, H.; Itoh, T.; Kinoshita, M.; Nakai, Y.; Kurotaki, M.; Kobayashi, M., Cytotoxic sesterterpenes, 6-epi-ophiobolin G and 6-epi-ophiobolin N, from marine derived fungus *Emericella variecolor* GF10. *Tetrahedron* **2004,** *60* (28), 6015-6019.

8. Wei, H.; Itoh, T.; Kinoshita, M.; Kotoku, N.; Aoki, S.; Kobayashi, M., Shimalactone A, a novel polyketide, from marine-derived fungus *Emericella variecolor* GF10. *Tetrahedron* **2005,** *61* (33), 8054-8058.

9. Matsuda, Y.; Wakimoto, T.; Mori, T.; Awakawa, T.; Abe, I., Complete biosynthetic pathway of anditomin: nature's sophisticated synthetic route to a complex fungal meroterpenoid. *Journal of the American Chemical Society* **2014,** *136* (43), 15326-15336.

10. Matsuda, Y.; Awakawa, T.; Itoh, T.; Wakimoto, T.; Kushiro, T.; Fujii, I.; Ebizuka, Y.; Abe, I., Terretonin biosynthesis requires methylation as essential step for cyclization. *ChemBioChem* **2012,** *13* (12), 1738-1741.

11. Kosemura, S.; Miyata, H.; Matsunaga, K.; Yamamura, S., Biosynthesis of citreohybridones, the metabolites of a hybrid strain KO 0031 derived from *Penicillium citreo-viride* B. IFO 6200 and 4692. *Tetrahedron Letters* **1992,** *33* (27), 3883-3886.

12. Kosemura, S.; Matsunaga, K.; Yamamura, S.; Kubota, M.; Ohba, S., The structures of citreohybridone A and B novel sesterterpenoid-type metabolites of a hybrid strain KO 0031 derived from *Penicillium citreo-viride* B. IFO 6200 and

4692. *Tetrahedron Letters* **1991,** *32* (29), 3543-3546.

13. Kosemura, S.; Yamamura, S., Isolation and biosynthetic pathway for citreohybridones from the hybrid strain KO 0031 derived from *Penicillium* species. *Tetrahedron Letters* **1997,** *38* (35), 6221-6224.

14. Kosemura, S., Structure and absolute configuration of citreohybridones isolated from *Penicillium* species. *Tetrahedron Letters* **2002,** *43* (7), 1253-1256.

15. Kosemura, S.; Matsunaga, K.; Yamamura, S., Citreohybriddiones A and B and related terpenoids, new metabolites of a hybrid strain KO 0031 derived from *Penicillium citreo-viride* B. IFO 6200 and 4692. *Chemistry Letters* **1991,** *20* (10), 1811-1814.

16. Kosemura, S., Meroterpenoids from *Penicillium* citreo-viride B. IFO 4692 and 6200 hybrid. *Tetrahedron* **2003,** *59* (27), 5055-5072.

17. Kosemura, S.; Matsuo, S.; Yamamura, S., Citreohybriddione C, a meroterpenoid of a hybrid strain KO 0031 derived from *Penicillium* citreo-viride B. IFO 6200 and 4692. *Phytochemistry* **1996,** *43* (6), 1231-1234.

18. Wang Filho, X.; JGS, H. A. R.; King, J. B.; Ellis, T. K.; Powell, D. R.; Cichewicz, R. H., Chemical epigenetics alters the secondary metabolite composition of guttate excreted by an atlantic-florest-soil-derived *Penicillium citreonigrum*. *Journal of Natural Products* **2010,** *73*, 942-948.

19. Dalsgaard, P. W.; Petersen, B. O.; Duus, J. Ø.; Zidorn, C.; Frisvad, J. C.; Christophersen, C.; Larsen, T. O., Atlantinone A, a meroterpenoid produced by *Penicillium ribeum* and several cheese associated *Penicillium* species. *Metabolites* **2012,** *2* (1), 214-220.

5. Summary and Prospect

Development of Genome Mining

Genome mining approach was proved to be a powerful tool in both biosynthetic research on known natural products (the project of ascochlorin described in chapter 3) and novel natural products discovery (the project of citreohybridonol described in chapter 4). Established at the beginning of 21st century, developed for over ten years, the methodology of genome mining has become a very common approach for natural products chemists.

Nowadays, it is possible to perform a biosynthetic gene cluster exploring using computer instead of human[56]. Furthermore, machine learning technology was also applied in genome mining to establish a smarter platform to search for BGC in bacteria, and to predict novel compounds[57]. It is believed that this platform will expand from bacteria to all microbes including fungi in near future.

Therefore, bottleneck of natural products research will be the isolation, identification, and bioactive assay of rare naturally occurring compounds. Fermentation of BGC heterologous expressing system to obtain natural products was proved to be one of the solutions against the small amount of these molecules.

Disadvantages of *A. oryzae* Heterologous Expression System

The fungal heterologous expression method was proved to be a useful approach to investigate natural products biosynthesis *in vivo*, as well as *E. coli* heterologous expression system for enzymatic research *in vitro* and gene disruption in wild type fungus. The advantages of *A. oryzae* heterologous expression system were already elaborated in chapter 2. During my research on fungal metabolites utilizing the *A. oryzae* as host organism, some disadvantages were also realized.

The first problem in *A. oryzae* heterologous expression is splicing. As far as I know, some genes cannot be correctly spliced to mature mRNAs due to the intron recognizing mistakes. In some cases (*ascB*, *ascD* in the *asc* cluster), heterologous expressing of a cDNAs reversely transcribed from mRNAs instead of full length genes will improve their expression.

The reducing and losing of enzymatic activity when enzymes are heterologous expressed in *A. oryzae* is also a big problem. In my research of ascochlorin biosynthesis, it is notable that the activities of both AscD and AscG are significantly reduced, while both enzymes in wild type *Fusarium* are very efficient judged by the secondary metabolites production. I have no idea how to solve this problem to date.

The last problem is the accumulation in mycelia. In my investigation of ascochlorin biosynthesis, specific products of heterologous expressed genes were observed only accumulated in mycelia of *A. oryzae*, while they are distributed in both medium and mycelia of wild type *Fusarium*. The reason was predicted as lack of specific transporter for metabolite produced by heterologous expressed genes in *A. oryzae*. It is expected that if a proper transporter was co-expressed with the biosynthetic genes, the production would be improved.

[References]

56. Weber, T.; Blin, K.; Duddela, S.; Krug, D.; Kim, H. U.; Bruccoleri, R.; Lee, S. Y.; Fischbach, M. A.; Müller, R.; Wohlleben, W., antiSMASH 3.0—a comprehensive resource for the genome mining of biosynthetic gene clusters. *Nucleic Acids Research* **2015,** *43* (W1), W237-W243.

57. Skinnider, M. A.; Dejong, C. A.; Rees, P. N.; Johnston, C. W.; Li, H.; Webster, A. L.; Wyatt, M. A.; Magarvey, N. A., Genomes to natural products prediction informatics for secondary metabolomes (PRISM). *Nucleic Acids Research* **2015,** *43* (20), 9645-9662.

6. Experiments

6.1. General

Experimental Equipments

The experimental equipments were purchased as following:
Pipetter: Pipetman (Gilson)
Water deionizer: Milli-Q Integral 5 (Millipore)
Autoclave apparatus: BS-325, KS243 (TOMY)
Shaker: innova4230 (New Brunswick Scientific), NR-20, Bio-Shaker BR-42FL, Double Shaker NR-30 (TAITEC), Orbital Shaking Incubator Model: OSI-502LD (FIRSTEK)
Rotary Evaporator: Rotary Evaporator N-1000 (EYELA)
Centrifugal Evaporator: Centrifugal Evaporator CVE-3100 (EYELA)
Freeze-drier: FDU-2200 (EYELA)
Scales: BP3100S (Sartorius), PJ400, PG203 (METTLE TOLEDO)
Spectrophotometer: GeneSpec III (Hitachi)
Refrigerator: Medicool (SANYO)
Freezer: Deep Freezer MDF-292, Medical Freezer (SANYO), ULT-2586-35D (REVCO)
Thermostat bath: SM-05, SD Thermo Minder, Personal-11, EX Thermo Minder (TAITEC)
Incubator: M-203F (TAITEC), CI-610 (ADVANTEC)
Clean bench: CCV (Hitachi)
pH meter: SevenEasy pH Meter S20, InLab Routine Pro (METTLER TOLEDO)
Vortex: Vortex Genie2 (Scientific Industries Inc.)
Cooled centrifuges: MX-300, MX-305 (TOMY)
Centrifuges: Kubota 6900, Kubota 6800 (Kubota), M201-IVD (SAKUMA)
Agarose gel electrophoresis tank: Mupid-2plus (ADVANCE)
Gel scanner: AE-6905H Image Saver HR (ATTO)
PCR Thermal Cyclers: PTC-100, PTC-200 (MJ Research Inc.), TaKaRa PCR Thermal Cycler Dice Gradient (TaKaRa)
LC/MS: micro TOF mass spectrometer (Bruker Daltonics) with a Shimadzu Prominence system HPLC (Shimadzu)
HPLC: LC-20AD, DGU-20A3, CTO-20A, SPD-M20A (SHIMADZU)
HR-MS: JMS-SX-102A (JEOL)
NMR: JNM-A 500, JNM-ECA 500 (JEOL)
NMR Data Analysis Software: Delta 5.0.3 (JEOL)

Biochemical Materials

The biochemical materials were purchased as following:
Restriction enzymes: TaKaRa
Dephosphorylation enzyme: Bacteria Alkaline Phosphatase (life technologies)
DNA polymerase: iProof High Fidelity DNA Polymerase (BIO-RAD), PrimeStar HS DNA polymerase (TaKaRa), KAPA Taq DNA Polymerase (KAPA Biosystems), KOD FX Neo DNA polymerase (TOYOBO)
DNA ligation: DNA ligation kit Ver.2.1 (TaKaRa), In-fusion HD cloning kit (TaKaRa)
Plasmid DNA preparation from E. coli: Wizard Plus Minipreps (Promega)
DNA purification: Wizard SV Gel and Clean-Up system (Promega)

Medium for *E. coli*:
Luria-Bertani (LB) medium: LB medium (miller), granulated (Cica-Reagent), 2.5%
Luria-Bertani (LB) agar plate: LB-agar miller (Formedium), 4%
All medium was autoclaved at 394 K for 20 min before use.

Medium for fungi:

DPY: dextrin 2%, hi-polypepton 1%, yeast ext. 0.5%, $MgSO_4/7H_2O$ 0.05%, KH_2PO_4 0.5%
Czapek-Dox Broth without KCl: glucose 2%, $NaNO_3$ 0.3%, KH_2PO_4 0.1%, $MgSO_4/7H_2O$ 0.05%, $FeSO_4/7H_2O$ 0.002%, pH=5.5
Czapek-Dox Broth without KCl plus KF: glucose 2%, $NaNO_3$ 0.3%, KF 0.2%, KH_2PO_4 0.1%, $MgSO_4/7H_2O$ 0.05%, $FeSO_4/7H_2O$ 0.002%, pH=5.5
Czapek-Dox Broth: glucose 2%, $NaNO_3$ 0.3%, KCl 0.2%, KH_2PO_4 0.1%, $MgSO_4/7H_2O$ 0.05%, $FeSO_4/7H_2O$ 0.002%, pH=5.5
Czapek-Dox Broth without KCl plus KBr: glucose 2%, $NaNO_3$ 0.3%, KCl 0.2%, KH_2PO_4 0.1%, $MgSO_4/7H_2O$ 0.05%, $FeSO_4/7H_2O$ 0.002%, pH=5.5
Czapek-Dox Broth without KCl plus KI: glucose 2%, $NaNO_3$ 0.3%, KI 0.2%, KH_2PO_4 0.1%, $MgSO_4/7H_2O$ 0.05%, $FeSO_4/7H_2O$ 0.002%, pH=5.5
CD-starch: $NaNO_3$ 0.3%, KCl 0.2%, hi-polypepton 1%, $MgSO_4/7H_2O$ 0.05%, KH_2PO_4 0.1%, $FeSO_4/7H_2O$ 0.002%, starch 2%, pH=5.5
CD-starch with 5% KCl: $NaNO_3$ 0.3%, KCl 5%, hi-polypepton 1%, $MgSO_4/7H_2O$ 0.05%, KH_2PO_4 0.1%, $FeSO_4/7H_2O$ 0.002%, starch 2%, pH=5.5
CD-starch with 5% KBr: $NaNO_3$ 0.3%, KBr 5%, hi-polypepton 1%, $MgSO_4/7H_2O$ 0.05%, KH_2PO_4 0.1%, $FeSO_4/7H_2O$ 0.002%, starch 2%, pH=5.5
M agar plate: NH_4Cl 0.2%, $(NH_4)_2SO_4$ 0.1%, KCl 0.05%, NaCl 0.05%, KH_2PO_4 0.1%, $MgSO_4/7H_2O$ 0.05%, $FeSO_4/7H_2O$ 0.002%, glucose 2%, agar 1.5%, pH=5.5
M-sorbitol agar plate: NH_4Cl 0.2%, $(NH_4)_2SO_4$ 0.1%, KCl 0.05%, NaCl 0.05%, KH_2PO4 0.1%, $MgSO_4/7H_2O$ 0.05%, $FeSO_4/7H2O$ 0.002%, glucose 2%, sorbitol 1.2 M, agar 1.5%, pH=5.5
PDA: Potato Dextrose Agar (Nissui), 3.9%
All medium was autoclaved at 394 K for 20 min before use.

Reagents for Fungal Transformation:
TF solution 0: Maleic acid 50 mM, pH=7.5
TF solution 1: Yatalase 0.1 g (1%), $(NH_4)_2SO_4$ 0.79 g (0.6M), TF solution 0 10 mL
TF solution 2: Sorbitol 1.2 M, $CaCl_2 \cdot H_2O$ 50 mM, NaCl 35 mM, Tris-HCl (pH 7.5) 10 mM
TF solution 3: PEG4000 60%, $CaCl_2 \cdot H_2O$ 50 mM, Tris-HCl (pH 7.5) 10mM
All solutions were autoclaved at 394 K for 20 min before use.

Escherichia coli Strain

Escherichia coli DH5α strain was purchased from Clontech (Mountain View, CA).
DH5α: hsrdR17($r^- m^+$), F^-. recA1, endA1, gyrA96, thi-1, supE44, relA1, $mcrA^-$, $mcrB^+$, λ^-, Δ(argF - laczya) U169, ϕ80dlacZΔM15

Aspergillus oryzae Strain

Aspergillus oryzae NSAR1 strain was kindly provided by Prof. K. Gomi (Graduate School of Agricultural Sciences, Tohoku University) and Prof. K. Kitamoto (Graduate School of Agricultural Sciences, The University of Tokyo).
NSAR1: $niaD^-$, sC^-, ΔargB, $adeA^-$

Fungal Transformation of *Aspergillus oryzae* NSAR1 (PEG-protoplast method)

A. oryzae NSAR1 strain was cultivated in DPY medium (5 mL) at 303 K for 3 days, then the broth suspension was inoculated into DPY medium (100 mL) at 303 K for 1 days. Mycelia were collected by filtration.

Protoplasting was performed using Yatalase (10 mg/mL) in TF solution 0 at 303 K for 3 h. Protoplasts were centrifuged at 1,500 rpm for 10 min and washed with TF solution 2 (15 mL). Then, protoplasts were diluted to 6.5 x 105 cells/mL in TF solution 2. Appropriate plasmid (10 μg, < 20 μL) was added to the protoplast solution (200 μL). The aliquot was incubated for 30 min and then TF Solution 3 was added in 250 μL, 250 μL, and 850 μL aliquots subsequently. After 20 minutes incubation, TF Solution 2 (5 mL) was added to the mixtures and the

mixture was centrifuged at 1,500 rpm for 10 min. The supernatant was removed, and the pellet was suspended with TF solution 2 (500 μL).

The transformation mixture was poured onto the M-sorbitol agar plate with appropriate nutrients and then overlaid with the soft-top M-sorbitol agar (0.8% agar w/v). The agar plates were incubated at 303 K for 3-10 days. All the operations were performed at room temperature.

Colony PCR

Fungal colony PCR was performed with KOD FX Neo DNA polymerase. Samples were denatured at 369 K for 10 min before PCR. Reaction for each sample was performed in 5 μL scale.

Bacteria colony PCR was performed with KAPATaq DNA Polymerase. Reaction for each sample was performed in 5 μL scale.

All the operations and reactions were following manual.

NMR

chloroform-d reference:
^{1}H: 7.26 ppm, ^{13}C: 77.0 ppm
methanol-d4 reference:
^{1}H: 4.84 ppm (H_2O), ^{13}C: 49.0 ppm

6.2. Experiments of Biosynthesis Research of Fungal Meroterpenoid Ascochlorin

Incubation of Wild Type *Fusarium* sp. NBRC100844

Wild type *Fusarium* sp. NBRC100844 strain, the reported ascochlorin producing strain, was purchases from Biological Resource Center, National Institute of Technology and Evaluation (Chiba, Japan).

This fungus was cultivated in DPY medium (10 mL) at 298 K, 200 rpm, for 3 days, then the broth suspension was inoculated into DPY medium (100 mL) at 298 K, 160 rpm, for 3 days for pre-incubation. After pre-incubation, the broth suspension was inoculated into Czapek-Dox (CD) broth (6 L) in 298 K, 160 rpm, for 3 days, followed by an incubation at 303 K, 160 rpm, for 5 days. The broth and mycelia were collected for metabolites isolation and purification.

CD broth can be changed to CD broth without KCl, CD broth without KCl plus KF, CD broth without KCl plus KBr, and CD broth without KCl plus KI in order to obtain different metabolites.

Isolation of Metabolites from *Fusarium* sp. NBRC100844

Fusarium sp. was cultured at 303 K, 160 rpm, for 7 days in DPY medium (1 L in 2 L flask). After filtering, the mycelia were lyophilized to dryness. Dried mycelia were extracted by acetone. The extraction solution was concentrated *in vacuo* to remove the solvent. The extract (146 mg) was subjected to silica-gel column chromatography and eluted stepwise using a hexane/acetone gradient (100:0 to 70:30). Fractions containing **6**, **7**, **9**, and **1** were further purified by reverse-phase preparative HPLC equipped with an Ultimate AQ-C18 column (Welch Inc., Ellicott, MO, USA, 5 μm, 10 mm i.d. x 250 mm) using acetonitrile/water (70:30) as the eluting solvent (flow rate 3.0 mL/min) to yield **6** (2.1 mg), **7** (3.8 mg), **9** (10.1 mg) and **1** (24.9 mg).

For, **12** and **13**, *Fusarium* sp. was cultured at 303 K, 160 rpm, for 7 days in CD broth without KCl plus KBr (2 L in two 2 L flasks). After filtering, the mycelia were lyophilized to dryness. Dried mycelia were extracted by acetone. The extraction solution was concentrated *in vacuo* to remove the solvent. The extract (720 mg) was subjected to silica-gel column chromatography and eluted stepwise using a hexane/acetone gradient (95:5 to 70:30). Fractions that contained **12** and **13** were further purified by reverse-phase preparative HPLC using acetonitrile/water (70:30) as the eluting solvent (flow rate 3.0 mL/min) to yield **12** (7.0 mg), **13** (35 mg).

Isolation of Genomic DNA of *Fusarium* sp. NBRC100844

Wild type *Fusarium* sp. NBRC100844 strain, the reported ascochlorin producing strain, was purchases from NITE (Japan). This fungus was cultivated in DPY medium (10 mL) at 298 K, 200 rpm, for 3 days, then the broth suspension was inoculated into DPY medium (100 mL) at 298 K, 160 rpm, for 3 days. The mycelia were collected for genomic DNA isolation and purification.

Genomic DNA isolation and purification was performed with NucleoSpin® Plant II Maxi. NucleoSpin® Plant II Maxi genomic DNA isolation and purification kit was purchased from TaKaRa.

Genomic DNA of *Fusarium* sp. NBRC100844 was used as the source for the cloning of each gene in the ascochlorin biosynthetic gene cluster (*asc* cluster) except *ascB* and *ascD*.

All the operations and reactions were following the manual.

Analysis of Genomic DNA of *Fusarium* sp. NBRC100844

Draft genome sequencing analysis of genomic DNA isolated from *Fusarium* sp. NBRC100844 was purchased from Macrogen Crop. Japan (Japan). As the result of analysis, 94.7% of total nucleotides was read.

Annotation of genomic DNA of *Fusarium* sp. NBRC100844 was performed by Augustus.

Isolation and Reverse-Transcription of mRNA form *Fusarium* sp. NBRC100844

This fungus was cultivated in DPY medium (10 mL in 50 mL falcon) at 298 K, 200 rpm, for 3 days, then the broth suspension was inoculated into DPY medium (100 mL in 500 mL flask) at 303 K, 160 rpm, for 3 days. After filtering, the mycelia were lyophilized to dryness. The mycelia were prepared for mRNA isolation.

RNA isolation reagent ISOGEN was purchased from Nippon Gene Co., Ltd. (Japan). RT-PCR kit SuperScript® III First-Strand Synthesis Synstem was purchased from Life Technologies Japan Ltd. (Tokyo, Japan).

cDNA of *Fusarium* sp. NBRC100844 was used as the source for the cloning of *ascB* and *ascD* in the

ascochlorin biosynthetic gene cluster (the *asc* cluster).

All the operations and reactions were following the manuals.

Detailed Information of Primers Used in This Research

Primers are ordered from eurofins genomics Inc..

Primer	Sequence (5' to 3')
SmaI-ascA-Fw	TCGAGCTCGGTACCCATGGGTGCCACAACGAG
SmaI-ascA-Rv	CTACTACAGATCCCCTTATTTCCCTCGGTGAGCATTC
ascA-Mid-Fw	GCAAACAGGCTTCTGTTG
ascA-Mid-Rv	CAGAAGCCTGTTTGCCGAC
pAdeA-SpeI-Fw	TAGAGGATCTACTAGCGATATCATGGTGTTTTGATC
pAdeA-SpeI-Rv	AATCCATATGACTAGCTTTCCTATAATAGACTAGCGTG
SmaI-ascB-Fw	TCGAGCTCGGTACCCATGGGTTCTGCCATGG
SmaI-ascB-Rv	CTACTACAGATCCCCCTACTTCTTCAGGTATCCAATC
SmaI-ascC-Fw	TCGAGCTCGGTACCCATGGCCCCCAAACGC
SmaI-ascC-Rv	CTACTACAGATCCCCCTATGCGAATAGTGCGGGAG
pTA_Prm_Fw1	GCTCGCGAGCGCGTTCCACTGCATCATCAGTCTAG
pTA_Tmn_Rv1	AACGCGCTCGCGAGCAAGTACCATACAGTACCGCG
KpnI-ascE-Fw	CTGAATTCGAGCTCGGTACCATGAGTTGCGAAATTCCTC
KpnI-ascE-Rv	ACTACAGATCCCCGGGTACCCTAAGAGAAAATCTCGCTGGC
KpnI-ascF-Fw	CTGAATTCGAGCTCGGTACCATGGCATTCAACGAC
KpnI-ascF-Rv	ACTACAGATCCCCGGGTACCTTAAAGCTCCTTTCCTTC
pUSA-Prm-Fw1	GCTCGCGAGCGCGTTCGATATCATGGTGTTTTGATC
pUSA-Tmn-Rv1	AACGCGCTCGCGAGCCTTTCCTATAATAGACTAGCGTG
SmaI-ascG-Fw	TCGAGCTCGGTACCCATGGATAACCTATCGTCACTCG
SmaI-ascG-Rv	CTACTACAGATCCCCTTACATCTTTCTACGCTTAAACTCAAG
pPTRI-HIndIII-Fw	TGATTACGCCAAGCTCGATATCATGGTGTTTTGATC
pPTRI-HindIII-Rv	GCAGGCATGCAAGCTCTTTCCTATAATAGACTAGCGTG
KpnI-ascD-Fw	CTGAATTCGAGCTCGGTACCATGGCTGCCCAAATTC
KpnI-ascD-Rv	ACTACAGATCCCCGGGTACCTTAAGCCGAGACGTCAAC
ascF-M1-Fw	GACGGCTCATTATAGCGCGGCGTCGTGGTGGATGGGC
ascF-M1-Rv	GCTATAATGAGCCGTCGCGC
ascF-M2-Fw	CATTATAGCTGGGCGTCGGCGGCGATGGGCAACGGC
ascF-M2-Rv	CGACGCCCAGCTATAATGAG
ascF-M3-Fw	GAACATCAGCTACGGAGCGGCTGCGTATACCTGGCCCGAG
ascF-M3-Rv	TCCGTAGCTGATGTTCAGGC
ascF-M4-Fw	GCCGGCAATCTTCCTTGCGGGAATCACCACCGTC
ascF-M4-Rv	AAGGAAGATTGCCGGCTC

Plasmids Construction and PCR conditions

Restriction enzymes were purchased from TaKaRa (Japan). Fungal transformation vectors were kindly provided by Prof. K. Gomi (Graduate School of Agricultural Sciences, Tohoku University) and Prof. K. Kitamoto (Graduate School of Agricultural Sciences, The University of Tokyo). iProof DNA polymerase was purchased from BIO-RAD (Japan). in-Fusion HD cloning kit was purchased from Clontech (Mountain View, CA).

Plasmids construction experiments were carried out utilizing *E. coli* DH5α strain.

Colony PCR and specific restriction enzyme digestions were used in the confirmation of constructed fungal transformation plasmids.

All the operations and reactions were following the manuals.

plasmid	vector	insert	primer 1	primer 2	PCR template	Ligation method
pUNA-ascA	pUNA digested with SmaI	ascA-F	SmaI-ascA-Fw	ascA-Mid-Rv	gDNA	in-fusion HD cloning kit
		ascA-R	ascA-Mid-Fw	SmaI-ascA-Rv		
pAdeA-ascA	pAdeA digested with SpeI	Prm-ascA-F	pAdeA-SpeI-Fw	ascA-Mid-Rv	pUNA-ascA	in-fusion HD cloning kit
		ascA-R-Tmn	ascA-Mid-Fw	pAdeA-SpeI-Rv		
pUNA-ascB	pUNA digested with SmaI	ascB	SmaI-ascB-Fw	SmaI-ascB-Rv	cDNA	in-fusion HD cloning kit
pTAex3-ascC	pTAex3 digested with SmaI	ascC	SmaI-ascC-Fw	SmaI-ascC-Rv	gDNA	in-fusion HD cloning kit
PTAex3-ascB+ascC	pTAex3 digested with SmaI	ascB+Tmn	SmaI-ascB-Fw	pTA_Tmn_Rv1	pUNA-ascB	in-fusion HD cloning kit
		Prm+ascC	pTA_Prm_Fw1	SmaI-ascC-Rv	pTAex3-ascC	in-fusion HD cloning kit
pUSA-ascE	pUSA digested with KpnI	ascE	KpnI-ascE-Fw	KpnI-ascE-Rv	gDNA	in-fusion HD cloning kit
pUSA-ascF	pUSA digested with KpnI	ascF	KpnI-ascF-Fw	KpnI-ascF-Rv	gDNA	in-fusion HD cloning kit
pUSA-ascF+ascE	pUSA digested with KpnI	ascF+Tmn	KpnI-ascE-Fw	pUSA-Tmn-Rv1	pUSA-ascE	in-fusion HD cloning kit
		Prm+ascE	pUSA-Prm-Fw1	KpnI-ascF-Rv	pUSA-ascF	
pUNA-ascG	pUNA digested with SmaI	ascG	SmaI-ascG-Fw	SmaI-ascG-Rv	gDNA	in-fusion HD cloning kit
pPTRI-ascG	pPTRI digested with HindIII	Prm-ascG-Tmn	pPTRI-HIndIII-Fw	pPTRI-HindIII-Rv	pUNA-ascG	in-fusion HD cloning kit
pUSA-ascD	pUSA digested with KpnI	ascD	KpnI-ascD-Fw	KpnI-ascD-Rv	cDNA	in-fusion HD cloning kit
pBARI-ascD	pBARI digested with HindIII	Prm-ascD-Tmn	pPTRI-HIndIII-Fw	pPTRI-HindIII-Rv	pUSA-ascD	in-fusion HD cloning kit
pUSA-ascF(mutant1)+ascE	pUSA digested with KpnI	ascF(mutant1)-F	KpnI-ascF-Fw	ascF-M1-Fw	pUSA-ascF+ascE	in-fusion HD cloning kit
		ascF(mutant1)-R+ascE	ascF-M1-Rv	KpnI-ascE-Rv		
pUSA-ascF(mutant2)+ascE	pUSA digested with KpnI	ascF(mutant2)-F	KpnI-ascF-Fw	ascF-M2-Fw	pUSA-ascF+ascE	in-fusion HD cloning kit
		ascF(mutant2)-R+ascE	ascF-M2-Rv	KpnI-ascE-Rv		
pUSA-ascF(mutant3)+ascE	pUSA digested with KpnI	ascF(mutant3)-F	KpnI-ascF-Fw	ascF-M3-Fw	pUSA-ascF+ascE	in-fusion HD cloning kit
		ascF(mutant3)-R+ascE	ascF-M3-Rv	KpnI-ascE-Rv		
pUSA-ascF(mutant4)+ascE	pUSA digested with KpnI	ascF(mutant4)-F	KpnI-ascF-Fw	ascF-M4-Fw	pUSA-ascF+ascE	in-fusion HD cloning kit
		ascF(mutant4)-R+ascE	ascF-M4-Rv	KpnI-ascE-Rv		

HPLC Analysis of metabolites extracted from *Fusarium* sp. and the *A. oryzae* transformants

Metabolites isolated from mycelia of *Fusarium* sp. NBRC100844 and the *A. oryzae* transformants were analyzed by HPLC, with a solvent system of 0.1% formic acid (solvent A) and acetonitrile containing 0.1% formic acid (solvent B), at a flow rate of 1.0 ml/min and a column temperature of 40 °C. HPLC column TSKgel ODS-80Tm 150 mm x 4.6 mm was purchase from TOSOH. Separation was performed with solvent B/solvent A (50:50), a linear gradient from 50:50 to 80:20 within the following 15 min, a linear gradient from 80:20 to 100:0 within the following 5 min, 100:0 for 5 additional min.

LC-MS Analysis of Metabolites Extracted from *Fusarium* sp. and the *A. oryzae* Transformants

Metabolites isolated from mycelia of *Fusarium* sp. NBRC100844 and the *A. oryzae* transformants were analyzed by LC-MS, with a solvent system of 0.1% formic acid (solvent A) and acetonitrile containing 0.1% formic acid (solvent B), at a flow rate of 0.2 ml/min and a column temperature of 40 °C, detected by ESI (-) mode. LC-MS column Cadenza CD-C18 150 x 2 mm was purchase from Imtakt. Separation was performed with solvent B/solvent A (50:50), a linear gradient from 50:50 to 80:20 within the following 15 min, a linear gradient from 80:20 to 100:0 within the following 15 min, 100:0 for 5 additional min.

Isolation and Purification of Metabolites from the *A. oryzae* Transformants

Isolation and purification of **4** from *A. oryzae* transformant harboring *ascA*, *B*, *C* and *E*:

A. oryzae transformant harboring *ascA*, *B*, *C*, and *E* was cultured at 303 K, 160 rpm, for 3 days in CD-starch medium (3 L in twenty 500 mL flask). After filtering, the mycelia were lyophilized to dryness. Dried mycelia were extracted by acetone/water (70:30). The extraction solution was concentrated *in vacuo* to remove the solvent.

The extract was subjected to silica-gel column chromatography and eluted using chloroform/methanol (100:0). Fractions that contained **4** yield 21.0 mg of a white solid.

Isolation and purification of **10** from *A. oryzae* transformant harboring *ascA*, *B*, *C*, *E*, and F (Mutant 1):

A. oryzae transformant harboring *ascA*, *B*, *C*, *E*, and F (W130AW131A) was cultured at 303 K, 160 rpm, for 3 days in CD-starch medium (1 L in thirty-four 100 mL flask). After filtering, the mycelia were lyophilized to dryness. Dried mycelia were extracted by acetone/water (70:30). The extraction solution was concentrated *in vacuo* to remove the solvent.

The extract from A. oryzae NSAR1 harboring ascABCE and ascF mutant1 was subjected to silica-gel column chromatography and eluted stepwise using a chloroform/methanol gradient (100:0 to 90:10). Fractions that contained **10** were further purified by reverse-phase preparative HPLC (30% aqueous acetonitrile, 3.5 mL/min) to yield 5.0 mg of a clear oil.

Isolation and purification of **6** from *A. oryzae* transformant harboring *ascA*, *B*, *C*, *E*, and *F*:

A. oryzae transformant harboring *ascA*, *B*, *C*, *E*, and F was cultured at 303 K, 160 rpm, for 3 days in CD-starch medium (1 L in five 500 mL flask). After filtering, the mycelia were lyophilized to dryness. Dried mycelia were extracted by acetone/water (70:30). The extraction solution was concentrated *in vacuo* to remove the solvent.

The extract was subjected to silica-gel column chromatography and eluted stepwise using a chloroform/methanol gradient (100:0 to 90:10). Fractions that contained **6** were further purified by reverse-phase preparative HPLC (40% aqueous acetonitrile, 3.0 mL/min) to yield 5.2 mg of a clear oil.

Cytotoxicity Assay of Ascochlorin and its Analogues

Cytotoxicity assay against MCF-7 breast cancer cell line was kindly performed by Prof. Dongmei Wang (School of Pharmaceutical Sciences, Sun Yat-Sen University).

6.3. Experiments of Discovery of a Cytochrome P450 for Biosynthesis of Citreohybridonol

Isolation of Genomic DNA of *Emericella variecolor* NBRC32302

Emericella variecolor NBRC32302 was purchased from the Biological Resource Center, National Institute of Technology and Evaluation (Chiba, Japan).

E. variecolor NBRC32302 was cultivated at 303 K, 160 rpm, in DPY medium (100 mL in 500 mL flask) for 3 days. and used as the source for the cloning of each gene in the citreohybridonol biosynthetic gene cluster. After filtering, the mycelia were lyophilized to dryness. A phenol-chloroform extraction was conducted on dried mycelia of *E. variecolor* to isolate and purified the genomic DNA of this fungus.

Purified genomic DNA of E. variecolor was used as the source for the cloning of each gene in the *ctr* cluster.

Detailed Information of Primers Used in This Research

Primers are ordered from eurofins genomics Inc..

Primer	Sequence (5' to 3')
InF-ctr-P450-F	TCGAGCTCGGTACCCATGATCTCCAACATATTGCAG
InF-ctr-P450-R	CTACTACAGATCCCCTTAGGCCATGCATGGCAGAT
KpnI-PO-F	TCTCCCGGTACCATGGCACCAAGTCTTGACAAC
KpnI-PO-R	GTGGATGGTACCTCAGCATTTGCAAAGCGTG
KpnI-GO-F	GGTATACAGGTACCATGACTCTGTCCCATTTGG
KpnI-GO-R	AATCAGGTACCTCAGAGAGTGACCTGGATGGTC
InF-pBARI-F	TGATTACGCCAAGCTTCGACTCCAATCTTCAAGAGC
InF-pBARI-R	GCAGGCATGCAAGCTACTAGTAAGATACATGAGCT
InF-pBARI-F2	CATGTATCTTACTAGCCCATCATGGTGTTTTGATC
InF-pBARI-R2	CATGCAAGCTACTAGCATTAATCCGGATCCTTTCC
InF-linker-F1	GCTCGCGAGCGCGTTCCACTGCATCATCAGTCTAG
InF-linker-R1	AACGCGCTCGCGAGCAAGTACCATACAGTACCGCG
SpeI-PamyB-F	GAGGAACTAGTTCATGGTGTTTTGATCATTTTAA
SpeI-TamyB-R	GACCATACTAGTTTCCGTTCCTTTGCTTTCTGC
KpnI-adrA-F	CTGCTGGTACCATGGCCGTCGACAAGC
KpnI-adrA-R	TCTGGAGGTACCTCAGAAAGTGACCTCCTC

Plasmids Construction and PCR conditions

Restriction enzymes were purchased from TaKaRa (Japan). Fungal transformation vectors were kindly provided by Prof. K. Gomi (Graduate School of Agricultural Sciences, Tohoku University) and Prof. K. Kitamoto (Graduate School of Agricultural Sciences, The University of Tokyo). iProof DNA polymerase was purchased from BIO-RAD (Japan). in-Fusion HD cloning kit was purchased from Clontech (Mountain View, CA).

Plasmids construction experiments were carried out utilizing *E. coli* DH5α strain.

Colony PCR and specific restriction enzyme digestions were used in the confirmation of constructed fungal transformation plasmids.

All the operations and reactions were following the manuals.

Plasmid	Insert	vector	Primer 1	Primer 2	PCR Template	Ligation method
pTAex3-ctr-P450	*ctr-P450*	pTAex3 digested with *Sma*I	InF-ctr-P450-F	InF-ctr-P450-R	gDNA	In-Fusion® HD Cloning Kit
pTAex3-PO	*PO*	pTAex3 digested with *Kpn*I	KpnI-PO-F	KpnI-PO-R	gDNA	DNA Ligation Kit Ver.2.1
pTAex3-GO	*GO*	pTAex3 digested with *Kpn*I	KpnI-GO-F	KpnI-GO-R	gDNA	DNA Ligation Kit Ver.2.1
pBARI-ctr-P450	*PamyB-ctr-P450-TamyB*	pBARI digested with *Hin*dIII	InF-pBARI-F	InF-pBARI-R	pTAex3-ctr-P450	In-Fusion® HD Cloning Kit
pBARI-PO	*PamyB-PO-TamyB*	pBARI digested with *Hin*dIII	InF-pBARI-F	InF-pBARI-R	pTAex3-PO	In-Fusion® HD Cloning Kit
pBARI-GO	*PamyB-GO-TamyB*	pBARI digested with *Hin*dIII	InF-pBARI-F	InF-pBARI-R	pTAex3-GO	In-Fusion® HD Cloning Kit
pBARI-ctr-P450+PO+GO	*PamyB-ctr-P450-TamyB*	pBARI-GO digested with *Spe*I	InF-pBARI-F2	InF-linker-R1	pTAex3-ctr-P450	In-Fusion® HD Cloning Kit
	PamyB-PO-TamyB		InF-linker-F1	InF-pBARI-R2	pTAex3-PO	
pBARI-ctr-P450+PO	*PamyB-PO-TamyB*	pBARI-ctr-P450 digested with *Spe*I	SpeI-PamyB-F	SpeI-TamyB-R	pTAex3-PO	DNA Ligation Kit Ver.2.1
pBARI-ctr-P450+GO	*PamyB-GO-TamyB*	pBARI-ctr-P450 digested with *Spe*I	SpeI-PamyB-F	SpeI-TamyB-R	pTAex3-GO	DNA Ligation Kit Ver.2.1
pBARI-PO+GO	*PamyB-GO-TamyB*	pBARI-PO digested with *Spe*I	SpeI-PamyB-F	SpeI-TamyB-R	pTAex3-GO	DNA Ligation Kit Ver.2.1
pTAex3-adrA	*adrA*	pTAex3 digested with *Kpn*I	KpnI-adrA-F	KpnI-adrA-R	pUSA-adrA	DNA Ligation Kit Ver.2.1

HPLC Analysis of Each Product from *A. oryzae* transformant

Metabolites extracted from broth of each *A. oryzae* transformant were analyzed by HPLC, with a solvent system of 0.5% acetic acid (solvent A) and acetonitrile containing 0.5% acetic acid (solvent B), at a flow rate of 1.0 ml/min and a column temperature of 40 °C. HPLC column TSKgel ODS-80Tm 150 mm x 4.6 mm was

purchase from TOSOH. Separation was performed with solvent B/solvent A (20:80) for 5 min, a linear gradient from 20:80 to 100:0 within the following 20 min, 100:0 for 5 additional min, and a linear gradient from 100:0 to 20:80 within the following 3 min.

LC-MS Analysis of Each Product from *A. oryzae* transformant

Metabolites isolated from broth of each *A. oryzae* transformant were analyzed by LC-MS, with a solvent system of 0.5% acetic acid (solvent A) and acetonitrile containing 0.5% acetic acid (solvent B), at a flow rate of 0.2 ml/min and a column temperature of 40 °C, detected by ESI (+) mode. LC-MS column COSMOSIL $5C_{18}$-MS-II 2.0 x 100 mm was purchase from nacalai tesque. Separation was performed with solvent B/solvent A (20:80) for 5 min, a linear gradient from 20:80 to 100:0 within the following 35 min, 100:0 for 5 additional min, a linear gradient from 100: 0 to 20:80 within the following 5 min, 20:80 for 10 additional min.

Preparing of Andrastin E for Feeding Experiments

A. oryzae transformant harboring *trt4*, *2*, *5*, *8*, and *adrI* were inoculated in DPY medium (10 mL in 50 mL falcon) at 303 K, 200 rpm, incubated overnight. Then the broth suspensions were inoculated into DPY medium (100 mL in 500 mL flask) at 303 K, 160 rpm, for two days. Finally, the pre-incubated culture was cultivated in CD-strach medium (2 L in two 2L flask) at 303 K, 160 rpm, for five days.

Medium and mycelia was separated from each other using Buchner funnel. After filtering, dried mycelia were extracted with acetone overnight. Extracts were concentrated, then combined with medium, re-extracted with ethyl acetate, then subjected to a silica gel column chromatography, eluted stepwise with a chloroform/methanol gradient (100:0 to 95:5).

After analyzed by HPLC, fractions containing andrastin E were combined, concentrated, and further purified by reverse-phase preparative HPLC (65% aqueous acetonitrile containing 0.5% acetic acid, 3.0 mL/min). Finally, andrastin E was obtained as a white solid with a yield of 25 mg/L CD-starch medium.

Andrastin E Feeding Experiment

Each *A. oryzae* transformants constructed in this research was first inoculated in DPY medium (5 mL in 50 mL falcon) at 303 K, 200 rpm, for two days. Then the broth suspensions were inoculated into DPY medium (30 mL in 100 mL flask). Andrastin E was dissolved in 2-methoxyethanol (0.2 mg/μL), and added to this culture (1.0 mg for each culture). After incubated at 303 K, 200 rpm, for three days, the broth was extracted by ethyl acetate, and the concentrated extract was subjected to HPLC and LC-MS analysis.

HR-MS analysis of each product from *A. oryzae* transformant

High resolution mass spectra analysis was conducted by JMS-SX-102A purchased from JEOL (Japan). All operations were following the manuals.

Isolation and Purification of Each Metabolite Isolated from *A. oryzae* transformant

For the isolation of each metabolite, two to eight liters of the culture media were extracted with ethyl acetate. Mycelia were extracted with acetone at room temperature overnight, concentrated, and re-extracted with ethyl acetate. Both extracts were combined and subjected to silica-gel column chromatography and further purification by preparative HPLC. The detailed purification procedures for each compound are described below.

Purification Conditions for Citreohybridonol:

The extract from a 2 L culture of A. oryzae NSAR1 with adrF, adrE, adrJ, adrA, and ctr-P450 was subjected to silica-gel column chromatography, and eluted stepwise with a chloroform/methanol gradient (100:0 to 90:10). Fractions that contained 4 were further purified by reverse-phase preparative HPLC (50% aqueous acetonitrile containing 0.5% acetic acid, 3.0 mL/min) to yield 4.8 mg of a colorless oil.

Citreohybridonol:

Colorless oil; $[\alpha]_{31}^{D}$=+17.0 (c=0.79, $CHCl_3$); HR-EI-MS found m/z 500.2418 $[M]^+$ (calcd 500.2410 for $C_{28}H_{36}O_8$).

Purification Conditions for 6α-hydroxylandrastin C:
The extract from a 2 L culture of A. oryzae NSAR1 with adrF, adrE, adrJ, adrA, and ctr-P450 was subjected to silica-gel column chromatography, and eluted stepwise with a chloroform/methanol gradient (100:0 to 90:10). Fractions that contained 5 were further purified by reverse-phase preparative HPLC (60% aqueous acetonitrile containing 0.5% acetic acid, 3.0 mL/min) to yield 10.5 mg of a white solid.

6α-hydroxylandrastin C:
White solid; $[\alpha]_{31}^{D}$ =-72.0 (c=1.85, $CHCl_3$); HR-EI-MS found m/z 488.2760 $[M]^+$ (calcd 488.2774 for $C_{28}H_{40}O_7$).

Purification Conditions for Deoxocitreohybridonol (**6**):
The extract from a 2 L culture of A. oryzae NSAR1 with adrF, adrE, adrJ, adrA, and ctr-P450 was subjected to silica-gel column chromatography, and eluted stepwise with a chloroform/methanol gradient (100:0 to 90:10). Fractions that contained 6 were further purified by reverse-phase preparative HPLC (65% aqueous acetonitrile containing 0.5% acetic acid, 3.0 mL/min), to yield 1.1 mg of a white amorphous solid.

Deoxocitreohybridonol:
White amorphous solid; $[\alpha]_{28}^{D}$=-37.0 (c=0.12, $CHCl_3$); HR-EI-MS found m/z 486.2607 $[M]^+$ (calcd 486.2618 for $C_{28}H_{38}O_7$).

Purification Conditions for Dihydrocitreohybridonol:
The extract from an 8 L culture of A. oryzae NSAR1 with adrF, adrE, adrJ, adrA, and ctr-P450 was subjected to silica-gel column chromatography, and eluted stepwise with a chloroform/methanol gradient (100:0 to 80:20). Fractions that contained 8 were further purified by reverse-phase preparative HPLC (50% aqueous acetonitrile containing 0.5% acetic acid, 3.0 mL/min), to yield 3.8 mg of a white amorphous solid.

Dihydrocitreohybridonol:
White amorphous solid; $[\alpha]_{25}^{D}$=+28.3 (c=0.30, $CHCl_3$); HR-EI-MS found m/z 502.2544 $[M]^+$ (calcd 502.2567 for $C_{28}H_{38}O_8$).

Purification Conditions for 6α-hydroxylandrastin B:
The extract from an 8 L culture of A. oryzae NSAR1 with adrF, adrE, adrJ, adrA, and ctr-P450 was subjected to silica-gel column chromatography, and eluted stepwise with a chloroform/methanol gradient (100:0 to 80:20). Fractions that contained 7 were further purified by reverse-phase preparative HPLC (50% aqueous acetonitrile containing 0.5% acetic acid, 3.0 mL/min), to yield 4.7 mg of a white solid.

6α-hydroxylandrastin B:
White solid; $[\alpha]_{25}^{D}$=+9.0 (c=0.41, $CHCl_3$); HR-EI-MS found m/z 504.2723 $[M]^+$ (calcd 504.2723 for $C_{28}H_{40}O_8$).

7. Appendix

7.1. Appendix of Biosynthesis Research of Fungal Meroterpenoid Ascochlorin

NMR Data for Peak c: LL-Z1272ε (**6**)

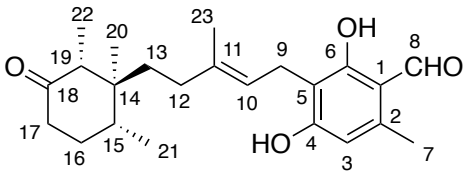

Table 7-1. NMR data for LL-Z1272ε (6).

1H NMR: 500 MHz, 13C NMR: 125 MHz (in CDCl3)

Position	**6**	
	δ_H (mult, Hz)	δ_C
1	-	112.2
2	-	142
3	6.24 (1H, s)	110.8
4	-	163.9
5	-	113.3
6	-	162.5
7	2.48 (3H, s)	18.1
8	10.06 (1H, s)	193.4
9	3.37 (2H, d, J = 7.1 Hz)	21.3
10	5.27 (1H, t, J =7.2 Hz)	121.5
11	-	138.3
12	1.97 (1H, m), 1.88 (1H, m)	32.8
13	1.40 (2H, m)	35.7
14	-	43.7
15	2.00 (1H, m)	36.2
16	1.84 (1H, m) 1.61 (1H, m)	31.1
17	2.33 (2H, m)	41.7
18	-	215.1
19	2.47 (1H, m)	50.7
20	0.57 (3H, s)	15.5
21	0.92 (3H, d, J = 6.7 Hz)	15.2
22	0.88 (3H, d, J = 6.6 Hz)	7.7
23	1.83 (3H, s)	16.5

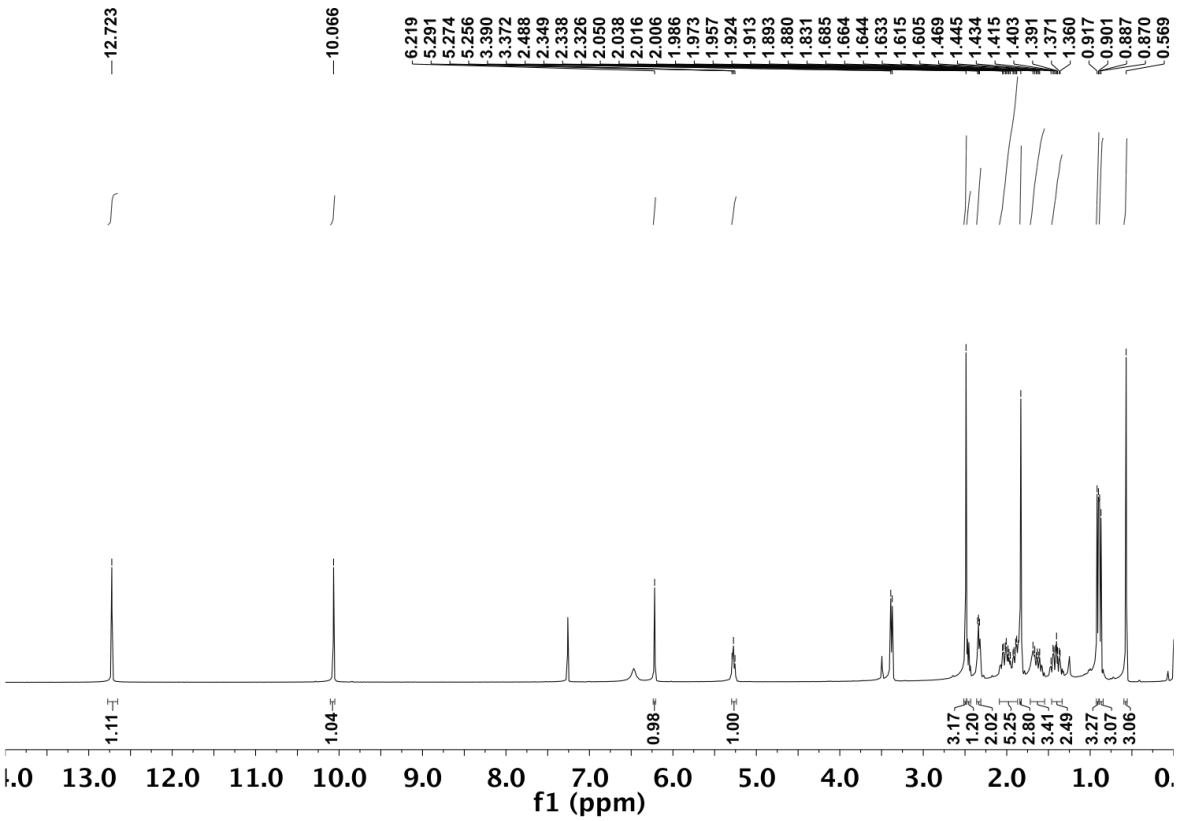

Figure 7-1. ^{1}H NMR spectrum of **6**.

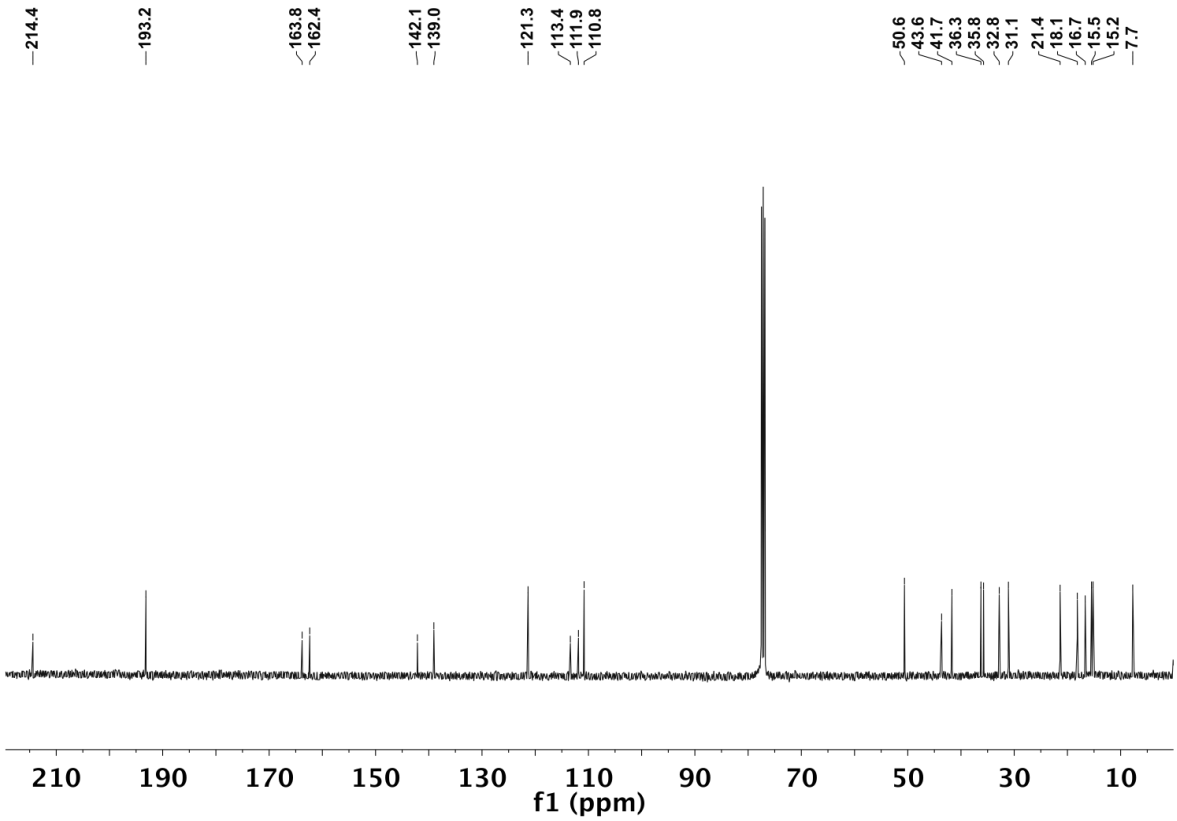

Figure 7-2. ^{13}C NMR spectrum of **6**.

NMR Data for Peak c′: LL-Z1272δ (9)

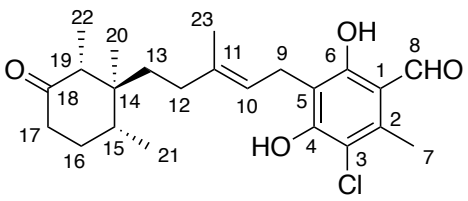

Table 7-2. NMR data for LL-Z1272δ (**9**).

^{1}H NMR: 500 MHz, ^{13}C NMR: 125 MHz (in $CDCl_3$)

Position	**9**	
	δ_H (mult, Hz)	δ_C (Hz)
1	-	113.3
2	-	137.8
3	-	113.8
4	-	156.4
5	-	114.4
6	-	162.4
7	2.45 (1H, m)	50.6
8	10.14 (1H, s)	193.4
9	3.39 (2H, d, *J* = 7.1 Hz)	22.2
10	5.25 (1H, t, *J* =7.1 Hz)	121
11	-	136.8
12	2.00 (1H, m), 1.84 (1H, m)	32.8
13	1.39 (2H, m)	35.7
14	-	43.6
15	2.00 (1H, m)	36.2
16	1.84 (1H ,m) 1.63 (1H, m)	31.1
17	2.32 (2H, m)	41.7
18	-	214.3
19	2.45 (1H, m)	50.6
20	0.56 (3H, s)	15.5
21	0.87 (1H, d, *J* = 6.7 Hz)	15.2
22	0.90 (3H, d, *J* = 6.7 Hz)	7.7
23	1.81 (3H, s)	16.5

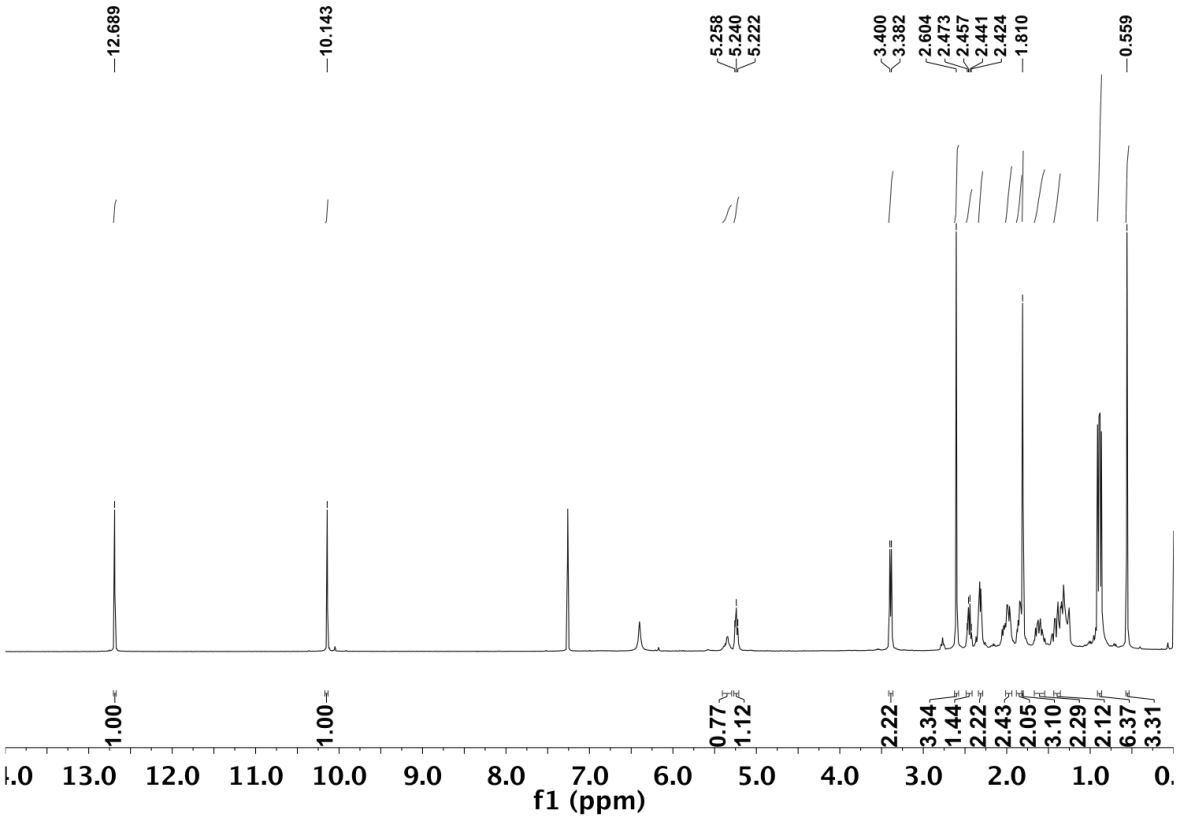

Figure 7-3. ^{1}H NMR spectrum of **9**.

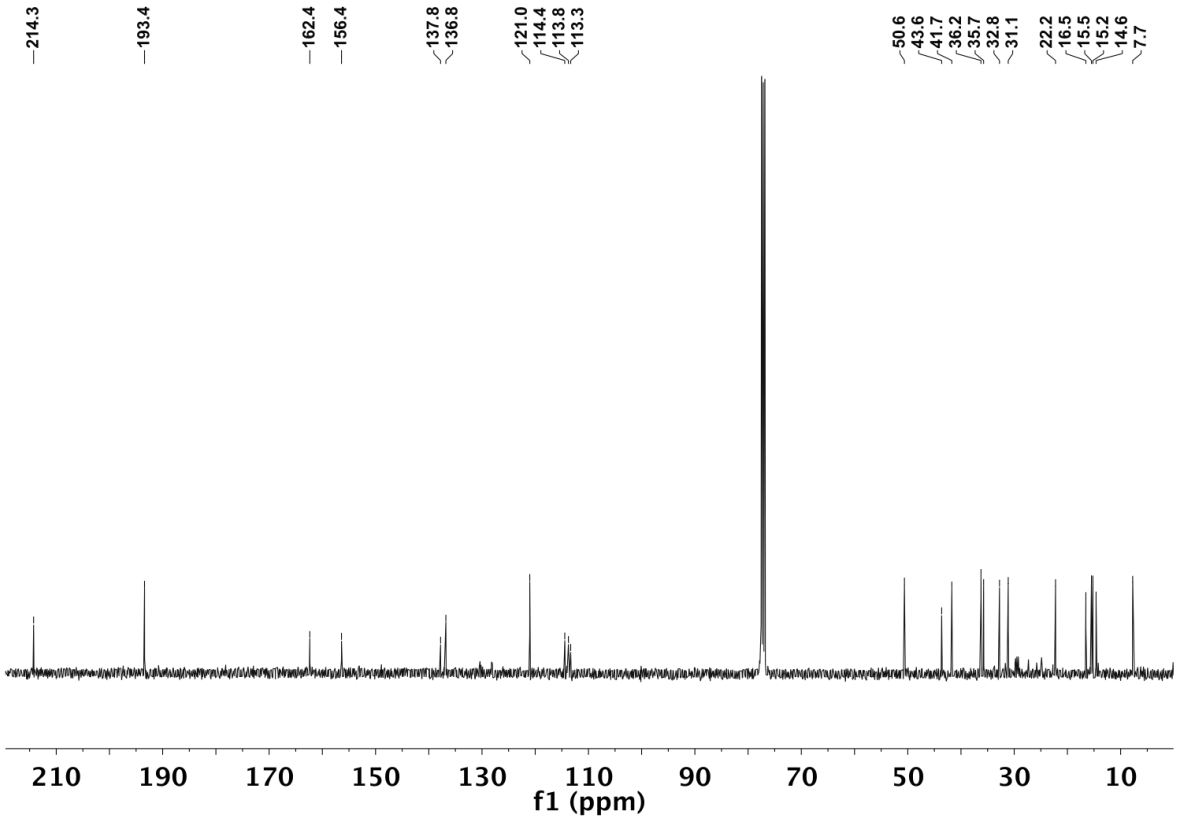

Figure 7-4. ^{13}C NMR spectrum of **9**.

NMR Data for Peak c″: Bromo Analogue of LL-Z1272δ (12)

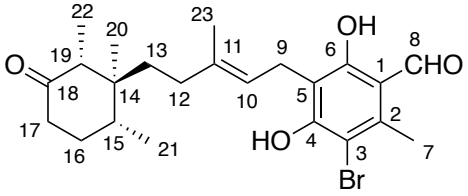

Table 7-3. NMR data for bromo analogue of LL-Z1272δ (**12**).

^{1}H NMR: 500 MHz, ^{13}C NMR: 125 MHz (in $CDCl_3$)

Position	**12**	
	δ_H (mult, Hz)	δ_C (Hz)
1	-	114.3
2	-	139.8
3	-	106.2
4	-	157.1
5	-	114.5
6	-	162.9
7	2.45 (1H, m)	50.6
8	10.16 (1H, s)	193.6
9	3.41 (2H, d, *J* = 7.2 Hz)	22.5
10	5.24 (1H, t, *J* =7.5 Hz)	121
11	-	136.8
12	1.98 (1H, m), 1.84 (1H, m)	32.8
13	1.39 (2H, m)	35.7
14	-	43.6
15	1.98 (1H, m)	36.2
16	1.83 (1H ,m) 1.61 (1H, m)	31.1
17	2.31 (2H, m)	41.7
18	-	214.3
19	2.45 (1H, m)	50.6
20	0.56 (3H, s)	15.5
21	0.88 (1H, d, *J* = 6.8 Hz)	15.2
22	0.91 (3H, d, *J* = 6.8 Hz)	7.7
23	1.81 (3H, s)	16.5

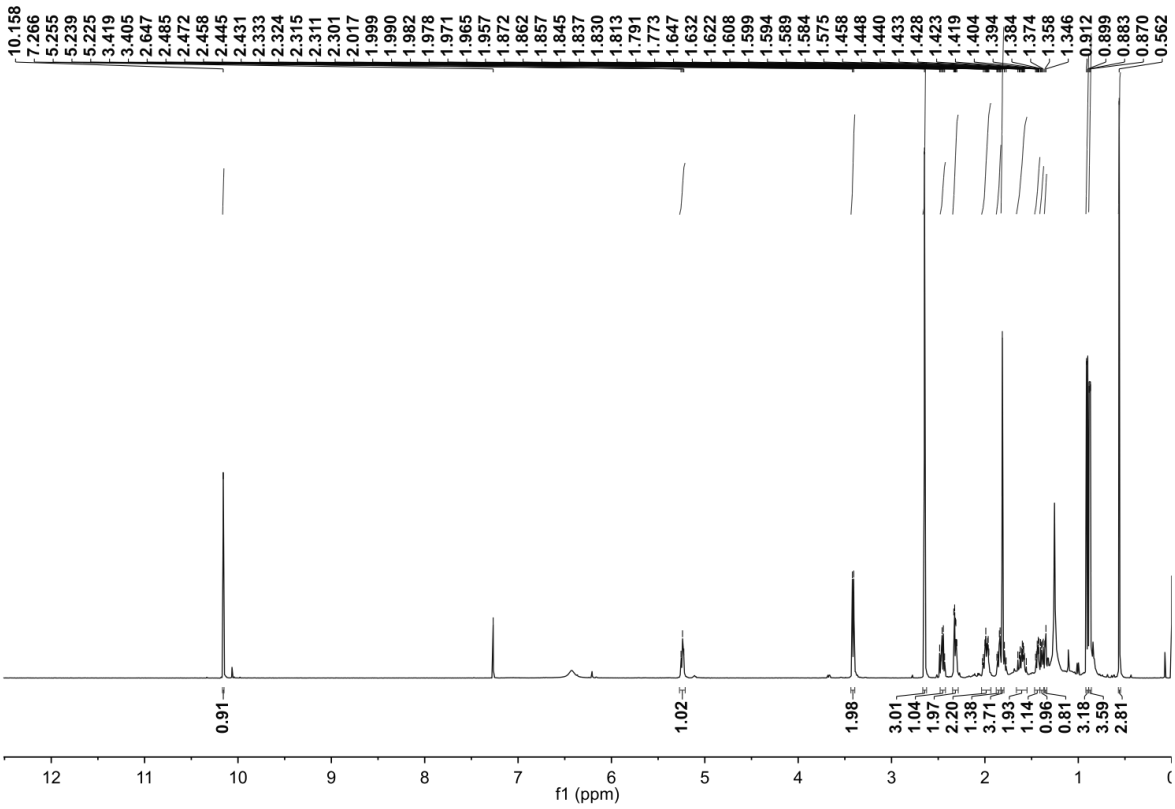

Figure 7-5. ^{1}H NMR spectrum of **12**.

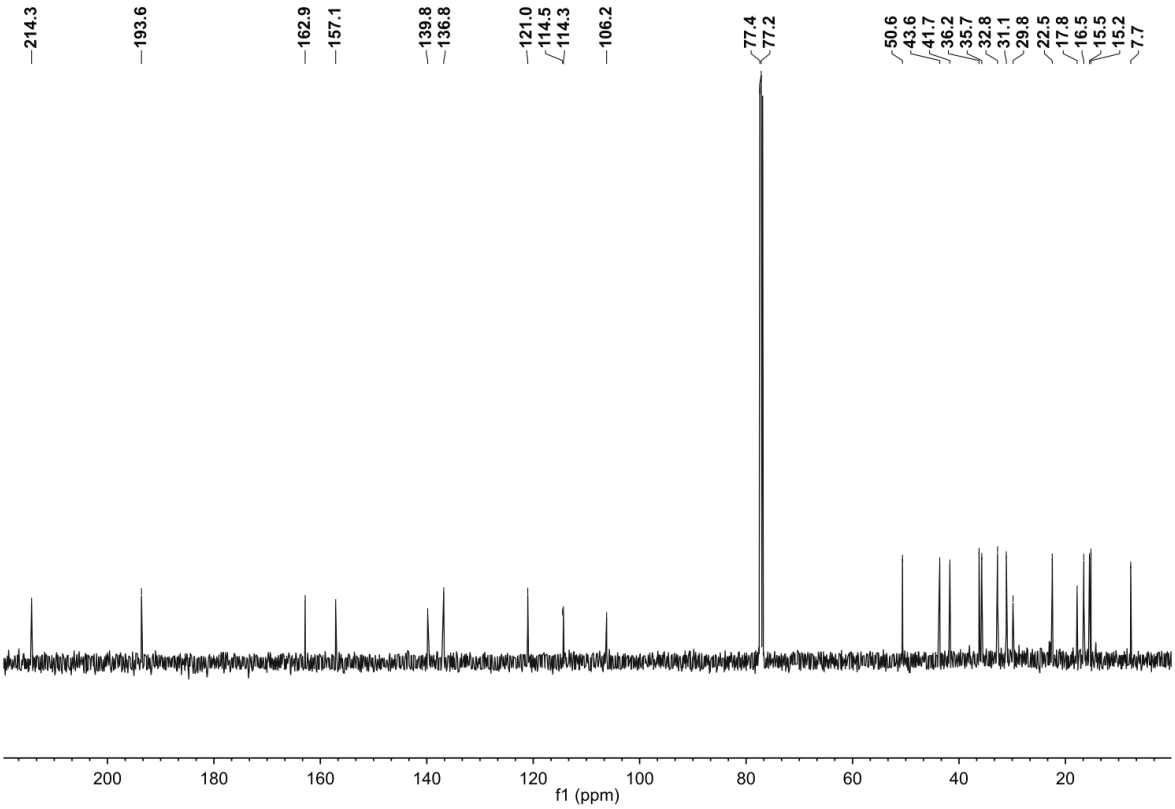

Figure 7-6. ^{13}C NMR spectrum of **12**.

NMR Data for Peak d: Dechloroascochlorin (7)

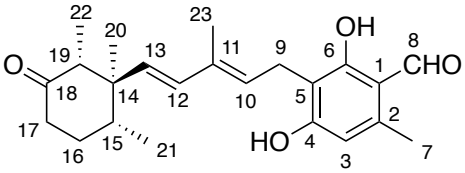

Table 7-4. NMR data for dechloroascochlorin (**7**)

^{1}H NMR: 500 MHz, ^{13}C NMR: 125 MHz (in $CDCl_3$)

Position	**7**	
	δ_H (mult, Hz)	δ_C (Hz)
1	-	111.9
2	-	142.2
3	6.22 (1H, s)	110.6
4	-	163.8
5	-	113.5
6	-	161.6
7	2.49 (3H, s)	18.1
8	10.07 (1H, s)	193.1
9	3.50 (2H, d, *J* = 7.4 Hz)	21.4
10	5.52 (1H, t, *J* =7.2 Hz)	127.5
11	-	136.4
12	5.92 (1H, d, *J* = 16.1 Hz)	132.9
13	5.40 (1H, d, *J* = 15.8 Hz)	135.4
14	-	48.6
15	1.98-1.90 (1H, m)	40.9
16	1.98-1.90 (1H, m) 1.62 (1H, m)	31.2
17	2.38 (2H, m)	41.7
18	-	212.9
19	2.38 (1H, m)	53.7
20	0.70 (3H, s)	10.4
21	0.84 (3H, d, *J* = 6.7 Hz)	16.4
22	0.81 (3H, d, *J* = 6.7 Hz)	9
23	1.94 (3H, s)	12.8

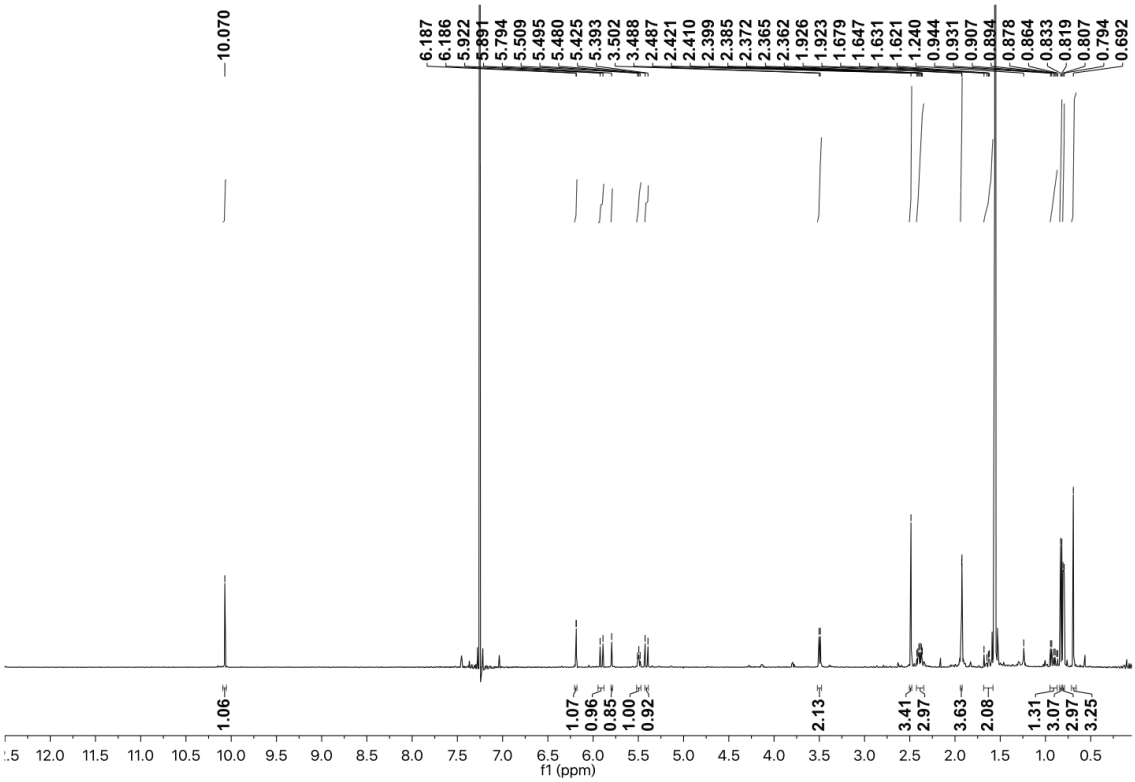

Figure 7-7. ^{1}H NMR spectrum of **7**.

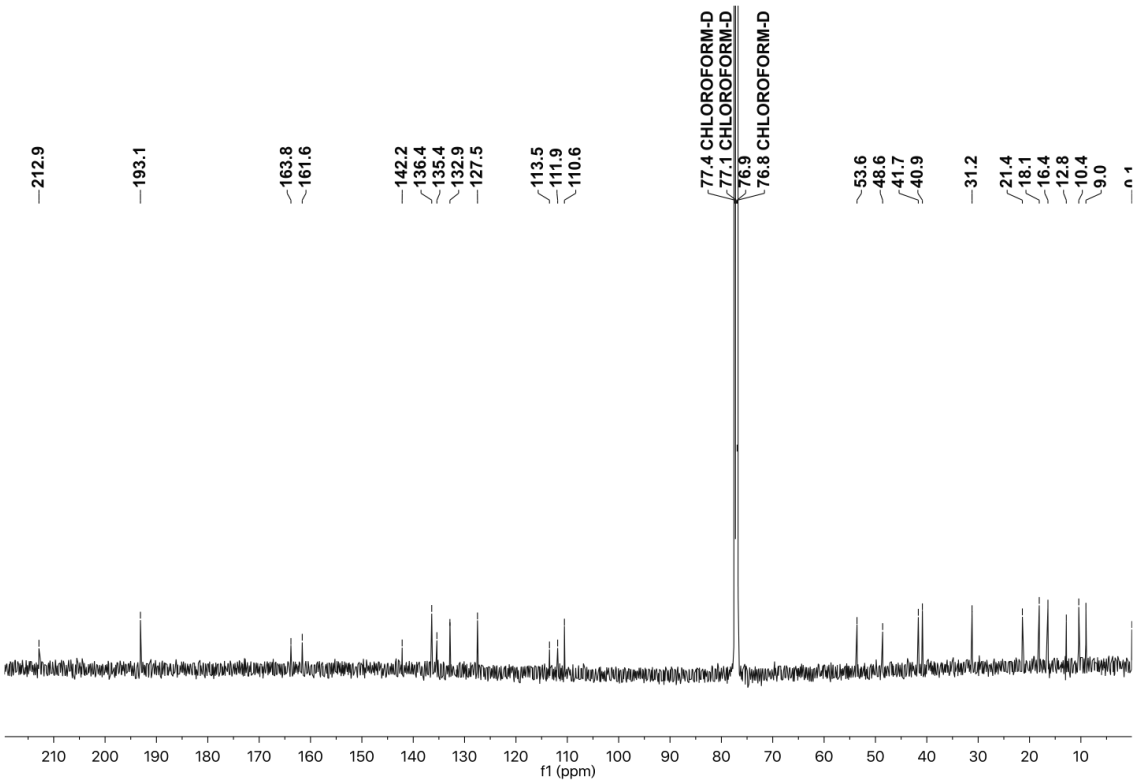

Figure 7-8. ^{13}C NMR spectrum of **7**.

NMR Data for Peak d′: Ascochlorin (1)

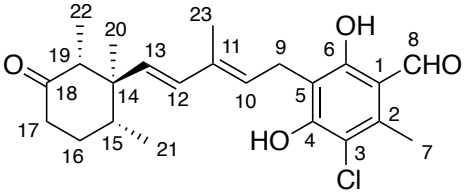

Table 7-5. NMR data for ascochlorin (**1**)

^{1}H NMR: 500 MHz, ^{13}C NMR: 125 MHz (in $CDCl_3$)

Position	**1**	
	δ_H (mult, Hz)	δ_C
1	-	113.9
2	-	137.9
3	-	113.3
4	-	156.3
5	-	113.8
6	-	162.3
7	2.60 (3H, s)	14.3
8	10.13 (1H, s)	193.4
9	3.53 (2H, d, *J* = 7.4 Hz)	22.4
10	5.52 (1H, t, *J* =7.3 Hz)	127.7
11	-	134.2
12	5.89 (1H, d, *J* = 16.0 Hz)	133.3
13	5.36 (1H, d, *J* = 16.0 Hz)	135.8
14	-	48.6
15	1.95-1.92 (1H, m)	41
16	1.95-1.92 (1H, m) 1.61 (1H, m)	31.3
17	2.39 (2H, m)	41.7
18	-	212.9
19	2.39 (1H, m)	53.7
20	0.69 (3H, s)	10.5
21	0.83 (3H, d, *J* = 6.8 Hz)	16.5
22	0.80 (3H, d, *J* = 6.6 Hz)	9
23	1.92 (3H, s)	12.8

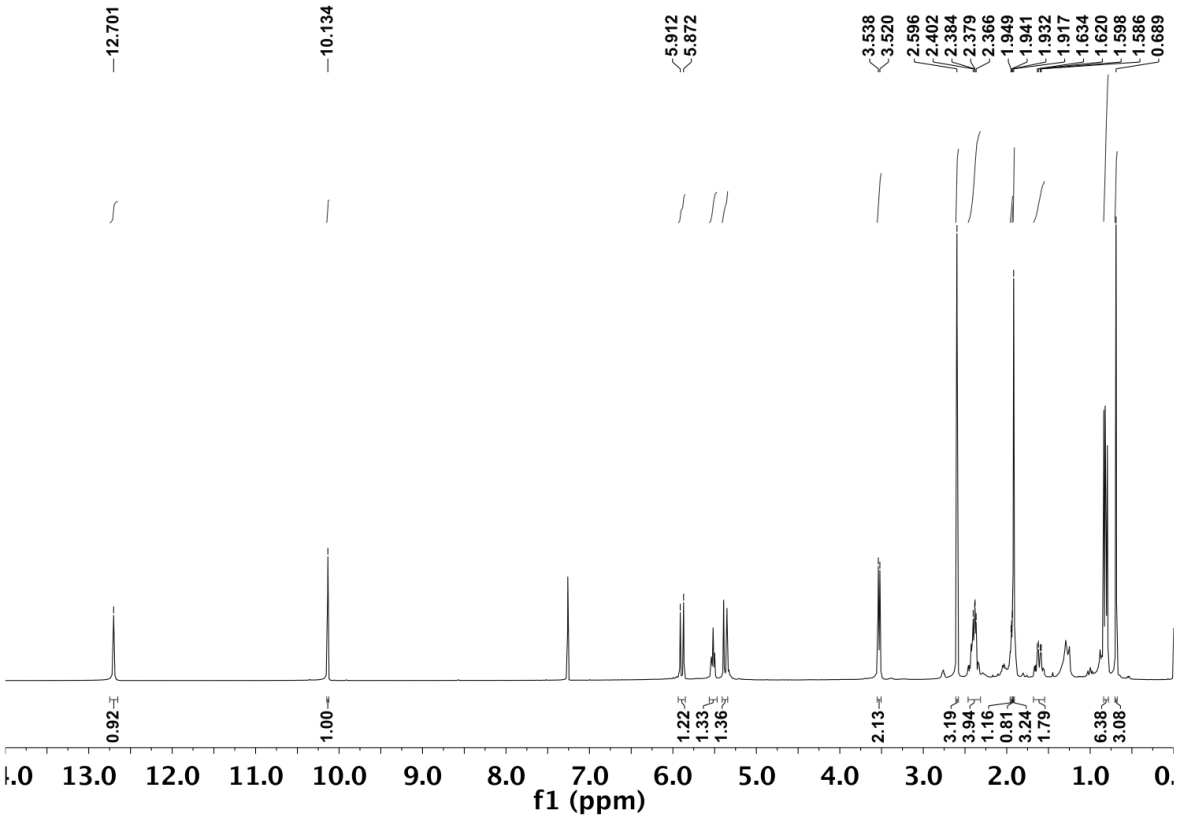

Figure 7-9. ^{1}H NMR spectrum of **1**.

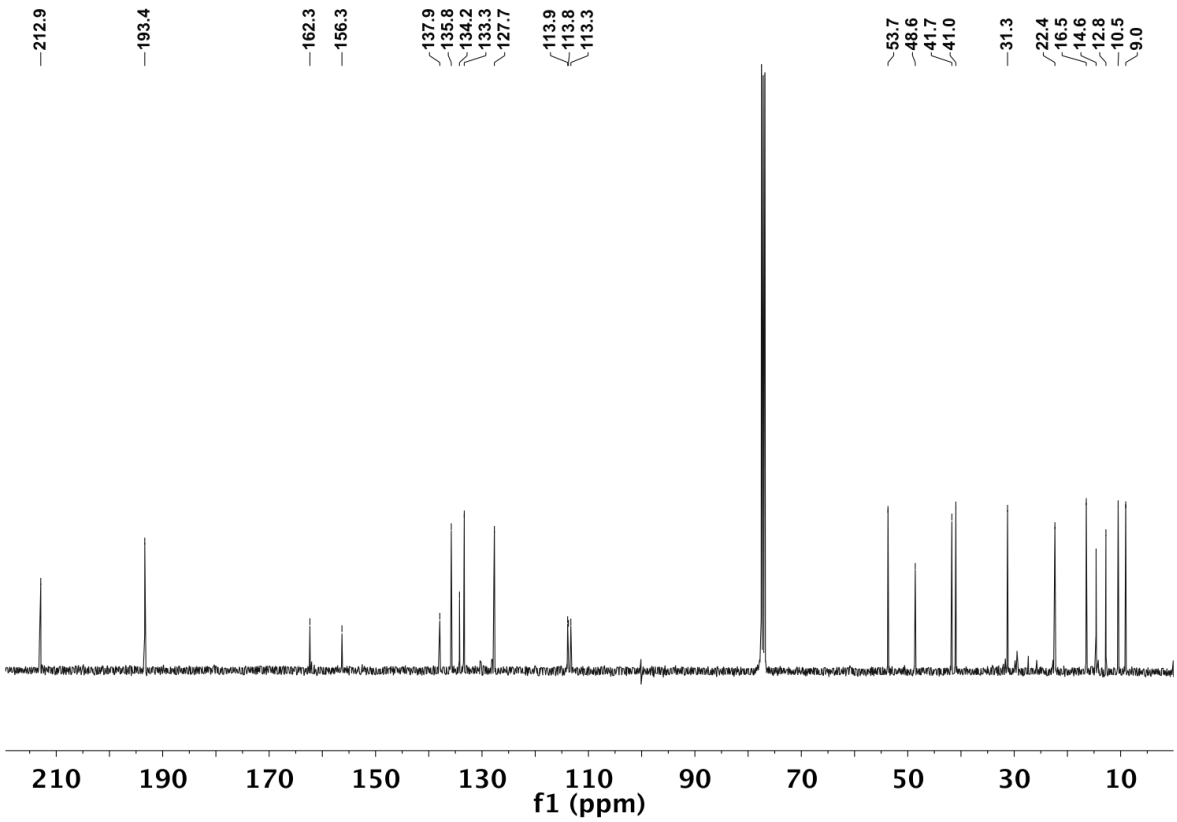

Figure 7-10. ^{13}C NMR spectrum of **1**.

NMR Data for Peak d″: Bromo Analogue of Ascochlorin (13)

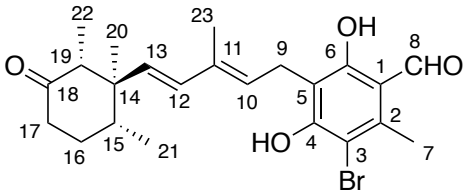

Table 7-6. NMR data for bromo analogue of ascochlorin (**13**)

^{1}H NMR: 500 MHz, ^{13}C NMR: 125 MHz (in $CDCl_3$)

Position	**13**	
	δ_H (mult, Hz)	δ_C
1	-	114.4
2	-	139.9
3	-	106.2
4	-	157
5	-	113.9
6	-	162.8
7	2.65 (3H, s)	14.3
8	10.16 (1H, s)	193.6
9	3.56 (2H, d, *J* = 7.4 Hz)	22.6
10	5.52 (1H, t, *J* =7.5 Hz)	127.7
11	-	134.3
12	5.90 (1H, d, *J* = 16.0 Hz)	133.4
13	5.38 (1H, d, *J* = 16.0 Hz)	135.8
14	-	48.6
15	1.98-1.92 (1H, m)	41
16	1.98-1.92 (1H, m) 1.61 (1H, m)	31.3
17	2.39 (2H, m)	41.7
18	-	212.9
19	2.39 (1H, m)	53.7
20	0.70 (3H, s)	10.5
21	0.83 (3H, d, *J* = 6.7 Hz)	16.5
22	0.81 (3H, d, *J* = 6.6 Hz)	9.1
23	1.92 (3H, s)	12.8

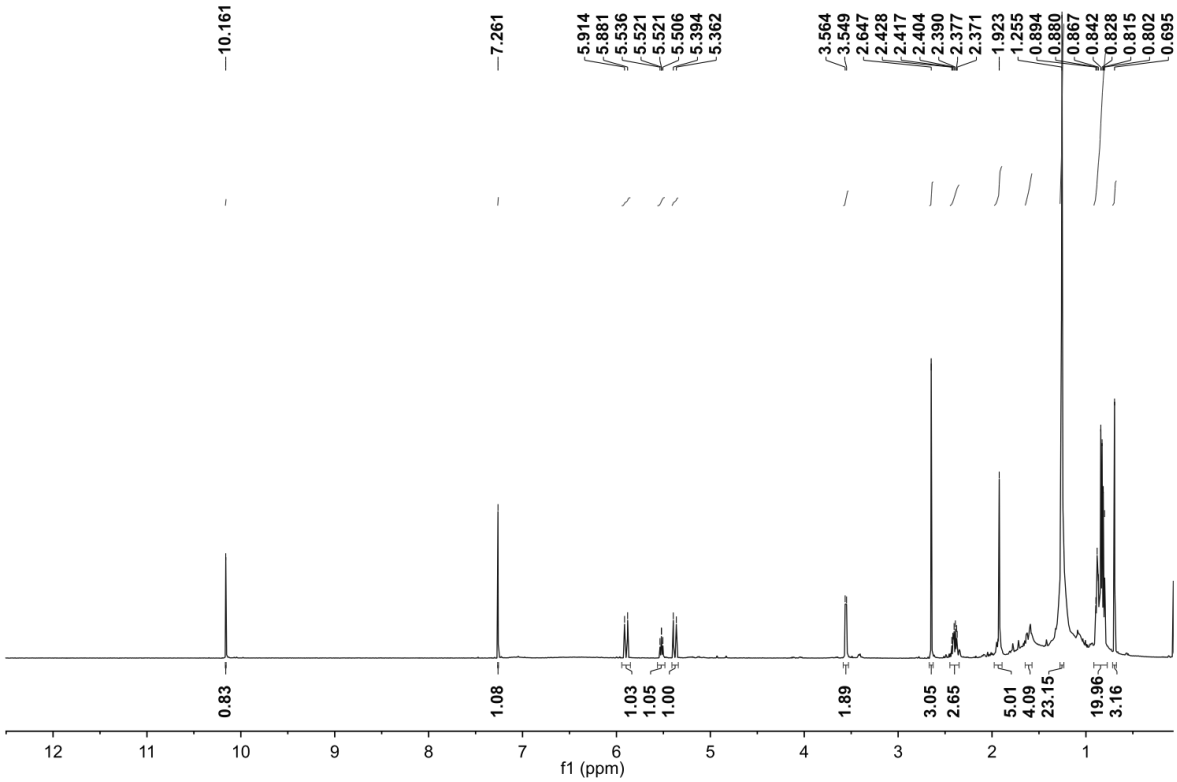

Figure 7-11. ^{1}H NMR spectrum of **13**.

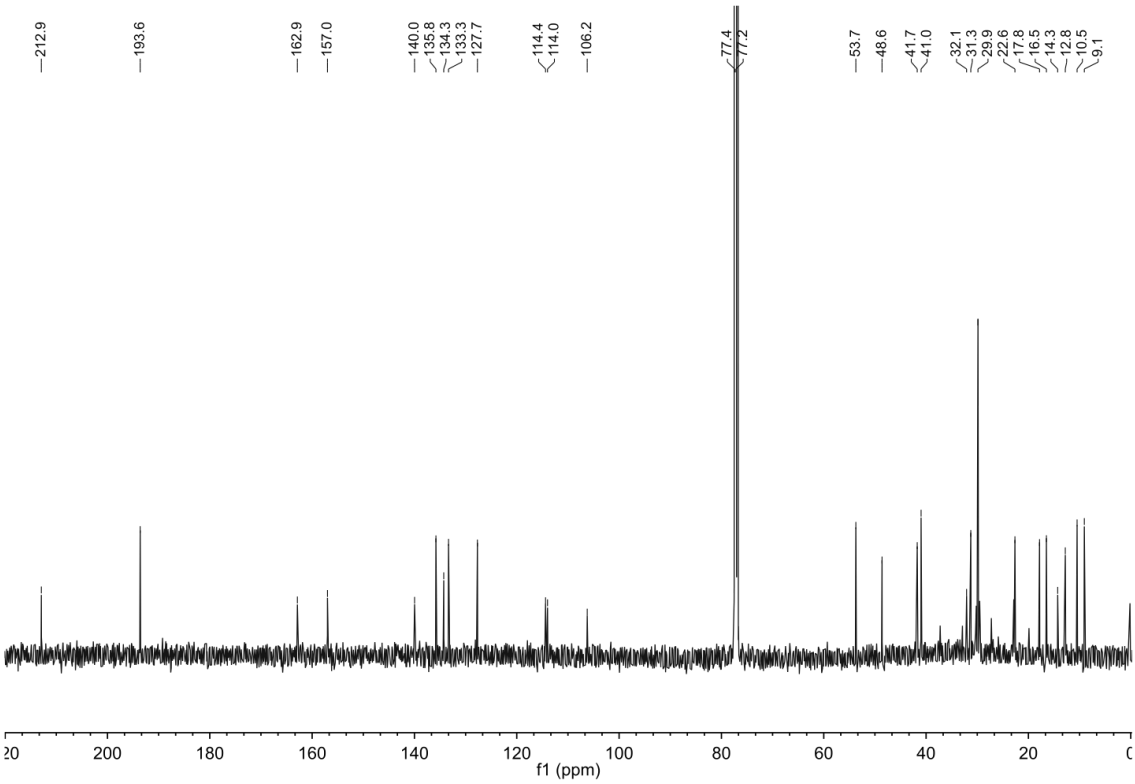

Figure 7-12. ^{13}C NMR spectrum of **13**.

NMR Data for the Peak b″: dihydroxy-LL-Z1272β (10)

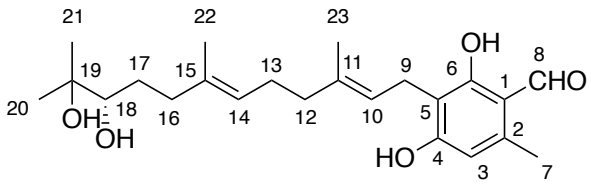

Table 7-7. NMR data for dihydroxy-LL-Z1272β (**10**)

^{1}H NMR: 500 MHz, ^{13}C NMR: 125 MHz (in $CDCl_3$)

Position	**10**	
	δ_H (mult, Hz)	δ_C (Hz)
1	-	113.2
2	-	141.9
3	6.19 (1H, s)	110.8
4	-	162.7
5	-	112.4
6	-	163.7
7	2.47 (3H, s)	18.1
8	10.05 (1H, s)	192.3
9	3.35 (2H, t, *J* = 6.6 Hz)	21.1
10	5.17 (1H, t, *J* =8.4 Hz)	122.3
11	-	137.6
12	2.05 (2H, m)	39.3
13	2.08 (2H, m)	25.5
14	5.12 (1H, t, *J* = 7.8 Hz)	124.8
15	-	135.2
16	2.13, 2.17 (2H, m)	36.6
17	1.42, 1.62 (2H, m)	29.8
18	3.39 (1H, dd, *J* =12.6, 1.8)	78.3
19	-	73.5
20	1.18 (3H, brs)	26.5
21	1.12 (3H, brs)	23.4
22	1.58 (3H, brs)	14.3
23	1.76 (3H, brs)	16.1
6-OH	12.7 (1H,s)	

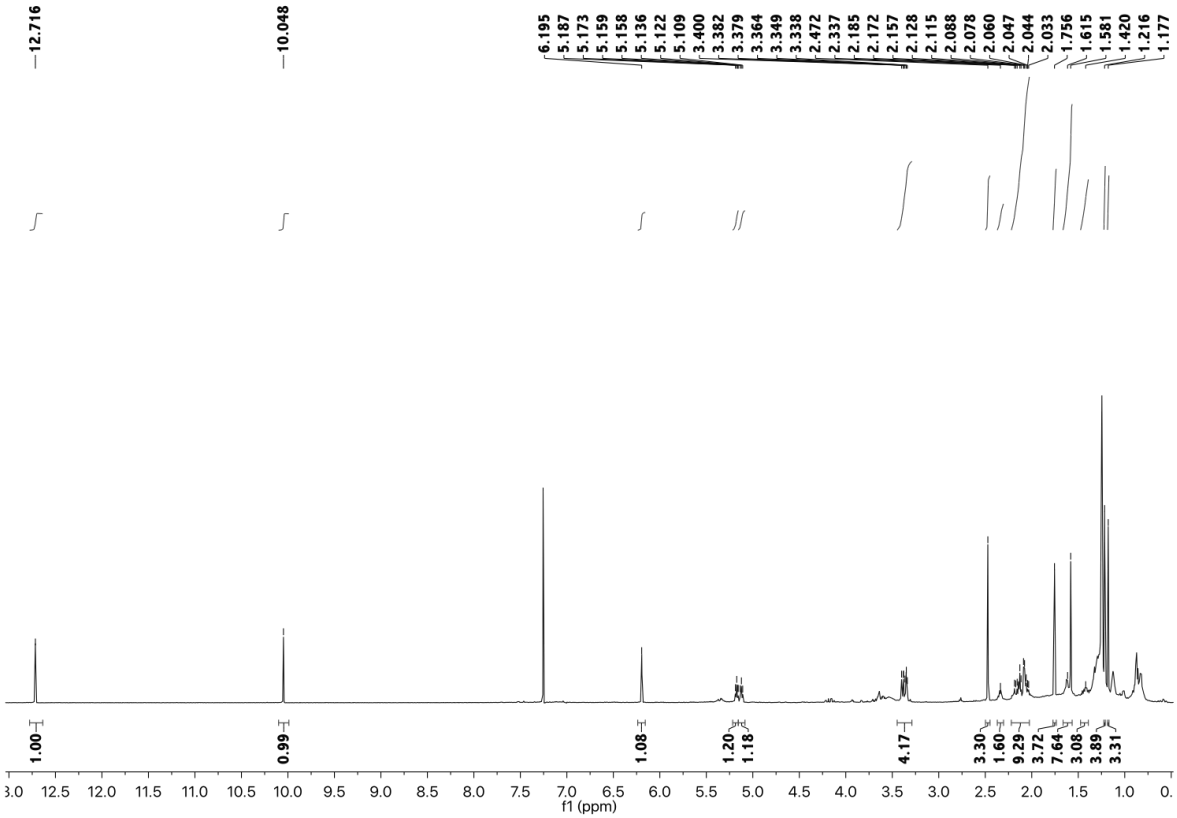

Figure 7-13. ^{1}H NMR spectrum of **10**.

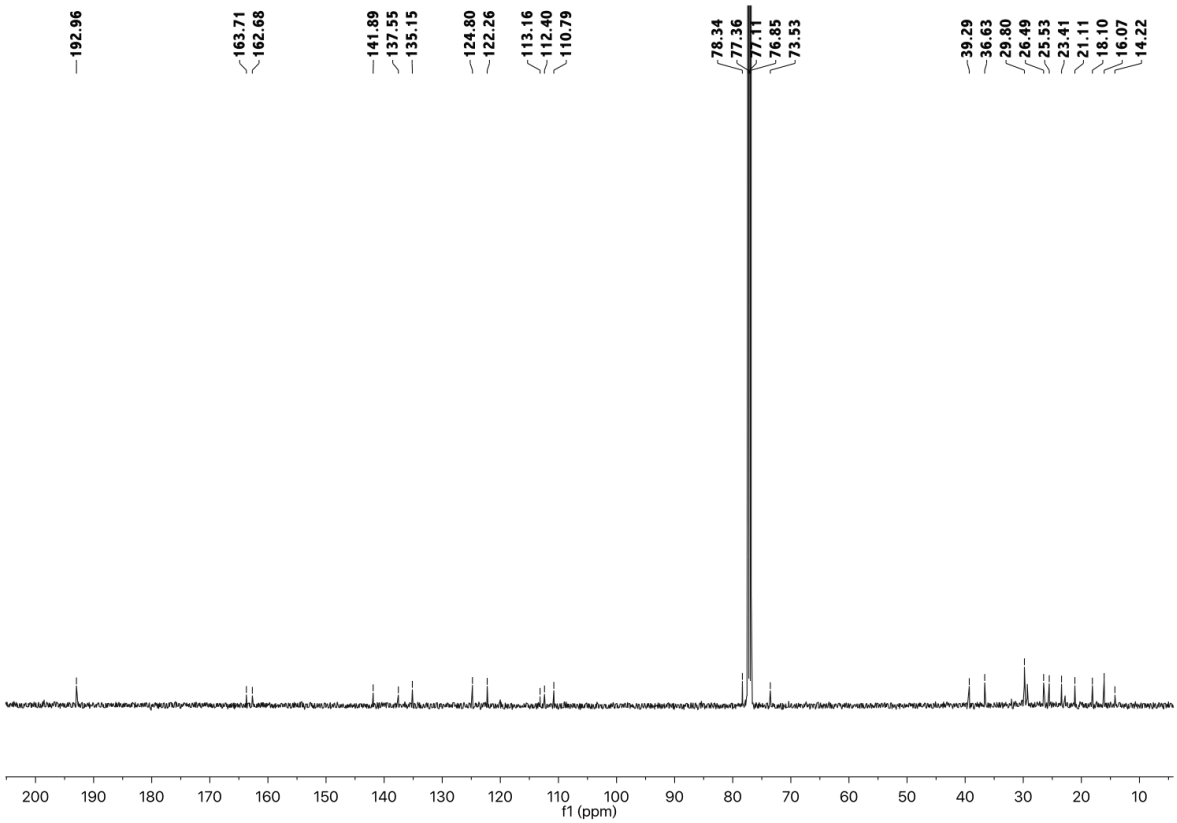

Figure 7-14. ^{13}C NMR spectrum of **10**.

UV Spectra of Metabolites Extracted from Mycelia of *Fusarium* sp. NBRC100844

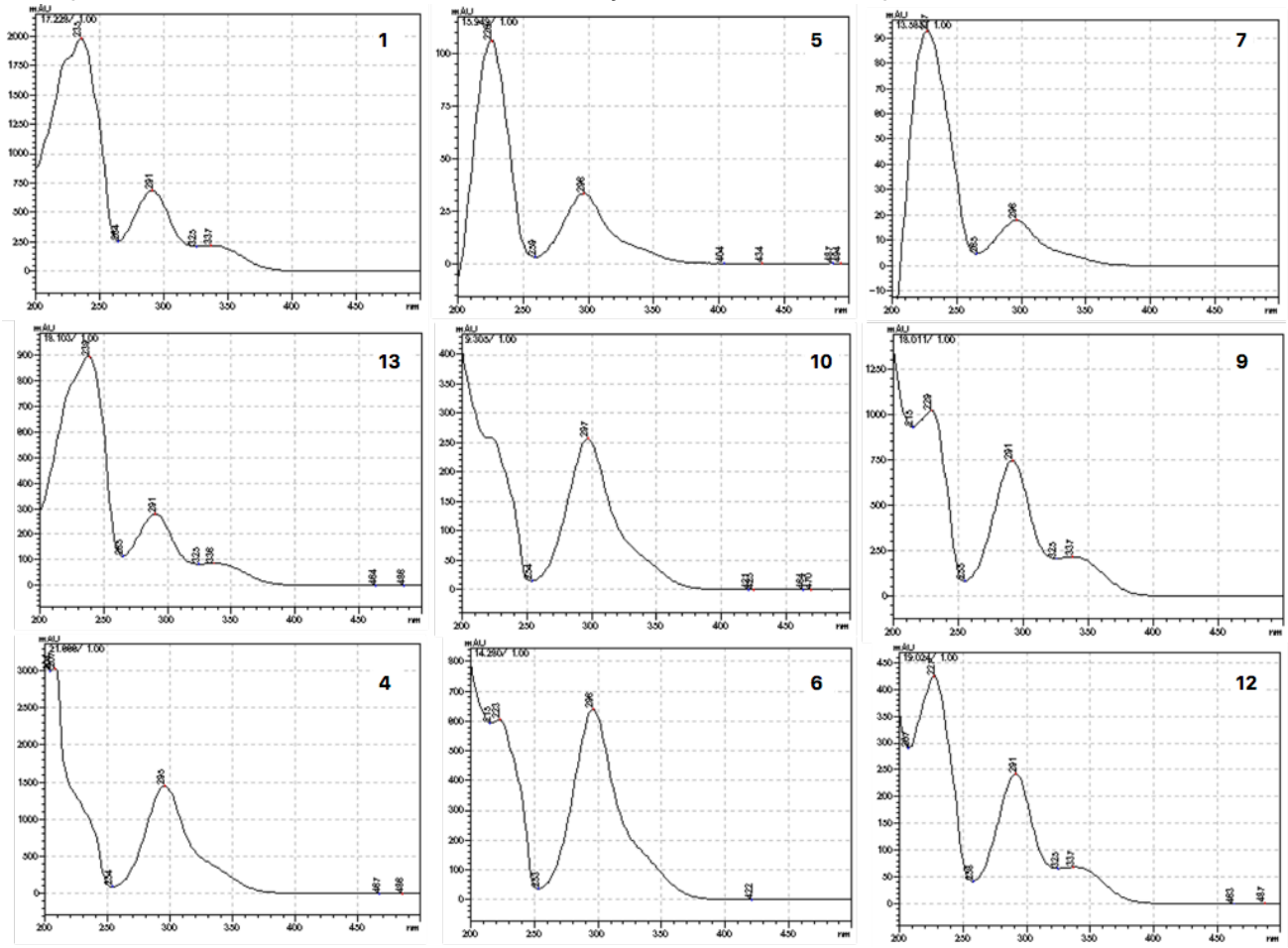

HR-MS Spectra of Metabolites Extracted from Mycelia of *Fusarium* sp. NBRC100844

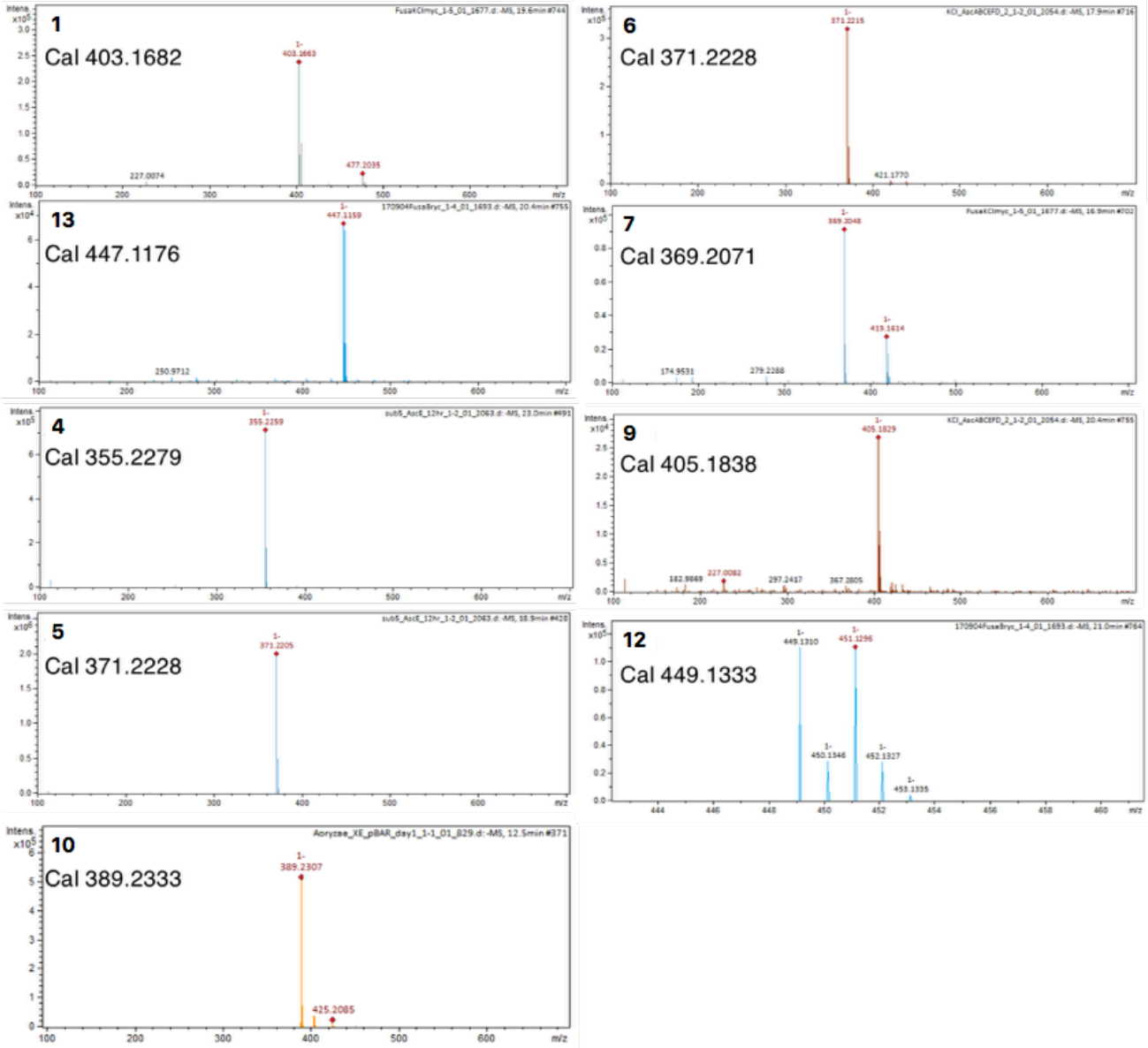

Cytotoxicity of Ascochlorin and its Analogues on MCF-7 Breast Cancer Cell Line

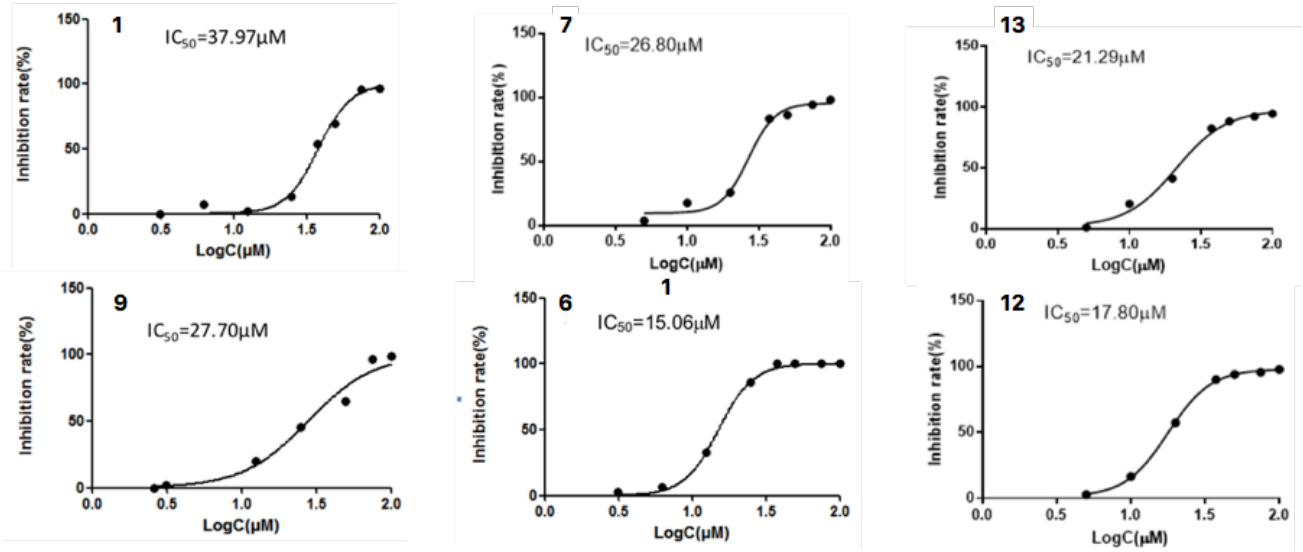

Phylogenetic Tree Analysis of Meroterpenoid Terpene Cyclases

Multiple sequence alignment, performed with Clustal Omega. The scale represents 0.10 amino acid substitutions per site. XiaH from *Streptomyces* sp. SCSIO 02999 was employed as out group.

Accession numbers:

AndB from Emericella variecolor, AtmB from Aspergillus flavus, AusL from Aspergillus nidulans FGSC A4, LtmB from Epichloe festucae var. lolii, MacJ from Penicillium terrestris, AdrI from Penicillium chrysogenum, PaxM from Penicillium paxilli, LtmB from Epichloe festucae var. lolii, MacJ from Penicillium terrestris, OclD from Penicillium oxalicum 114-2, PaxB from Penicillium paxilli, PrhH from Penicillium brasilianum NBRC6234, Pyr4 from Aspergillus fumigatus F37, Trt1 from Aspergillus terreus, AscF from Fusarium sp. NBRC100844, Verruculide_cyclase from Penicillium verruculosum, AFO69287 from Periglandula ipomoeae, AFO69298 from Epichloe gansuensis, AFO69305 from Aciculosporium take, AFO85421 from Claviceps paspali, AFP27270 from Epichloe festucae, AFP27292 from Claviceps purpurea, AGN73002 from Epichloe aotearoae, AGN73003 from Epichloe occultans, AGN73004 from Epichloe siegelii, AGN73005 from Neotyphodium sp. FaTG-3, AGN73006 from Neotyphodium sp. FaTG-2, AGN73007 from Neotyphodium sp. FaTG-2, AGN73062 from Epichloe funkii, AGN73076 from Epichloe coenophiala, AGN73086 from Neotyphodium sp. FaTG-4, AGZ20190 from Penicillium crustosum, AGZ20474 from Penicillium janthinellum, ABF20226 from Epichloe festucae var. lolii, BAM84047 from Tolypocladium album, BAU61559 from Penicillium simplicissimum, CAK48315 from Aspergillus niger, CDM27377 from Penicillium roqueforti FM164, CDM28239 from Penicillium roqueforti FM164, CEF79629 from Fusarium graminearum, CEJ61316 from Penicillium brasilianum, CEL08900 from Aspergillus calidoustus, CEL11271 from Aspergillus calidoustus, CRL19196 from Penicillium camemberti, CRL28507 from Penicillium camemberti, EDP47980 from Aspergillus fumigatus A1163, EDP52188 from Aspergillus fumigatus A1163, EHA26643 from Aspergillus niger ATCC 1015, EIT78655 from Aspergillus oryzae 3.042, EKG13729 from Macrophomina phaseolina MS6, EXU95682 from Metarhizium robertsii, EYB27998 from Fusarium graminearum, GAA83664 from Aspergillus kawachii IFO 4308, GAA83986 from Aspergillus kawachii IFO 4308, GAD99481 from Byssochlamys spectabilis No. 5, GAO83049 from Aspergillus udagawae, GAO85956 from Aspergillus udagawae, GAO85985 from Aspergillus udagawae, GAO89465 from Aspergillus udagawae, GAQ03682 from Aspergillus lentulus, GAQ05405 from Aspergillus lentulus, GAQ05411 from Aspergillus lentulus, GAQ09941 from Aspergillus lentulus, GAQ34046 from Aspergillus niger, KEY81846 from Aspergillus fumigatus var. RP-2014, KEY82996 from Aspergillus fumigatus var. RP-2014, KEY84148 from Aspergillus fumigatus var. RP-2014, KFG80376 from Metarhizium anisopliae, KFG81920 from Metarhizium anisopliae, KFH44079 from Acremonium chrysogenum ATCC 11550, KHN94001 from Metarhizium album ARSEF 1941, KIA75414 from Aspergillus ustus, KID81691 from Metarhizium guizhouense ARSEF 977, KIL84121 from Fusarium avenaceum, KJK74552 from Metarhizium anisopliae BRIP 53293, KJZ71105 from Hirsutella minnesotensis 3608, KJZ73006 from Hirsutella minnesotensis 3608, KJZ80338 from Hirsutella minnesotensis 3608, KKK13519 from Aspergillus rambellii, KKK13733 from Aspergillus ochraceoroseus, KMK56825 from Aspergillus fumigatus Z5, KOM20732 from Ophiocordyceps unilateralis, KOM21072 from Ophiocordyceps unilateralis, KOS19956 from Escovopsis weberi, KOS38981 from Penicillium nordicum, KUL81846 from Talaromyces verruculosus, KYK60562 from Drechmeria coniospora, B6H6U3 from Penicillium chrysogenum ATCC 28089, OAA32941 from Aschersonia aleyrodis RCEF 2490, OAA34864 from Metarhizium rileyi RCEF 4871, OBR09784 from Colletotrichum higginsianum IMI 349063, OCK81419 from Lepidopterella palustris CBS 459.81, ODA80718 from Drechmeria coniospora, XP_681413 from Aspergillus nidulans FGSC A4, XP_746967 from Aspergillus fumigatus Af293, XP_751270 from Aspergillus fumigatus Af293, XP_753197 from Aspergillus fumigatus Af293, XP_001259220 from Aspergillus fischeri NRRL 181, XP_001261883 from Aspergillus fischeri NRRL 181, XP_001262309 from Aspergillus fischeri NRRL 181, XP_001389192 from Aspergillus niger CBS 513.88, XP_001394250 from Aspergillus niger CBS 513.88, XP_001826324 from Aspergillus oryzae RIB40, XP_002378013 from Aspergillus flavus NRRL3357, XP_007813280 from Metarhizium acridum CQMa 102, XP_007814548 from Metarhizium acridum CQMa 102, XP_007816270 from Metarhizium robertsii ARSEF 23, XP_007823686 from Metarhizium robertsii ARSEF 23, XP_009262229 from Fusarium pseudograminearum CS3096, XP_011320986 from Fusarium graminearum PH-1, XP_014541493 from Metarhizium brunneum ARSEF 3297, XP_014573710 from Metarhizium majus ARSEF 297, XP_015406232 from Aspergillus nomius NRRL 13137, XP_016595032 from Penicillium expansum.

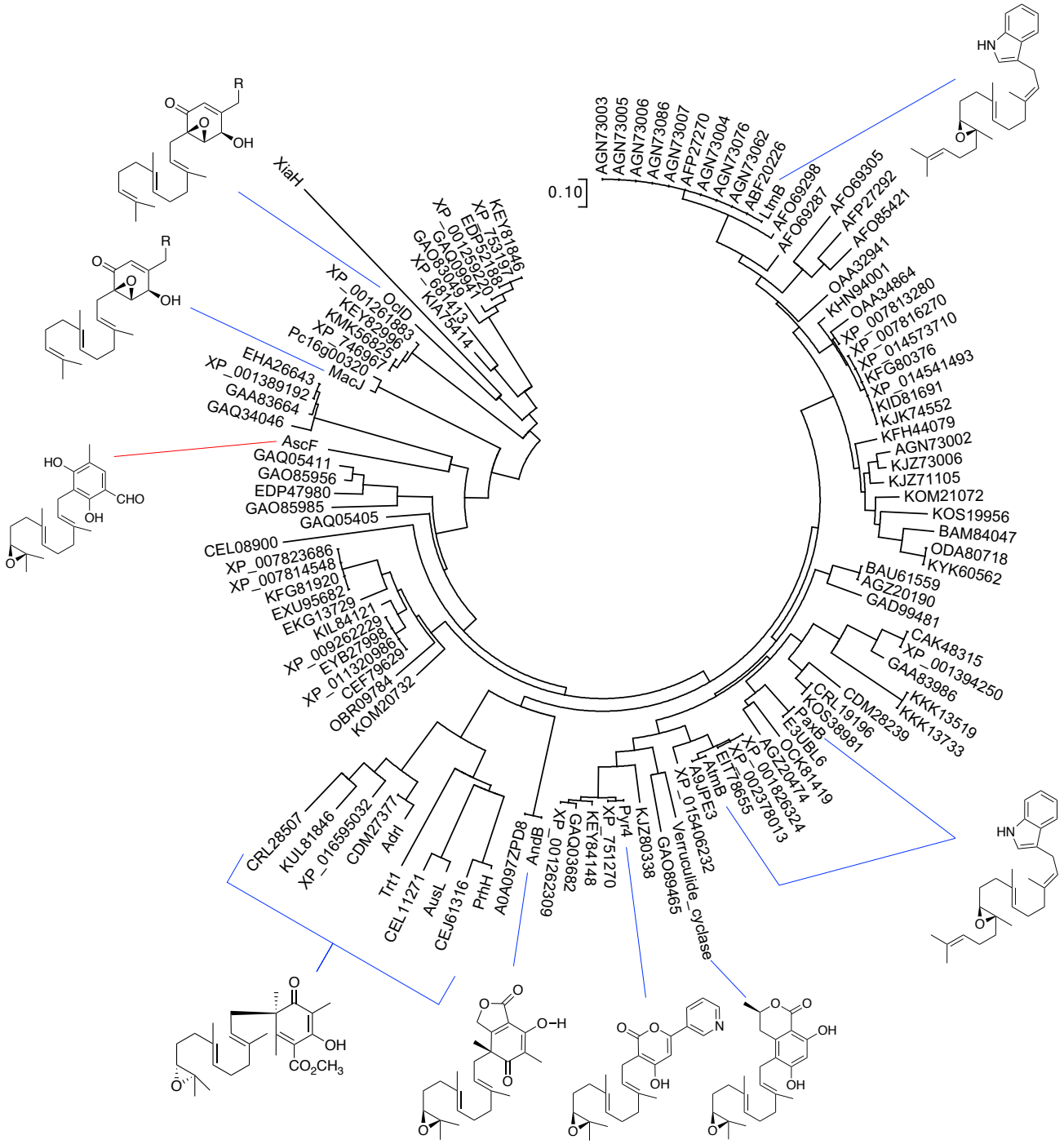
0.10
AGN73003
AGN73005
AGN73006
AGN73086
AGN73007
AFP27270
AGN73004
AGN73076
AGN73062
ABF20226
LtmB
AFO69298
AFO69287
AFO69305
AFP27292
AFO85421
OAA32941
KHN94001
OAA34864
XP_007813280
XP_007816270
XP_014573710
KFG80376
XP_014541493
KID81691
KJK74552
KFH44079
AGN73002
KJZ73006
KJZ71105
KOM21072
KOS19956
BAM84047
ODA80718
KYK60562
BAU61559
AGZ20190
GAD99481
CAK48315
XP_001394250
GAA83986
KKK13519
KKK13733
CDM28239
CRL19196
KOS38981
PaxB
E3UBL6
OCK81419
AGZ20474
XP_001826324
XP_002378013
EIT78655
AtmB
A9JPE3
XP_015406232
Verruculide_cyclase
GAO89465
KJZ80338
Pyr4
XP_751270
KEY84148
GAQ03682
XP_001262309
AnpB
A0A097ZPD8
PrhH
CEJ61316
AusL
CEL11271
Trt1
CDM27377
Adrl
XP_016595032
KUL81846
CRL28507
XiaH
OcID
XP_001261883
KEY82996
KMK56825
XP_746967
Pc16g00320
MacJ
EHA26643
XP_001389192
GAA83664
GAQ34046
AscF
GAQ05411
GAO85956
EDP47980
GAO85985
GAQ05405
CEL08900
XP_007823686
XP_007814548
KFG81920
EXU95682
EKG13729
KIL84121
XP_009262229
EYB27998
XP_011320986
CEF79629
OBR09784
KOM20732
KEY81846
XP_751197
EDP52188
XP_001259220
GAQ09941
GAO83049
XP_681413
KIA75414
HN
O
R
OH
HO
CHO
N
O-H
CO2CH3

7.2. Appendix of Discovery of a Cytochrome P450 for Biosynthesis of Citreohybridonol

NMR Data for Citreohybridonol

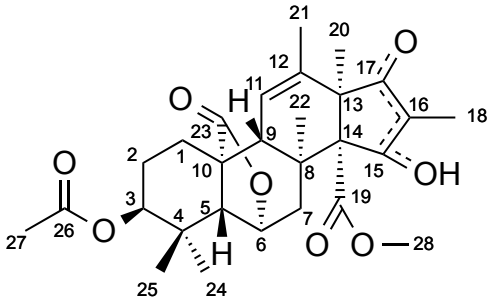

Table 7-8. NMR data for citreohybridonol.

^{1}H NMR: 500 MHz, ^{13}C NMR: 125 MHz (in CD_3OD)

	^{13}C	^{1}H					
position	δ (ppm)	δ (ppm)	intensitiy	multiplicity	HMBC correlation	COSY correlation	NOESY correlation
1	22.1	2.12 (α)	1H	m	3, 5	H-2	H-11
		1.33 (β)	1H	m	2, 3, 5, 10, 23	H-2	H-9
2	23.1	1.69	2H	m	10	H-1α, H-1β, H-3	
3	77.6	4.63	1H	dd (*J* = 3.0, 2.0 Hz)	1, 2, 5, 24, 26	H-2	H-24, H-25
4	35.5						
5	56.3	2.03	1H	brs	1, 4, 7, 9, 10, 23, 24, 25		H-6, H-7β, H-9, H-25
6	79.7	4.85	1H	m	4, 5, 8, 23	H-7α, H-7β	H-5, H-7α, H-7β, H-25
7	38.2	2.50 (α)	1H	dd (*J* = 14.6, 4.5 Hz)	5, 6, 8, 9, 22	H-6	H-6, H-22, H-28
		3.25 (β)	1H	brd (*J* = 14.6 Hz)	8, 14, 22	H-6	H-5, H-6, H-9
8	43.4						
9	53.2	2.40	1H	brt (*J* = 2.5 Hz)	5, 8, 10, 11, 12, 14, 22, 23	H-11, H-21	H-1β, H-5, H-7β, H-11
10	45.1						
11	123.3	5.59	1H	brs	8, 13, 21	H-9, H-21	H-1α, H-9, H-21, H-22
12	139.1						
13	57.3						
14	71.4						
15	191.8*						
16	114.8						
17	196.9*						
18	6.2	1.61	3H	s	15, 16, 17		
19	171.9						
20	17.7	1.26	3H	s	12, 13, 14, 17		H-21, H-28
21	20.4	1.84	3H	t (*J* = 2.0 Hz)	11, 12, 13	H-9, H-11	H-11, H-20
22	24.3	1.31	3H	s	7, 8, 9, 14		H-6α, H-11
23	181.6						
24	22.6	0.88	3H	s	3, 4, 5, 25		H-3, H-25
25	26.5	0.97	3H	s	3, 4, 5, 24		H-3, H-5, H-6, H-24
26	172.0						
27	20.8	2.02	3H	s	26		
28	52.0	3.60	3H	s	19		H-6α, H-20

Note: Two carbons indicated by * were identified in HMBC spectrum

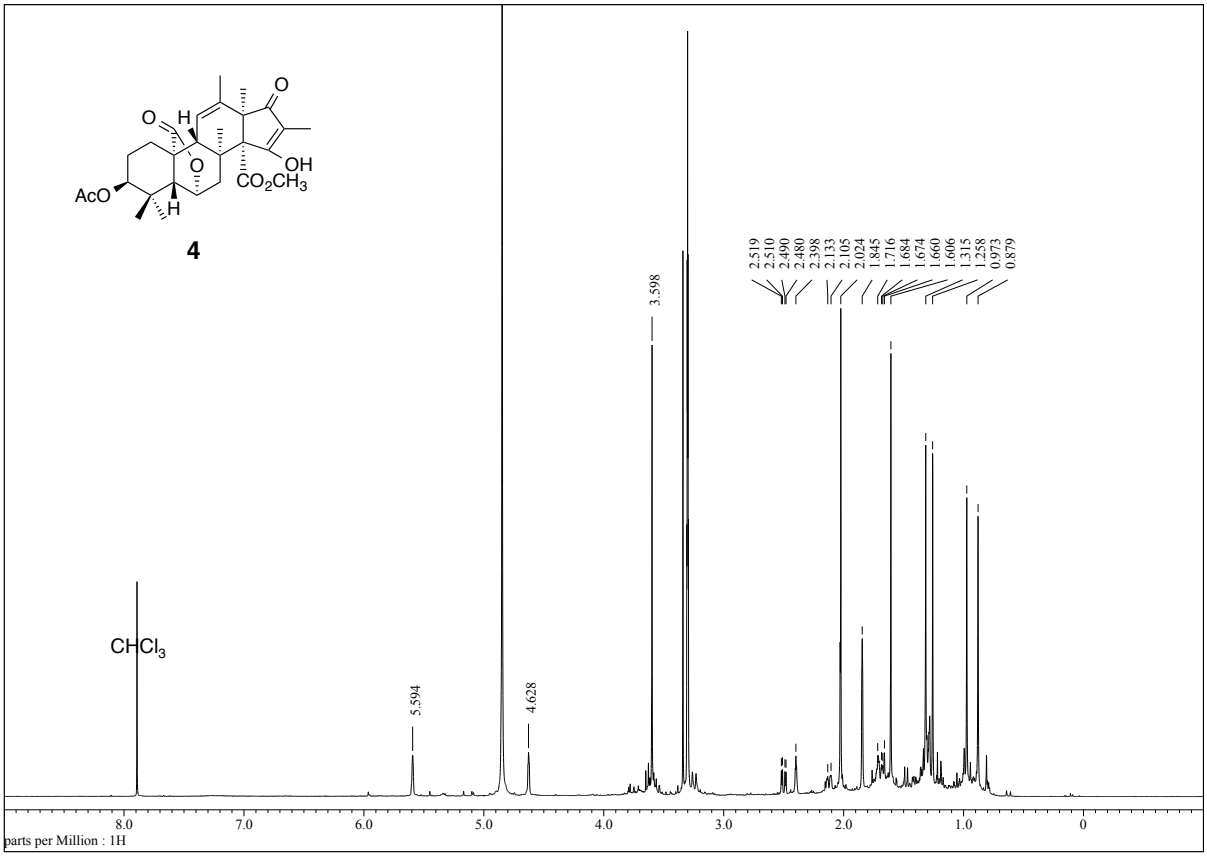

Figure 7-15. ^{1}H NMR spectrum of citreohybridonol.

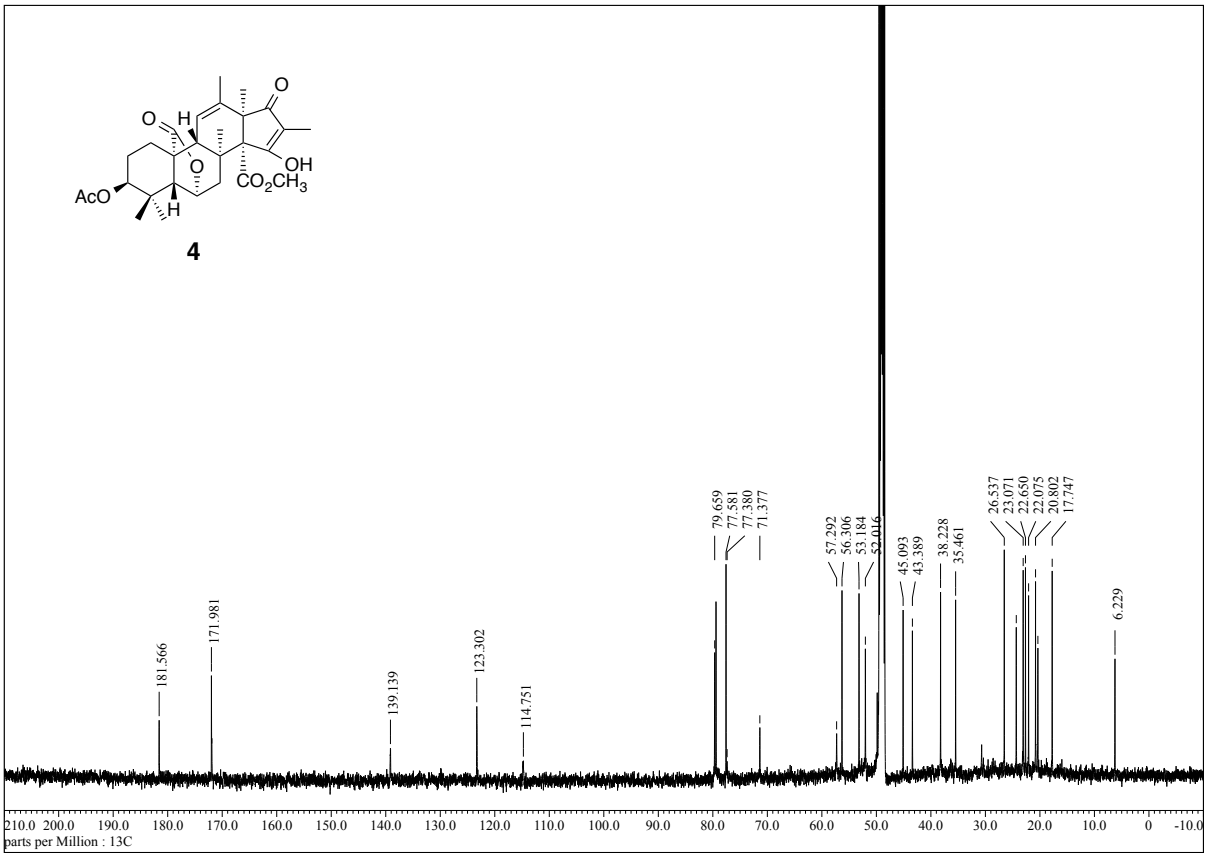

Figure 7-16. ^{13}C NMR spectrum of citreohybridonol.

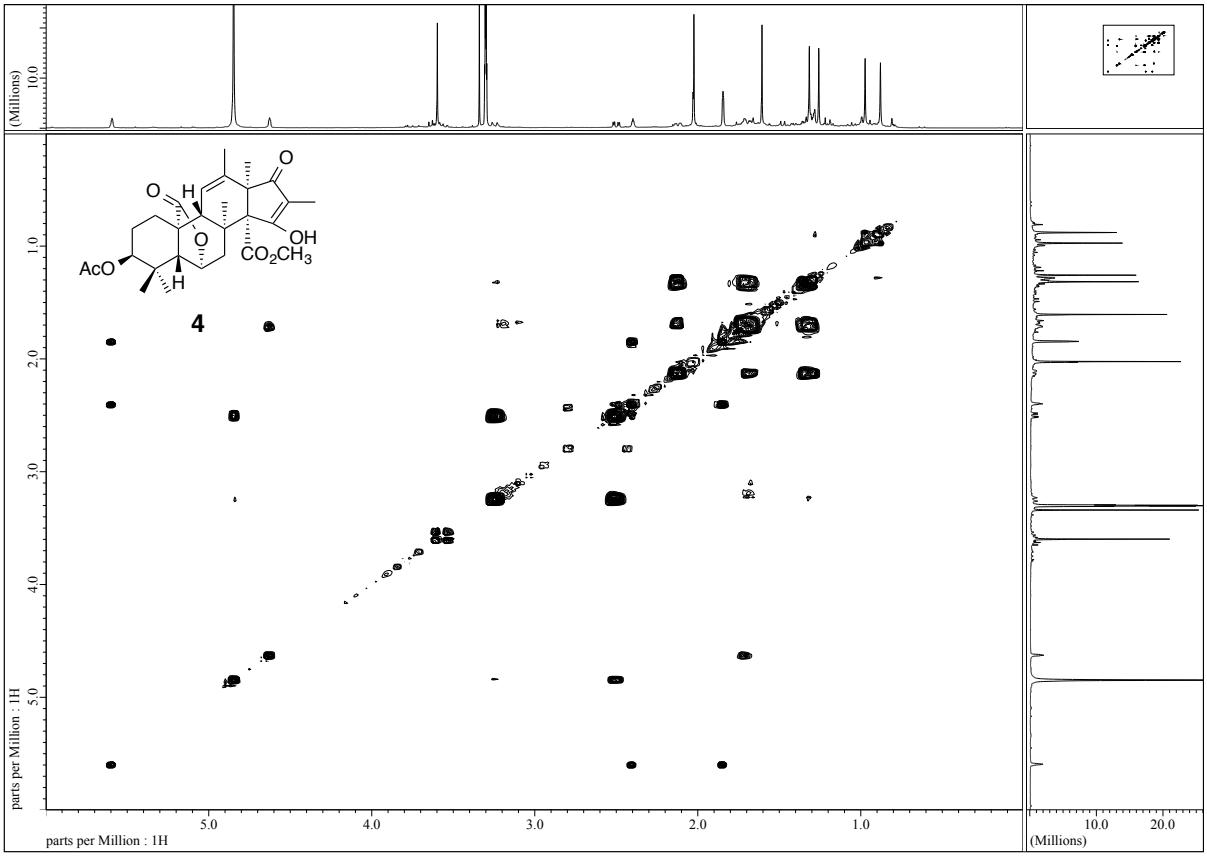

Figure 7-17. ^{1}H-^{1}H COSY NMR spectrum of citreohybridonol.

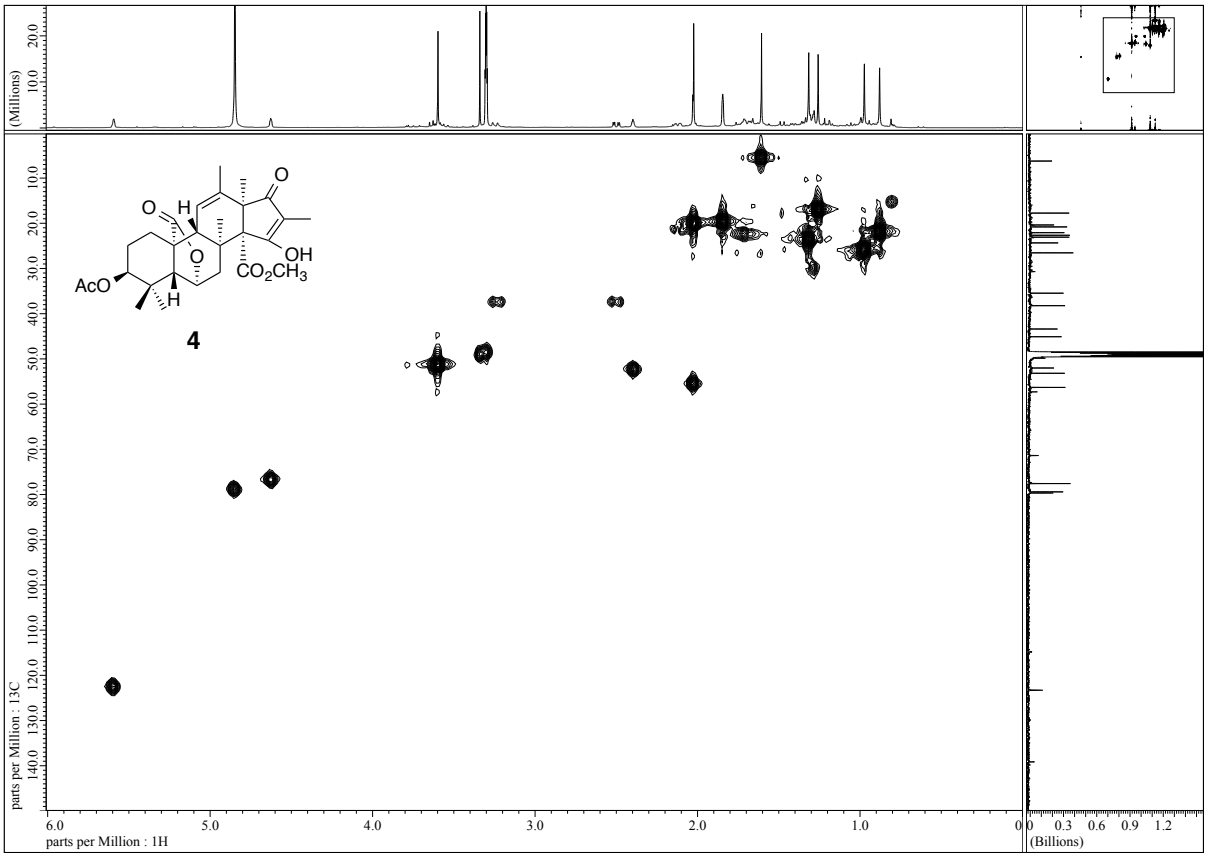

Figure 7-18. HMQC NMR spectrum of citreohybridonol.

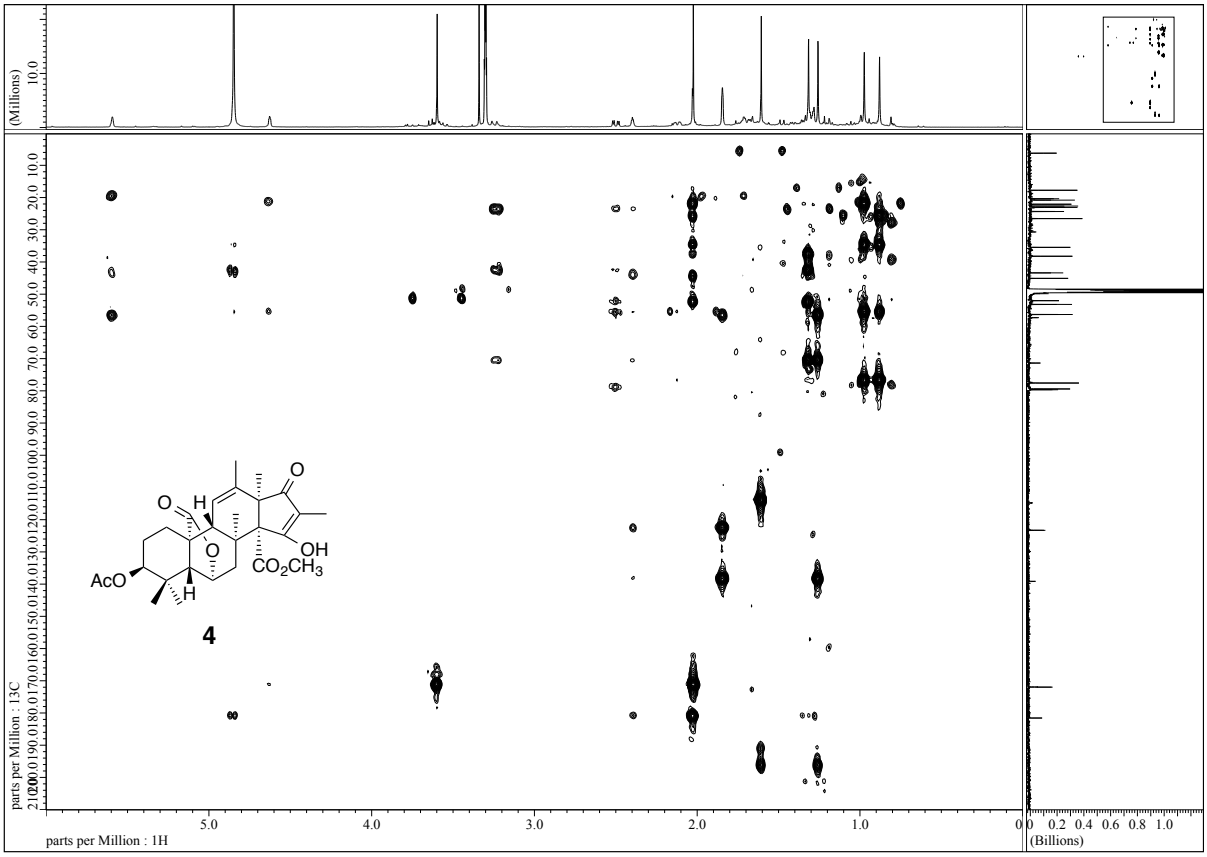

Figure 7-19. HMBC NMR spectrum of citreohybridonol.

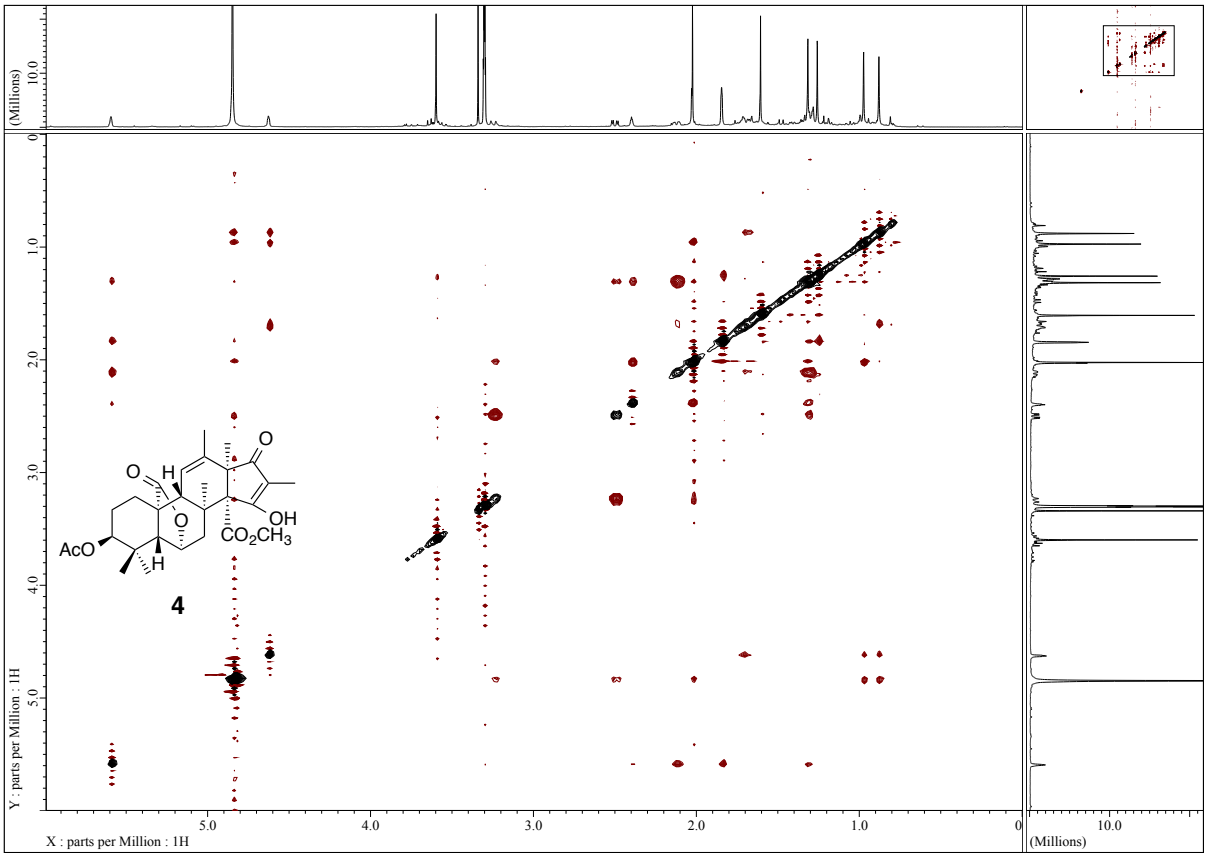

Figure 7-20. NOESY NMR spectrum of citreohybridonol.

NMR Data for 6α-hydroxyandrastin C

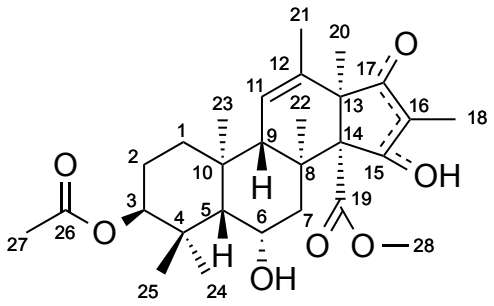

Table 7-9. NMR data for 6α-hydroxyandrastin C.

^{1}H NMR: 500 MHz, ^{13}C NMR: 125 MHz (in CD_3OD)

	^{13}C	^{1}H					
position	δ (ppm)	δ (ppm)	intensitiy	multiplicity	HMBC correlation	COSY correlation	NOESY correlation
1	36.6	1.53 (α)	1H	m		H-2α	H-11
		1.09 (β)	1H	m	3, 10	H-2α, H-2β	H-5, H-9
2	23.5	2.06 (α)	1H	m		H-1α, H-1β	H-3, H-23, H-24
		1.55 (β)	1H	m		H-1α	H-3
3	81.1	4.56	1H	t (*J* = 3.5 Hz)	1, 4, 5, 24, 26	H-2α, H-2β	H-2α, H-2β, H-24, H-25
4	38.6						
5	50.9	1.40	1H	d (*J* = 1.7 Hz)	1, 4, 6, 10, 23, 24	H-6	H-1β, H-6, H-7β, H-9, H-25
6	68.8	4.38	1H	m	4, 7, 10	H-5, H-7α, H-7β	H-5, H-7α, H-7β, H-25
7	42.1	2.36 (α)	1H	dd (*J* = 14.6, 2.2 Hz)	5, 6, 8, 9, 22	H-6	H-6, H-22
		3.00 (β)	1H	dd (*J* = 14.6, 3.7 Hz)	8, 22	H-6	H-5, H-6, H-9
8	42.7						
9	54.9	1.86	1H	brt (*J* = 2.2 Hz)	8, 10, 11, 12, 14, 22, 23	H-11, H-21	H-1β, H-5, H-7β, H-11
10	37.6						
11	126.1	5.43	1H	brs	8, 10, 13, 21	H-9, H-21	H-1α, H-9, H-21, H-23
12	136.3						
13	57.9						
14	69.4						
15	187.8*						
16	114.2						
17	201.6*						
18	6.3	1.58	3H	s	15, 16, 17		
19	172.1						
20	16.2	1.19	3H	s	12, 13, 14, 17		H-21, H-22, H-28
21	19.9	1.80	3H	brs	11, 12, 13	H-9, H-11	H-11, H-20
22	19.3	1.59	3H	s	7, 8, 9, 14		H-6α, H-20, H-23
23	18.7	1.29	3H	s	1, 5, 9, 10		H-2α, H-11, H-22
24	24.2	1.30	3H	s	3, 4, 5, 25		H-2α, H-3, H-25
25	28.1	0.94	3H	s	3, 4, 5, 24		H-3, H-5, H-6, H-24
26	172.5						
27	21.2	2.01	3H	s	26		
28	52.0	3.56	3H	s	19		H-20

Note: Two carbons indicated by * were identified in HMBC spectrum

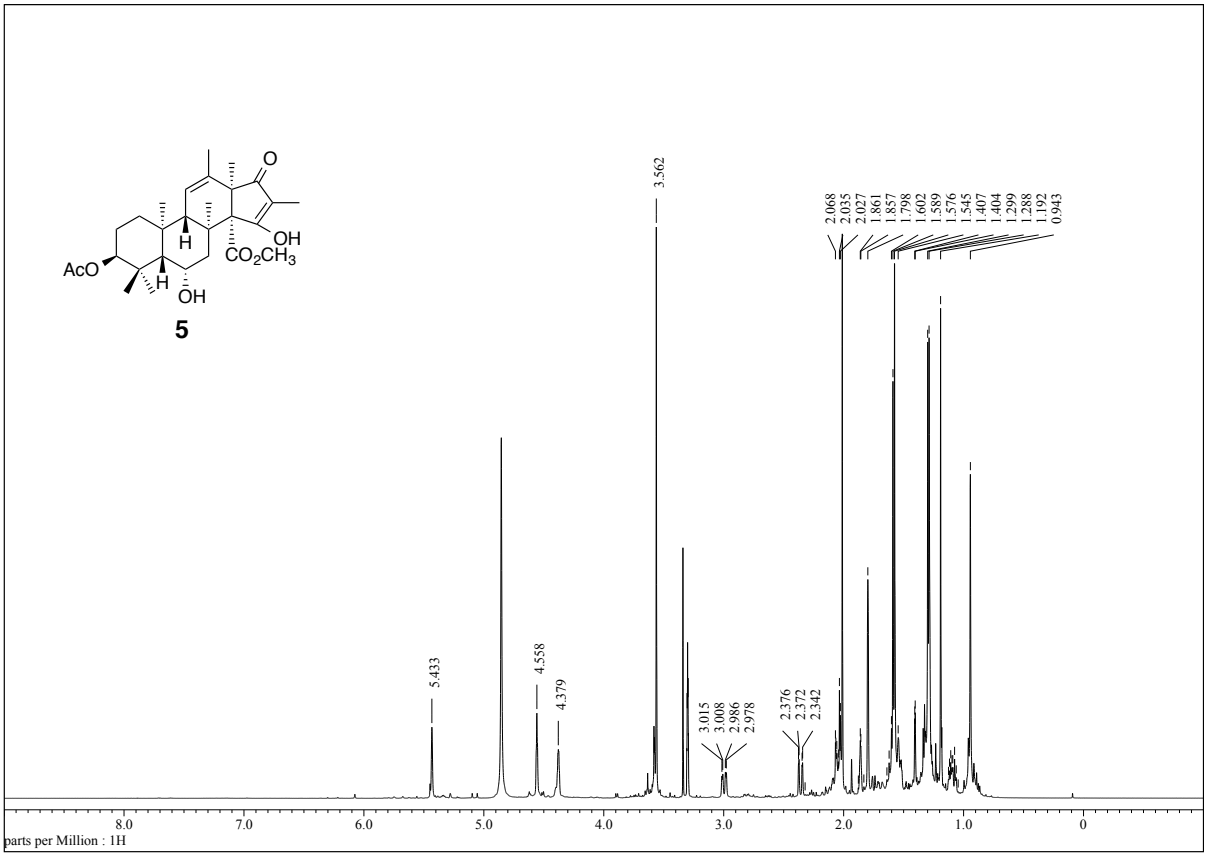

Figure 7-21. ^{1}H NMR spectrum of 6α-hydroxyandrastin C.

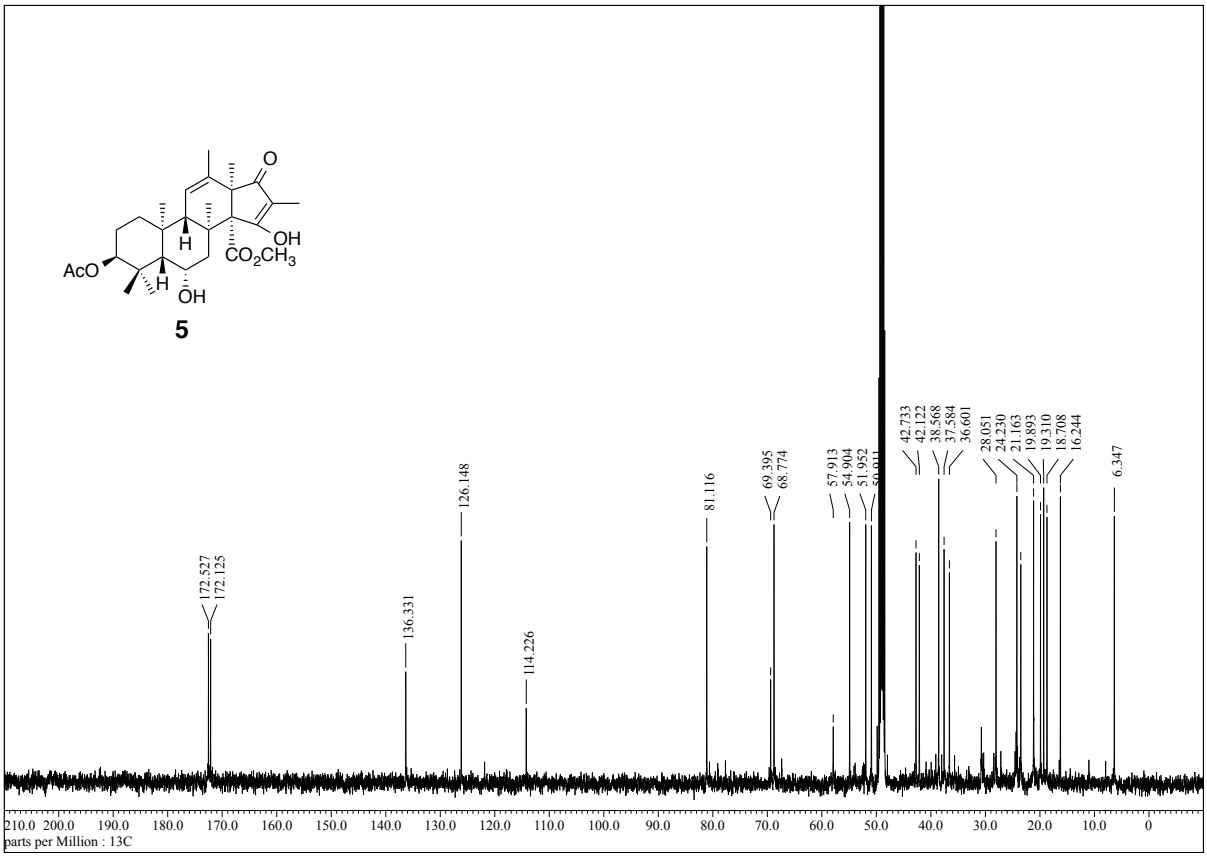

Figure 7-22. ^{13}C NMR spectrum of 6α-hydroxyandrastin C.

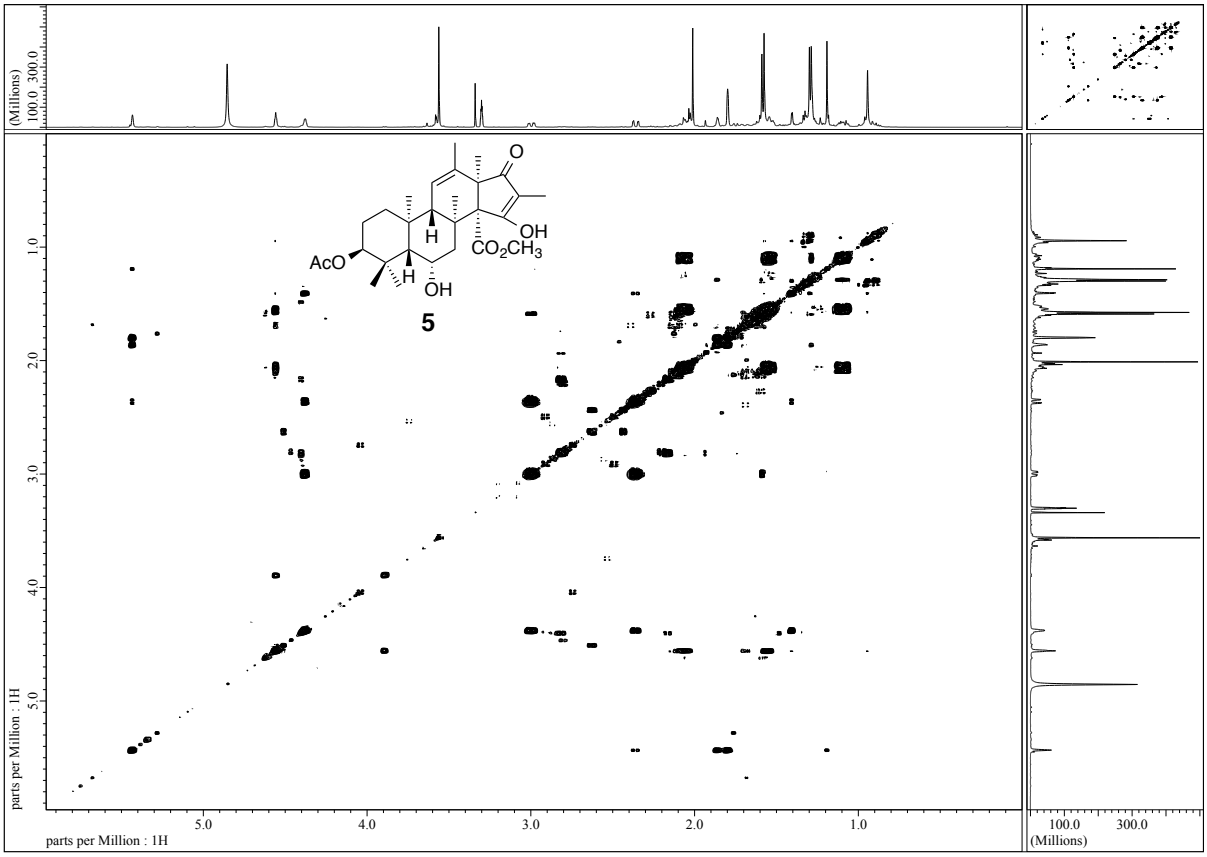

Figure 7-23. ^{1}H-^{1}H COSY spectrum of 6α-hydroxyandrastin C.

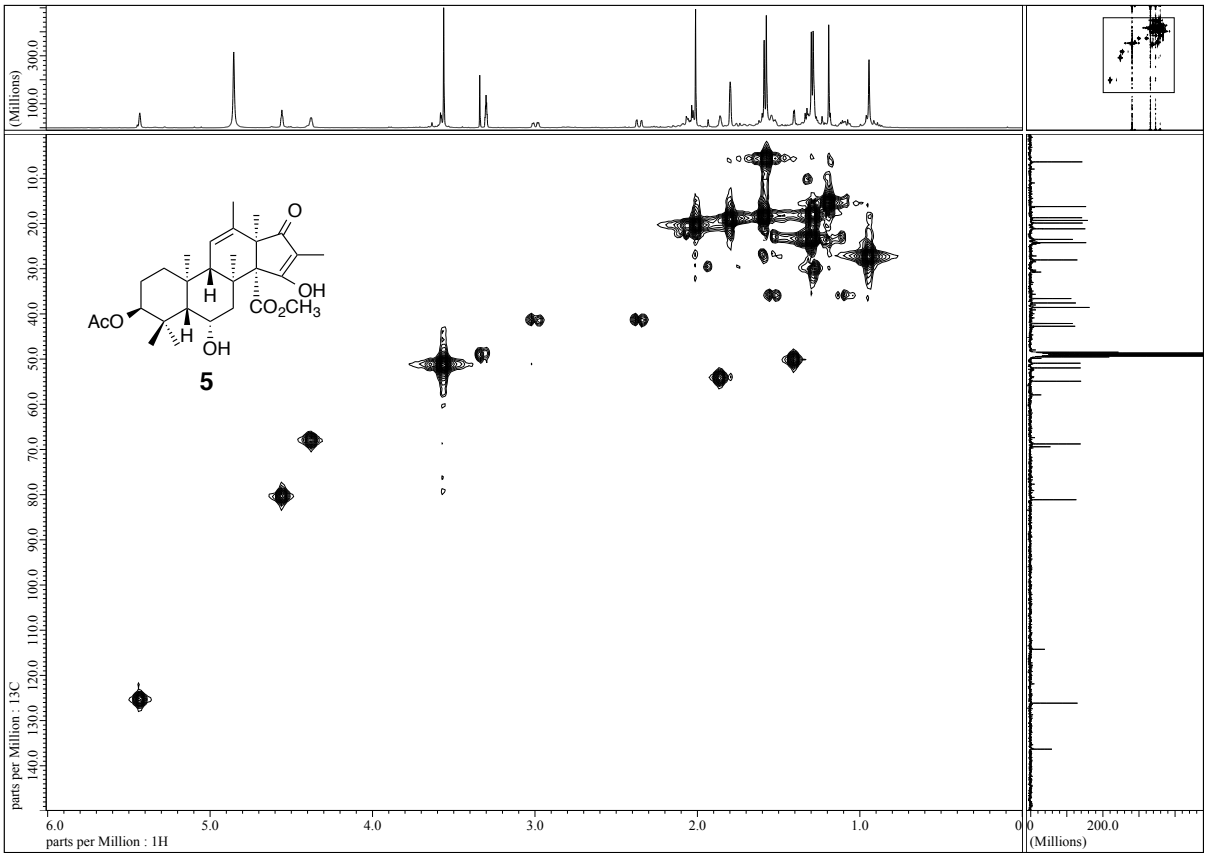

Figure 7-24. HMQC spectrum of 6α-hydroxyandrastin C.

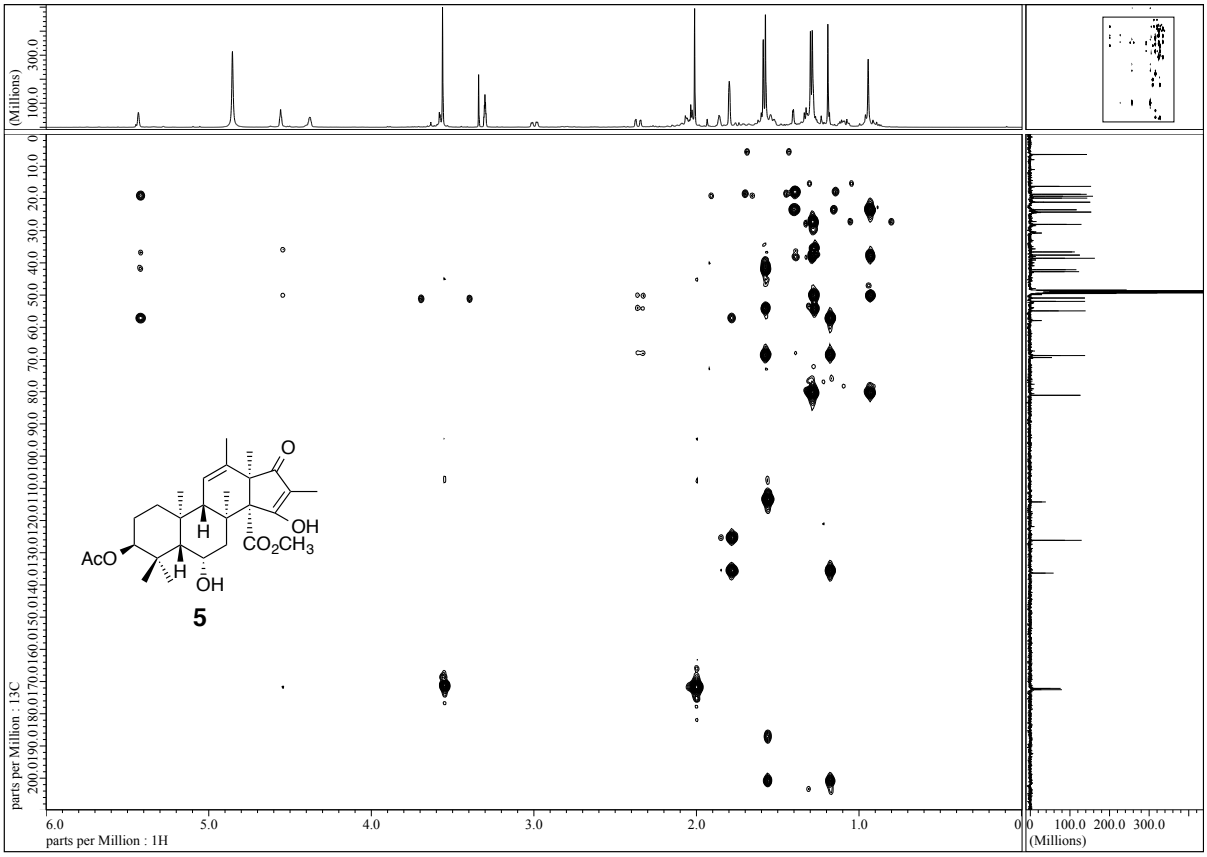

Figure 7-25. HMBC spectrum of 6α-hydroxyandrastin C.

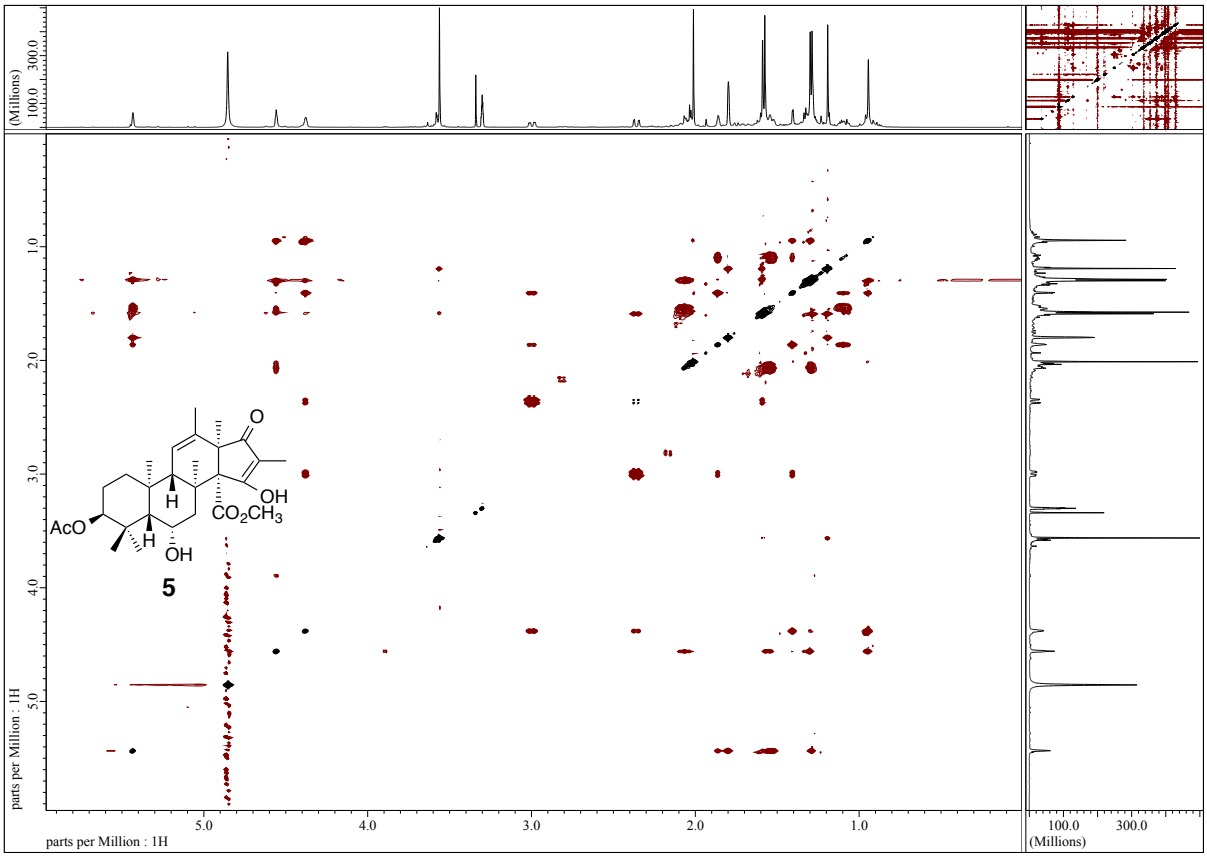

Figure 7-26. NOESY spectrum of 6α-hydroxyandrastin C.

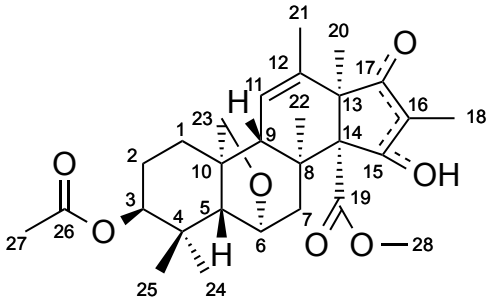

Table 7-10. NMR data for deoxocitreohybridonol.

^{1}H NMR: 500 MHz, ^{13}C NMR: 125 MHz (in CD_3OD)

	^{13}C	^{1}H					
position	δ (ppm)	δ (ppm)	intensitiy	multiplicity	HMBC correlation	COSY correlation	NOESY correlation
1	23.0	1.68 (α)	1H	m			
		1.33 (β)	1H	m	10	H-2α	H-9
2	22.9	1.88 (α)	1H	m		H-1β, H-3	H-3, H-23α
		1.66 (β)	1H	m		H-3	
3	78.6	4.62	1H	t (*J* = 3.0 Hz)	1, 2	H-2α, H-2β	H-2α, H-24, H-25
4	35.3						
5	55.8	1.77	1H	brs	1, 4, 7, 9, 10, 23, 24, 25		H-6, H-7β, H-9, H-25
6	81.3	4.38	1H	brd (*J* = 4.0 Hz)	8	H-7α, H-7β	H-5, H-7α, H-7β, H-24, H-25
7	41.5	2.37 (α)	1H	dd (*J* = 14.2, 4.0 Hz)	5, 22	H-6	H-6, H-22
		3.17 (β)	1H	brd (*J* = 14.2 Hz)	8, 14, 22	H-6	H-5, H-6
8	44.3						
9	53.9	2.33	1H	brs	5, 22	H-11, H-21	H-1β, H-5
10	45.9						
11	123.9	5.44	1H	brs	13, 21	H-9, H-21	H-21
12	140.1						
13	57.5						
14	71.8						
15	201.3						
16	111.2						
17	202.3						
18	7.0	1.53	3H	s	15, 16, 17		
19	174.0						
20	17.3	1.20	3H	s	12, 13, 14, 17		H-21, H-22, H-28
21	21.0	1.88	3H	t (*J* = 2.0 Hz)	11, 12, 13	H-9, H-11	H-11, H-20
22	21.2	1.51	3H	s	7, 8, 9, 14		H-6α, H-20, H-23β
23	70.2	3.60 (α)	1H	d (*J* = 8.5 Hz)	9		H-2α, H-24
		3.78 (β)	1H	d (*J* = 8.5 Hz)	5, 6, 9		H-22
24	22.9	1.01	3H	s	3, 4, 5, 25		H-3, H-6, H-23α
25	28.2	0.93	3H	s	3, 4, 5, 24		H-3, H-5, H-6
26	172.6						
27	21.0	2.04	3H	s	26		
28	51.3	3.51	3H	s	19		H-20

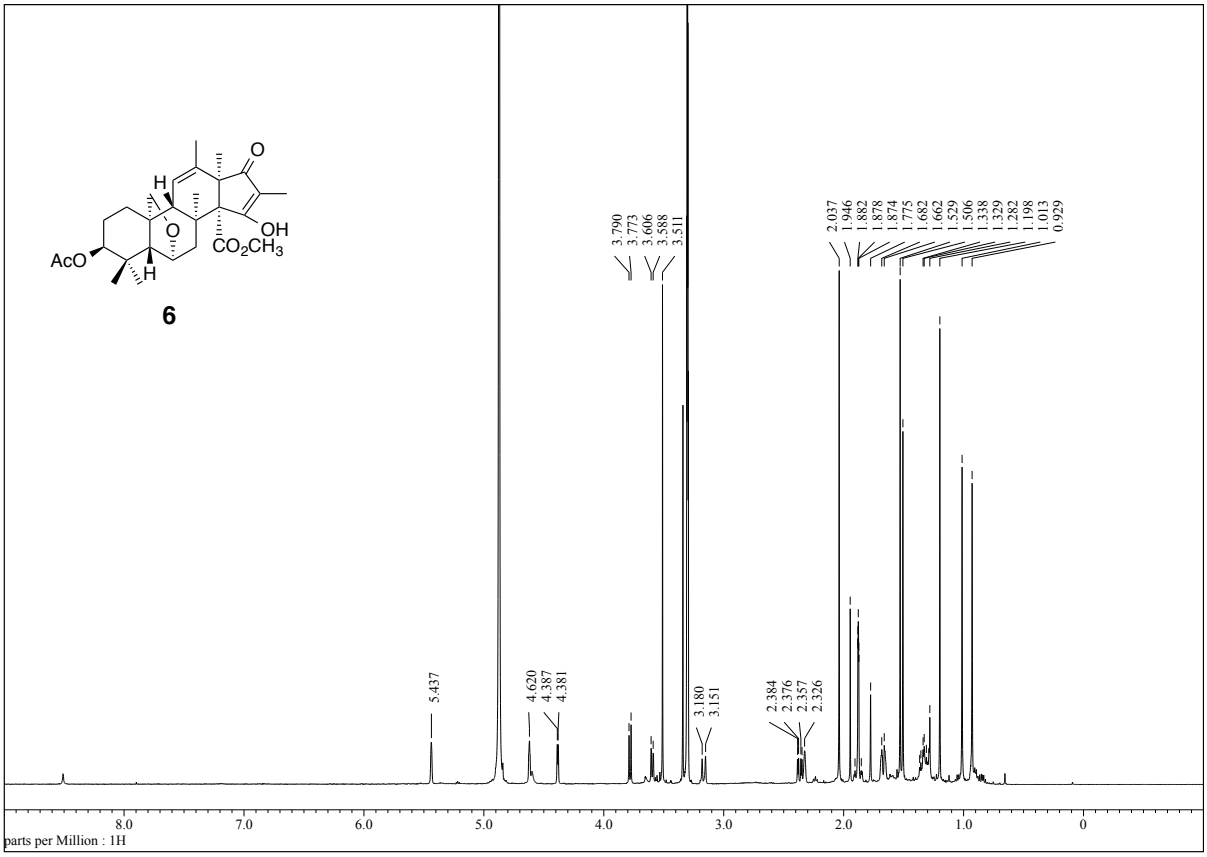

Figure 7-27. ^{1}H NMR spectrum of deoxocitreohybridonol.

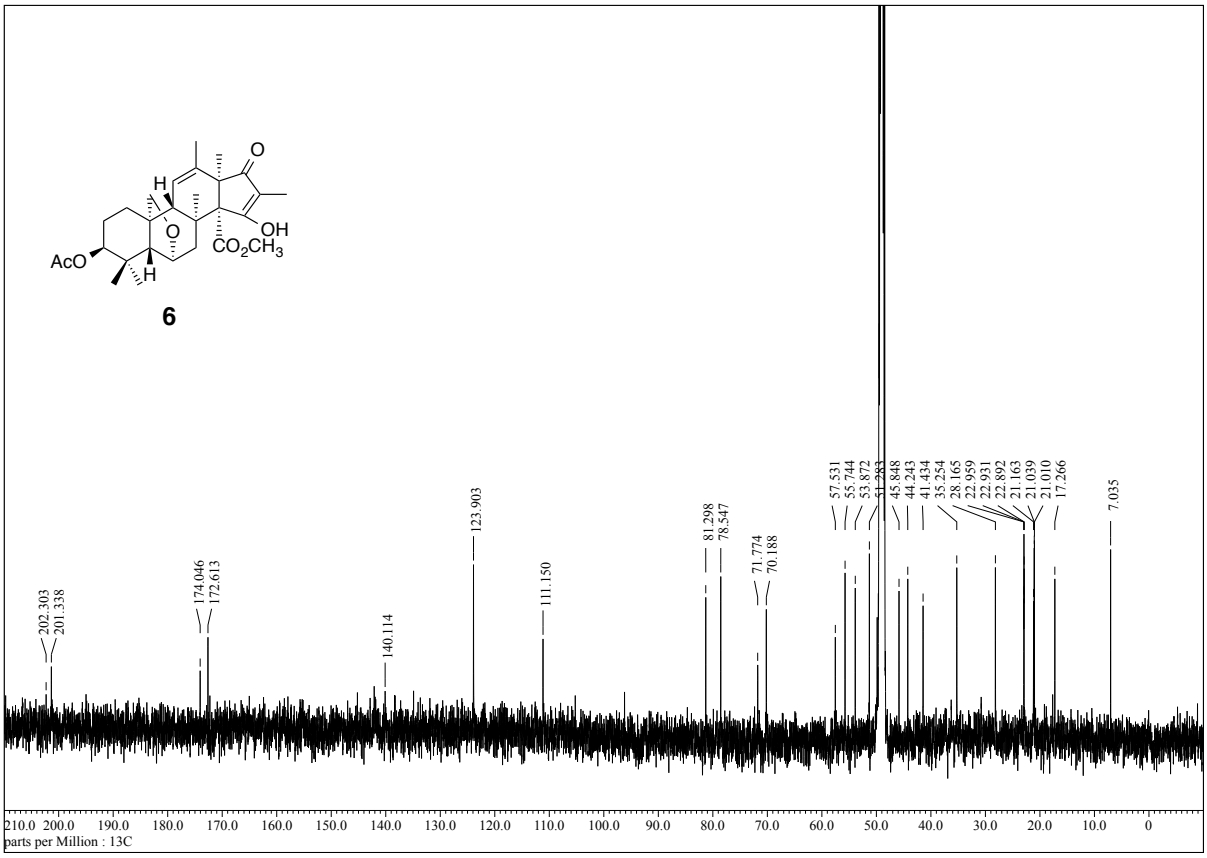

Figure 7-28. ^{13}C NMR spectrum of deoxocitreohybridonol.

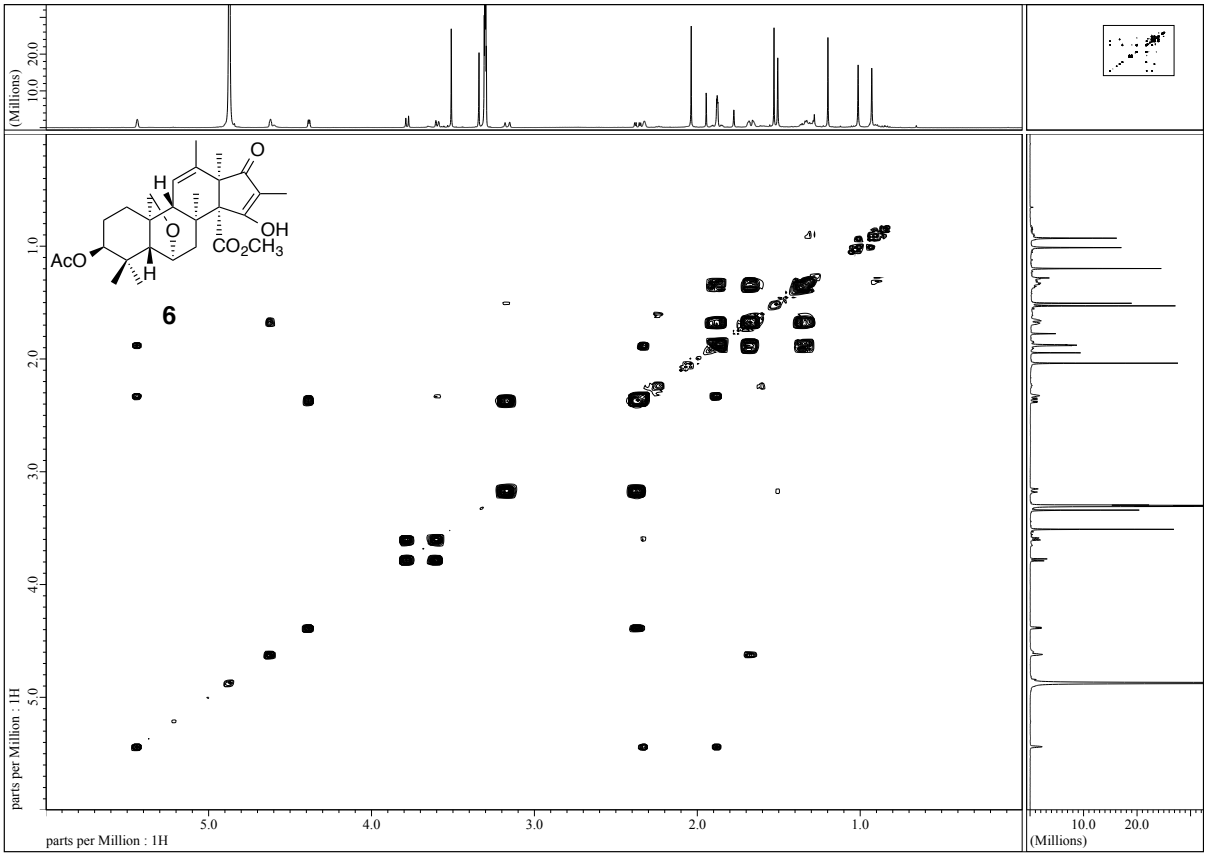

Figure 7-29. ^{1}H-^{1}H COSY spectrum of deoxocitreohybridonol.

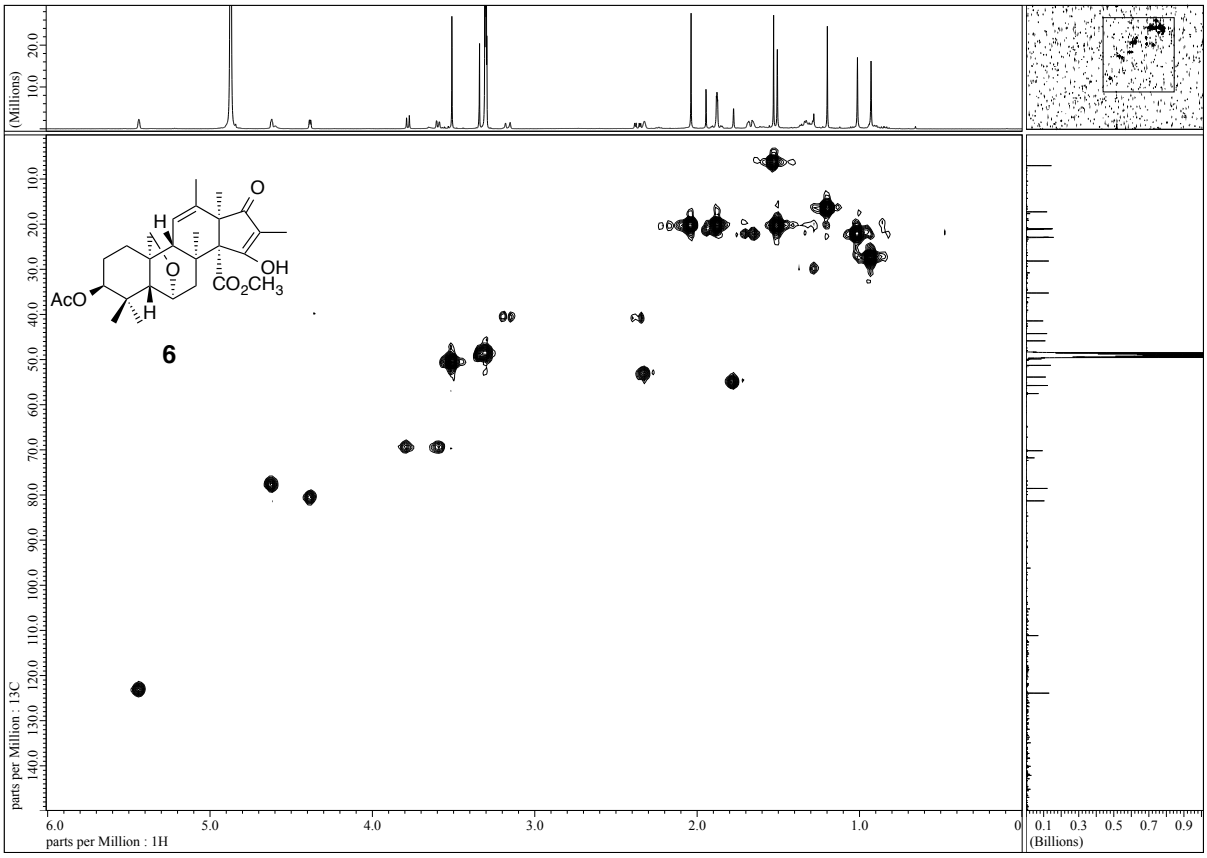

Figure 7-30. HMQC spectrum of deoxocitreohybridonol.

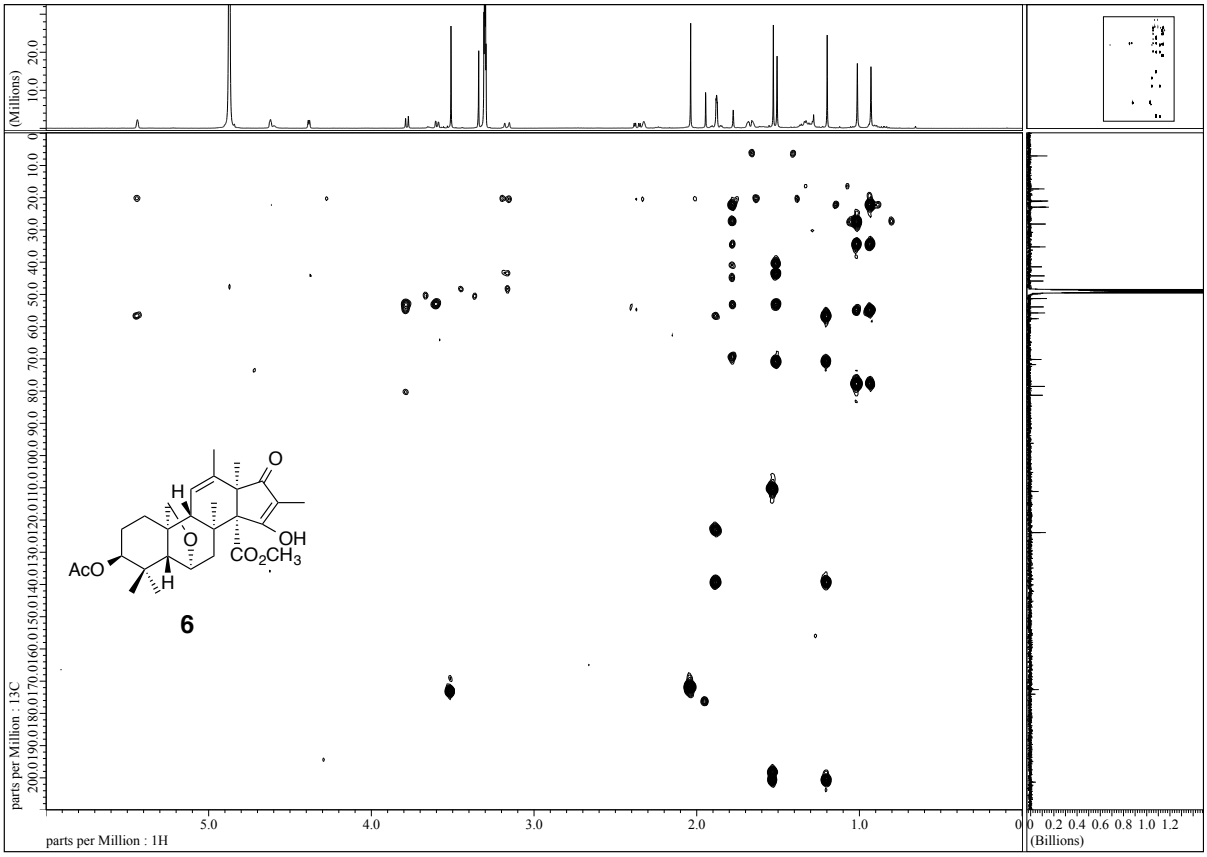

Figure 7-31. HMBC spectrum of deoxocitreohybridonol.

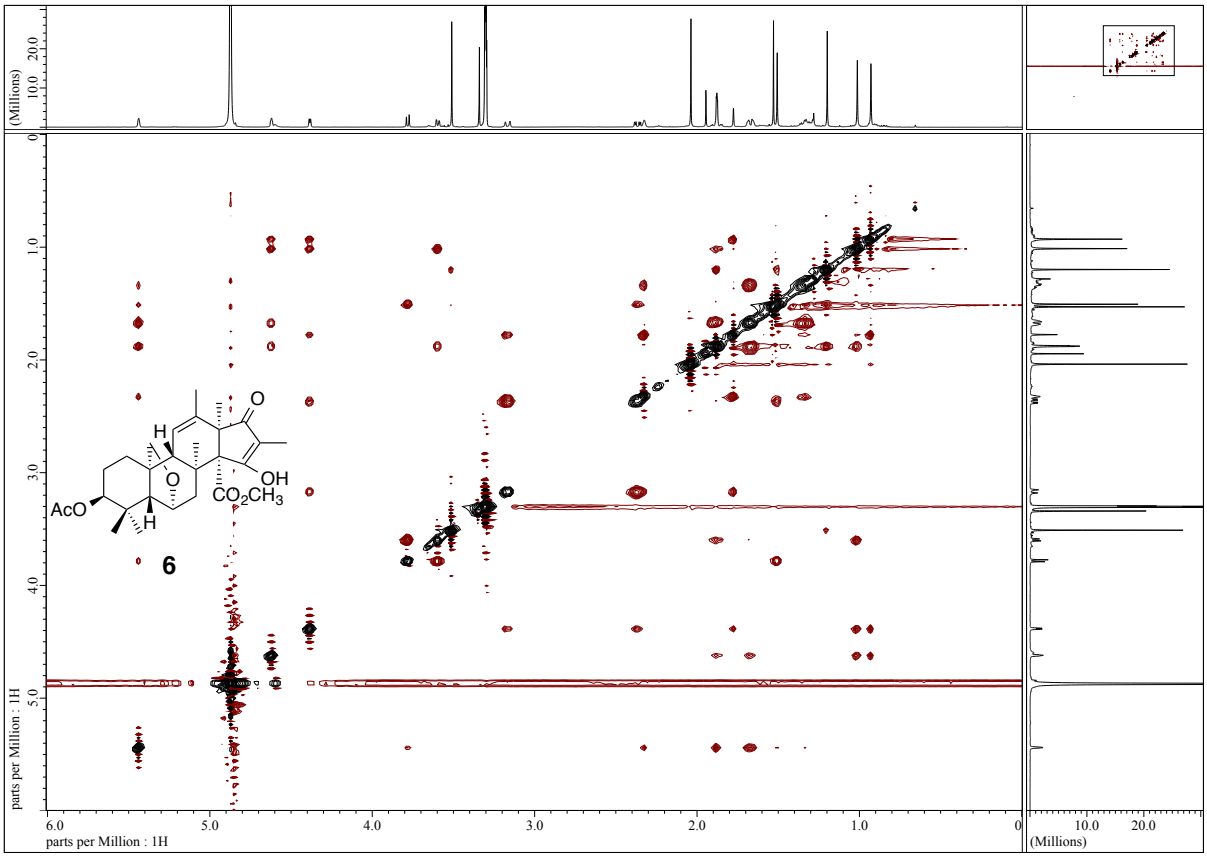

Figure 7-32. NOESY spectrum of deoxocitreohybridonol.

NMR Data for dihydrocitreohybridonol

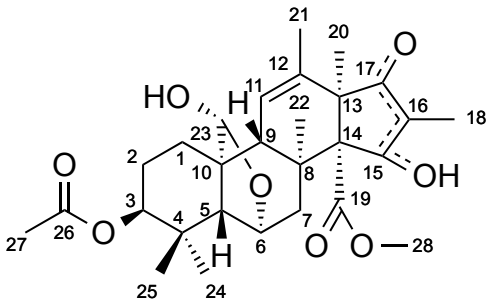

Table 7-11. NMR data for dihydrocitreohybridonol.

^{1}H NMR: 500 MHz, ^{13}C NMR: 125 MHz (in CD_3OD)

	^{13}C	^{1}H					
position	δ (ppm)	δ (ppm)	intensitiy	multiplicity	HMBC correlation	COSY correlation	NOESY correlation
1	23.6	1.82 (α)	1H	m	3, 9	H-2α, H-2β	H-11
		1.22 (β)	1H	td (*J* = 13.6, 5.7 Hz)	9, 10, 23	H-2α, H-2β	H-9
2	25.4	2.17 (α)	1H	m		H-1α, H-1β, H-3	H-3, H-24
		1.62 (β)	1H	m		H-1α, H-1β, H-3	H-3
3	79.4	4.63	1H	dd (*J* = 4.0, 2.0 Hz)		H-2α, H-2β	H-2α, H-2β, H-24, H-25
4	34.8						
5	55.6	1.86	1H	brs	1, 4, 7, 9, 10, 23, 24, 25	H-6	H-6, H-7β, H-9, H-24, H-25
6	79.5	4.46	1H	brd (J = 3.4 Hz)	8, 10	H-5, H-7α, H-7β	H-5, H-7α, H-7β, H-24, H-25
7	41.2	2.33 (α)	1H	dd (*J* = 13.6, 4.0 Hz)		H-6	H-6, H-22
		2.85 (β)	1H	brd (*J* = 13.6 Hz)	8, 22	H-6	H-5, H-6
8	44.2						
9	54.7	2.28	1H	brt (*J* = 2.8 Hz)	10, 14, 23	H-11, H-21	H-1β, H-5, H-11
10	48.1						
11	125.0	5.55	1H	brs	13, 21	H-9, H-21	H-1α, H-9, H-21, H-22, H-23
12	138.7						
13	58.1						
14	71.2						
15	193.1*						
16	113.4						
17	200.0*						
18	6.6	1.57	3H	s	15, 16, 17		
19	172.8						
20	17.0	1.19	3H	s	12, 13, 14, 17		H-22, H-28
21	20.5	1.84	3H	t (*J* = 1.7 Hz)	11, 12, 13	H-9, H-11	H-11
22	21.0	1.50	3H	s	7, 8, 9, 14		H-6α, H-11, H-23
23	100.9	5.23	1H	s	5, 6, 9, 10		H-11, H-22
24	22.3	1.15	3H	s	3, 4, 5, 25		H-2α, H-3, H-6, H-25
25	28.9	0.94	3H	s	3, 4, 5, 24		H-3, H-5, H-6, H-24
26	172.6						
27	21.0	2.02	3H	s	26		
28	51.7	3.54	3H	s	19		H-20

Note: Two carbons indicated by * were identified in HMBC spectrum

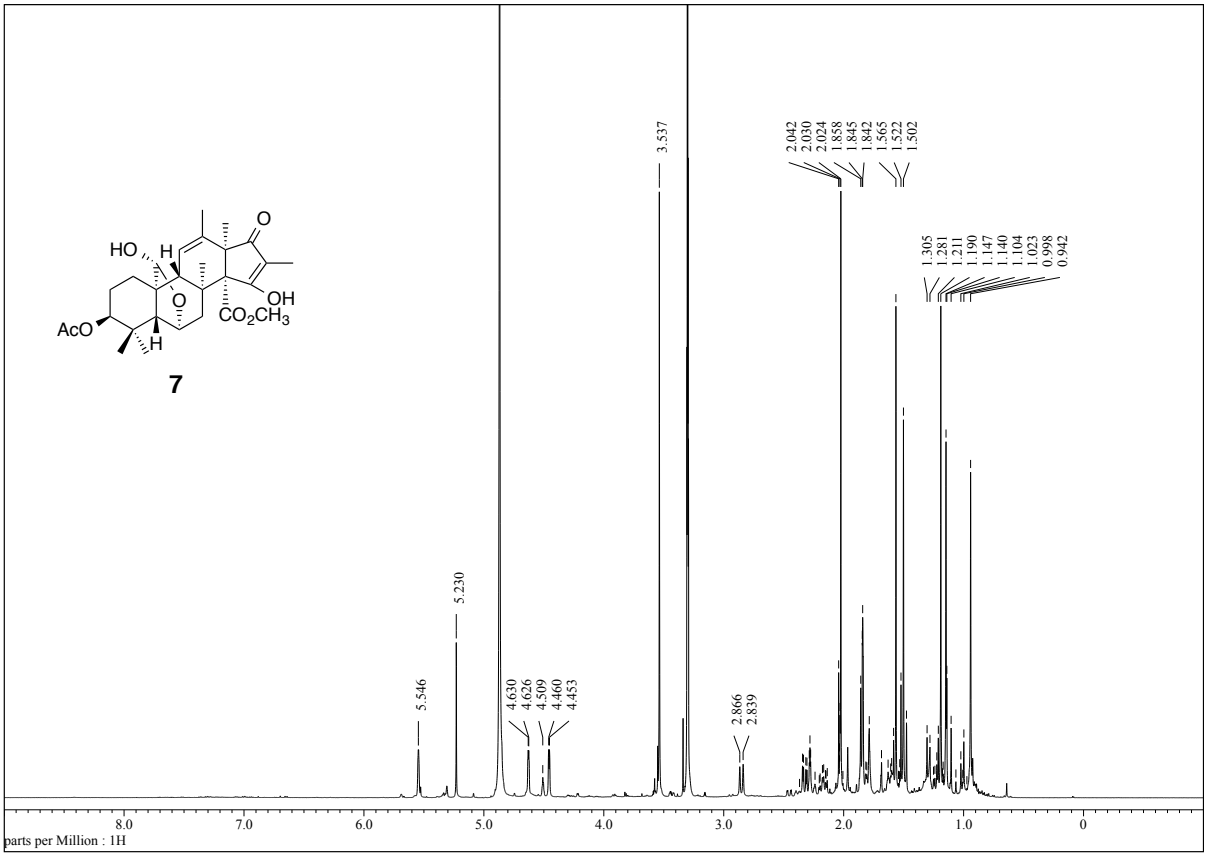

Figure 7-33. ^{1}H NMR spectrum of dihydrocitreohybridonol.

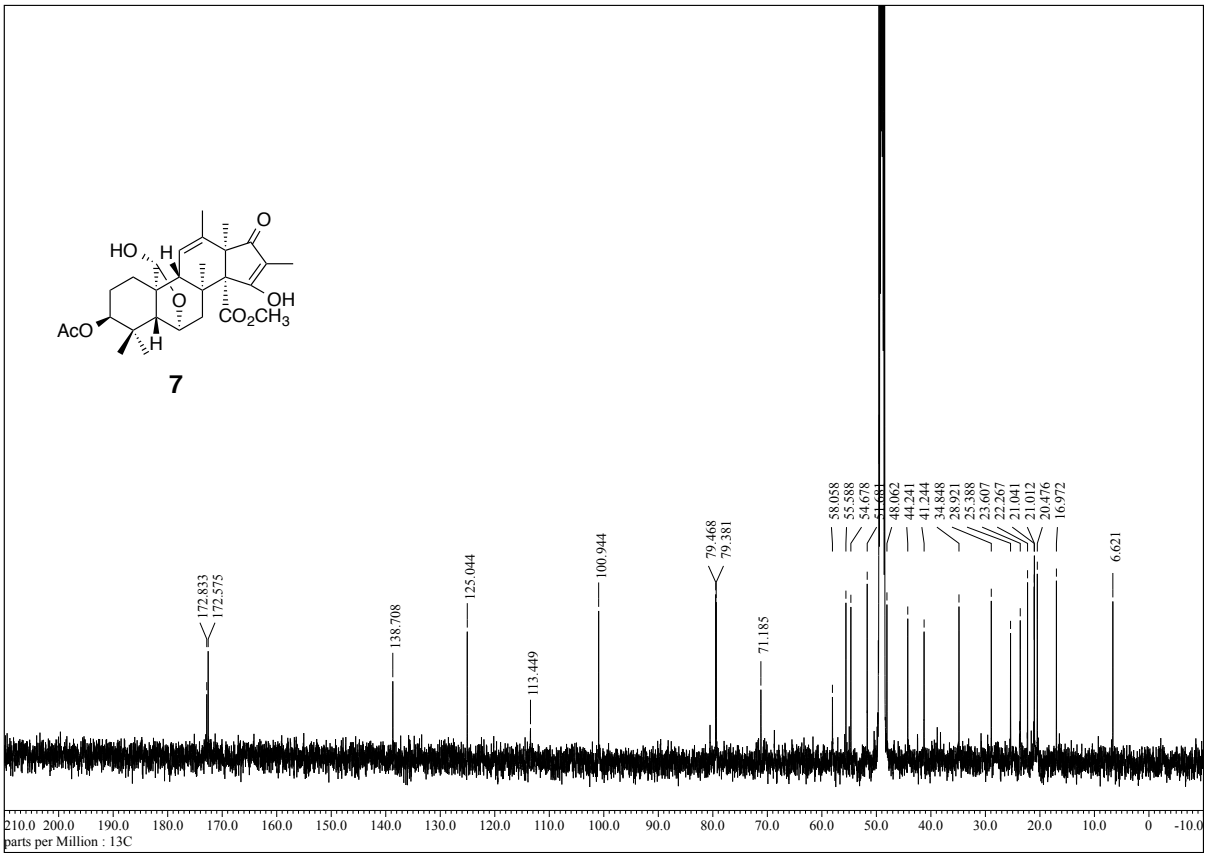

Figure 7-34. ^{13}C NMR spectrum of dihydrocitreohybridonol.

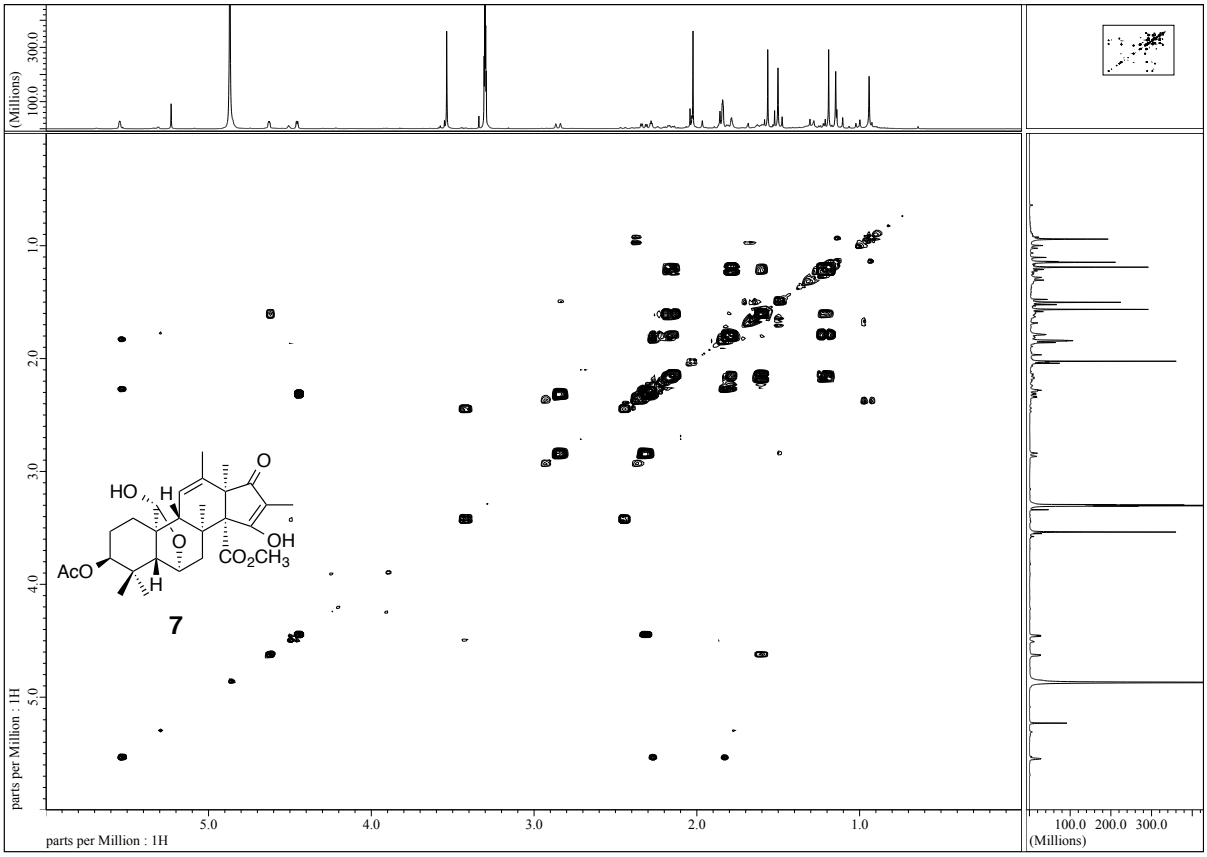

Figure 7-35. ^{1}H-^{1}H COSY spectrum of dihydrocitreohybridonol.

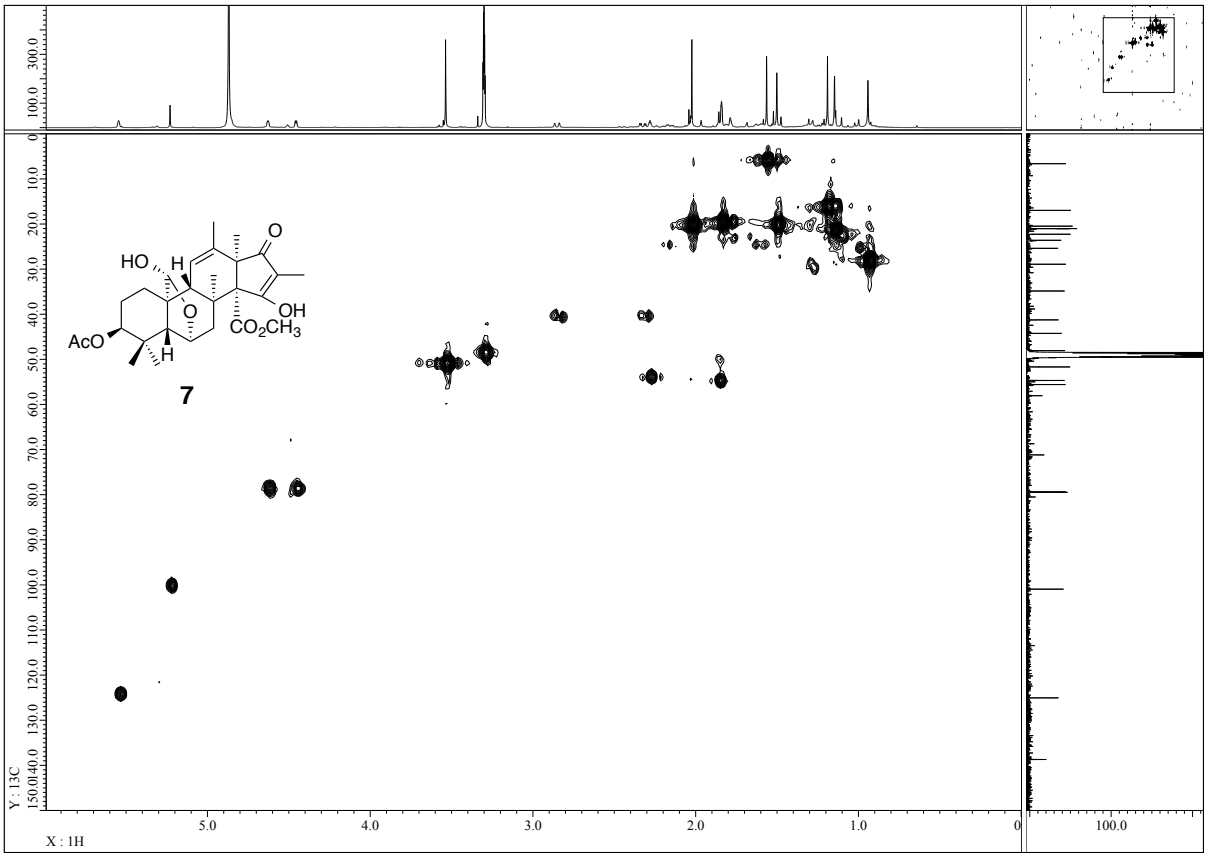

Figure 7-36. HMQC spectrum of dihydrocitreohybridonol.

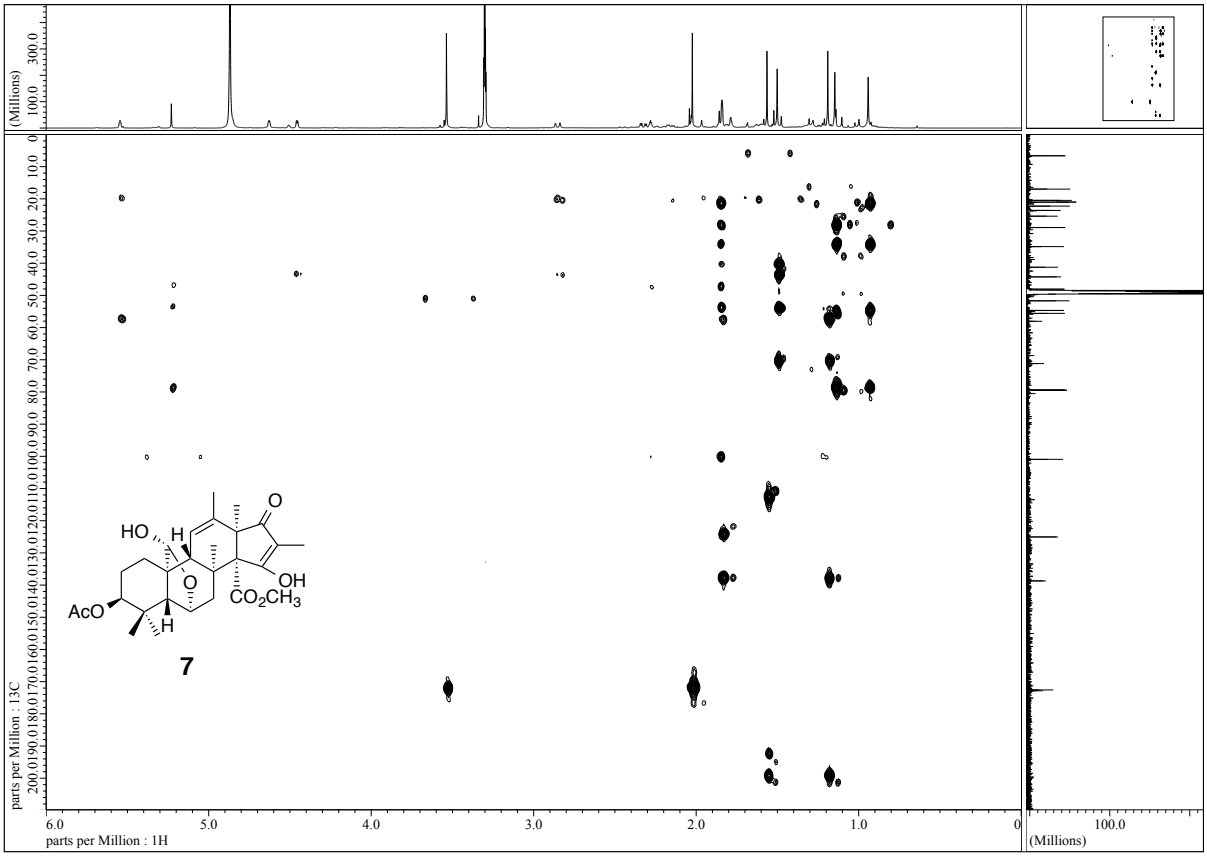

Figure 7-37. HMBC spectrum of dihydrocitreohybridonol.

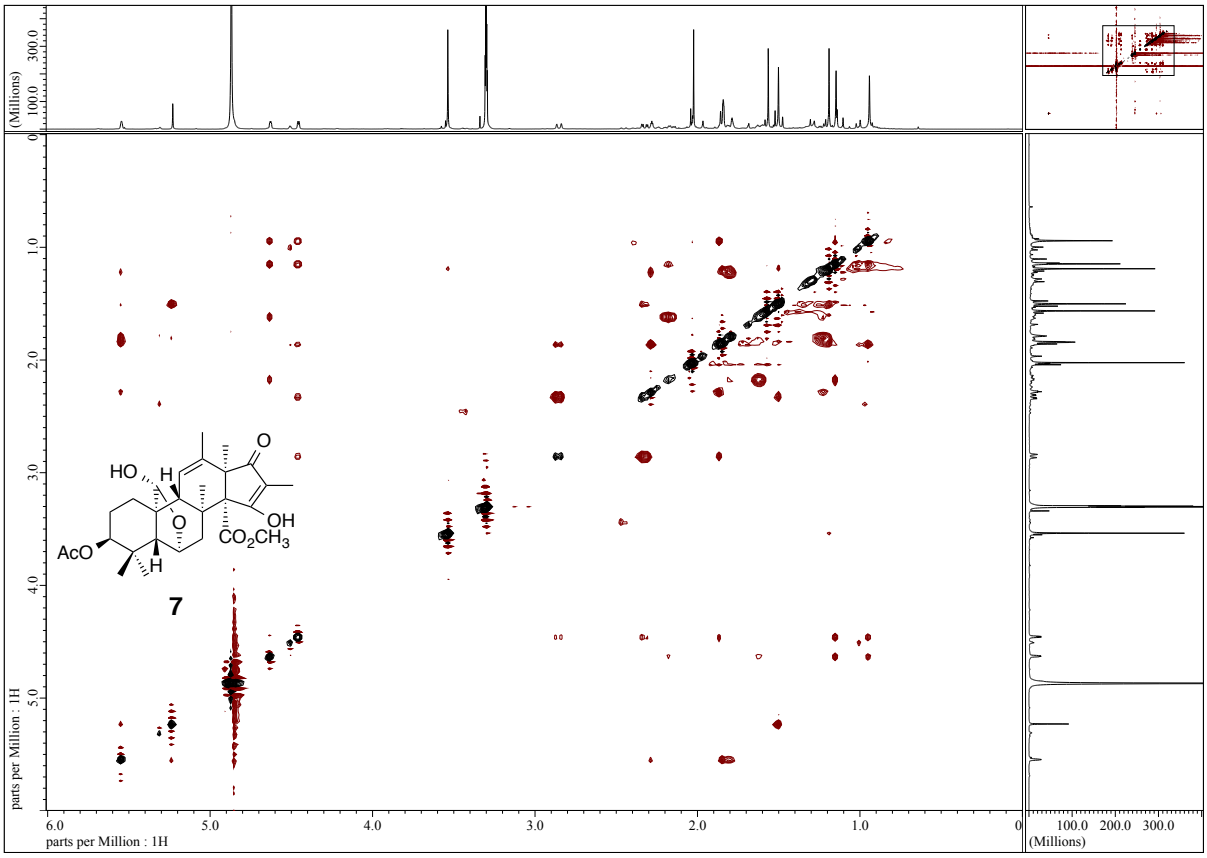

Figure 7-38. NOESY spectrum of dihydrocitreohybridonol.

NMR data for 6α-hydroxyandrastin B

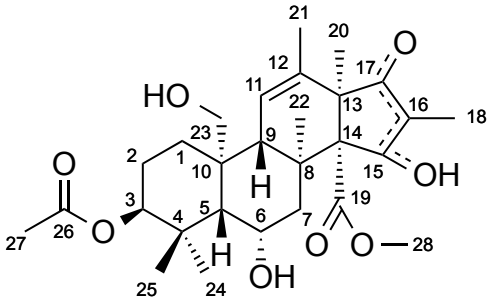

Table 7-12. NMR data for 6α-hydroxyandrastin B

^{1}H NMR: 500 MHz, ^{13}C NMR: 125 MHz (in CD_3OD)

	^{13}C	^{1}H					
position	δ (ppm)	δ (ppm)	intensitiy	multiplicity	HMBC correlation	COSY correlation	NOESY correlation
1	31.9	1.84 (α)	1H	dt (*J* = 13.5, 3.0 Hz)	3, 23	H-2α, H-2β	H-11
		1.05 (β)	1H	dt (*J* = 14.0, 3.9 Hz)	9	H-2α, H-2β	H-2β, H-5, H-9
2	23.4	2.14 (α)	1H	tt (J = 14.6, 3.2 Hz)		H-1α, H-1β	H-3, H-23, H-24
		1.56 (β)	1H	m		H-1α, H-1β	H-1β, H-3
3	79.6	4.59	1H	t (*J* = 2.7 Hz)	1, 5, 26	H-2α, H-2β	H-2α, H-2β, H-24, H-25
4	37.0						
5	50.5	1.73	1H	d (*J* = 2.2 Hz)	1, 4, 6, 9, 23, 24	H-6	H-1β, H-6, H-7β, H-9, H-25
6	66.4	4.28	1H	m		H-5, H-7α, H-7β	H-5, H-7α, H-7β, H-24, H-25
7	40.7	2.33 (α)	1H	dd (*J* = 15.2, 2.0 Hz)	5, 6, 8, 9, 22	H-6	H-6, H-22
		3.12 (β)	1H	dd (*J* = 15.2, 3.9 Hz)	8, 22	H-6	H-5, H-6, H-9
8	40.7						
9	54.0	1.99	1H	brt (*J* = 2.5 Hz)	11, 22, 23	H-11, H-21	H-1β, H-5, H-7β, H-11
10	41.7						
11	124.1	5.54	1H	brs	8, 9, 13, 21	H-9, H-21	H-1α, H-9, H-21, H-23
12	135.1						
13	56.5						
14	68.7						
15	189.2*						
16	112.4						
17	201.4*						
18	5.2	1.57	3H	s	15, 16, 17		
19	171.2						
20	15.1	1.20	3H	s	12, 13, 14, 17		H-21, H-22, H-28
21	18.7	1.80	3H	dd (*J* = 2.5, 1.0 Hz)	11, 12, 13	H-9, H-11	H-11, H-20
22	17.7	1.59	3H	s	7, 8, 9, 14		H-6α, H-20, H-23
23	60.7	3.97	1H	s	1, 5, 9, 10		H-2α, H-11, H-22, H-24
		3.93	1H	s			
24	22.9	1.28	3H	s	3, 4, 5, 25		H-2α, H-3, H-23, H-24, H-25
25	26.6	0.96	3H	s	3, 4, 5, 24		H-3, H-5, H-6, H-24
26	171.2						
27	19.8	2.04	3H	s	26		
28	50.6	3.56	3H	s	19		H-20

Note: Two carbons indicated by * were identified in HMBC spectrum

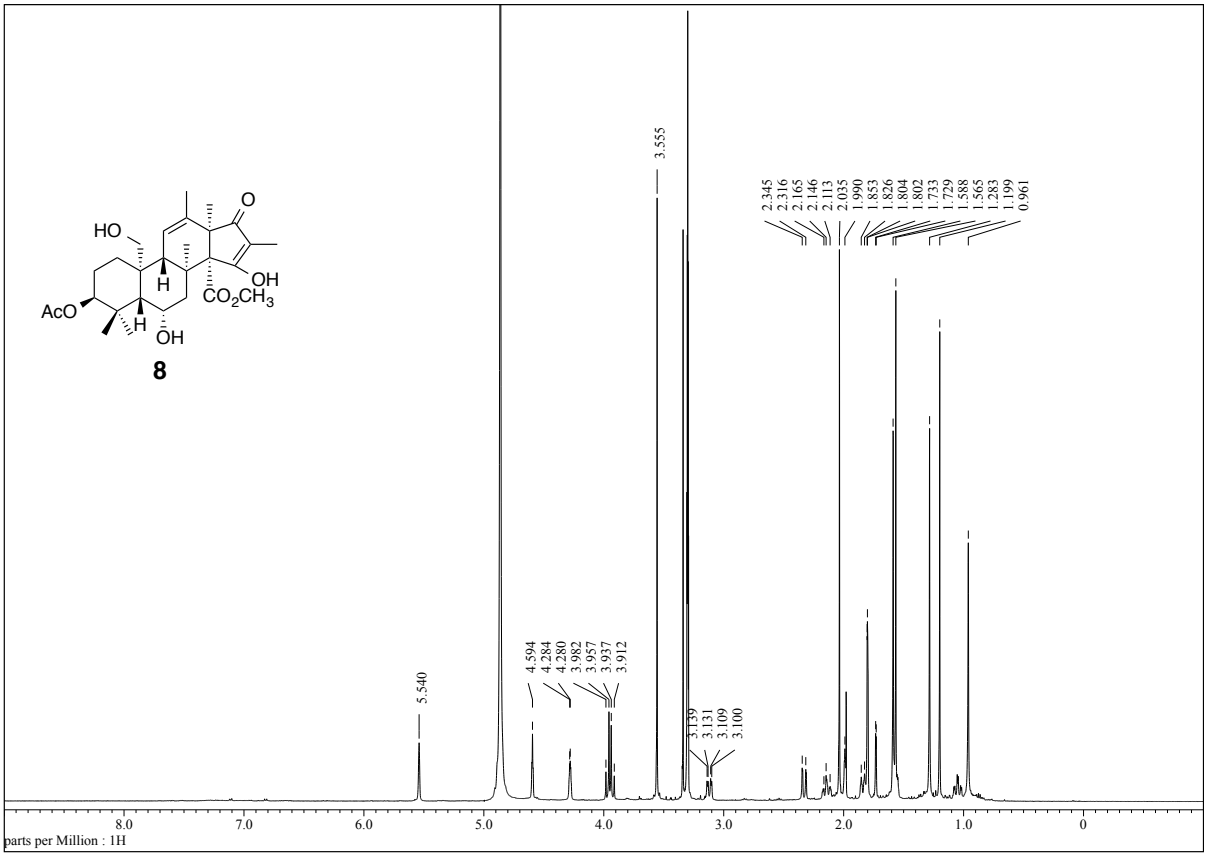

Figure 7-39. ^{1}H NMR spectrum of 6α-hydroxyandrastin B.

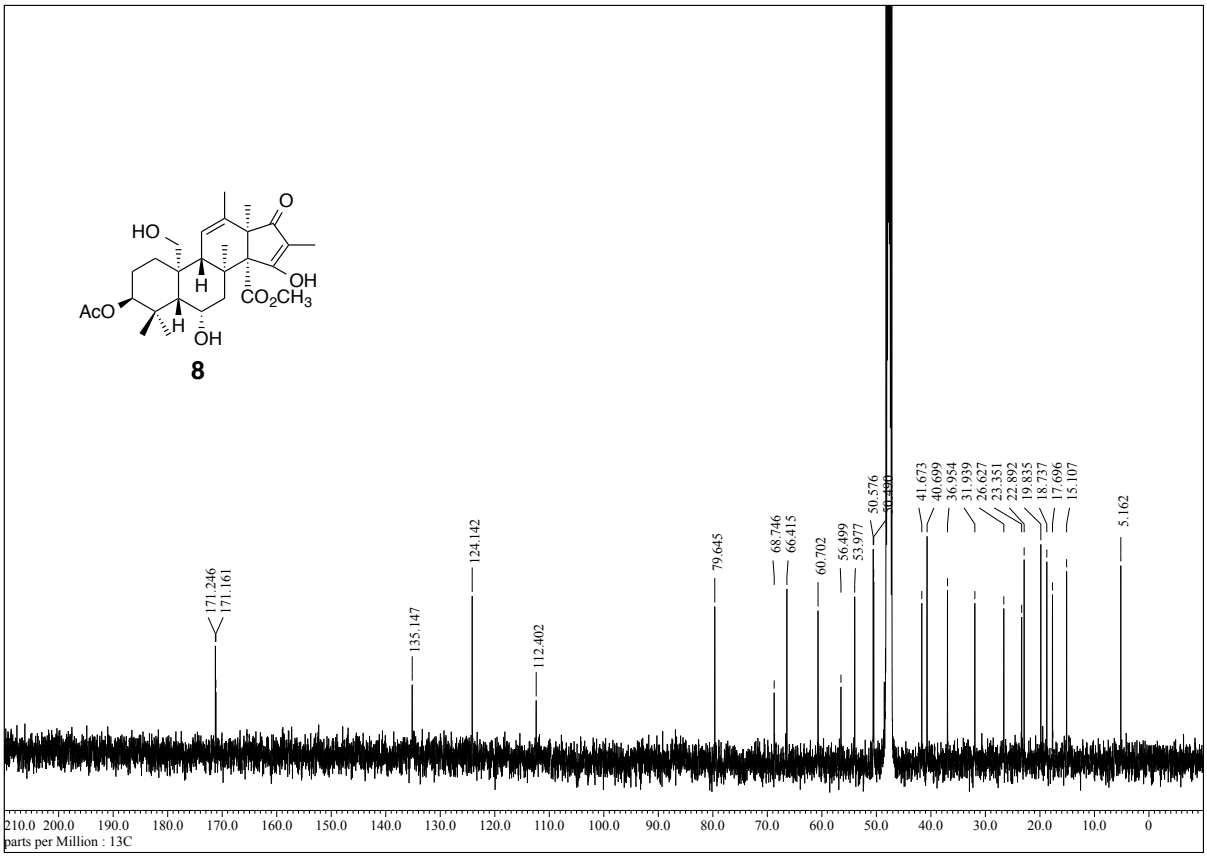

Figure 7-40. ^{13}C NMR spectrum of 6α-hydroxyandrastin B.

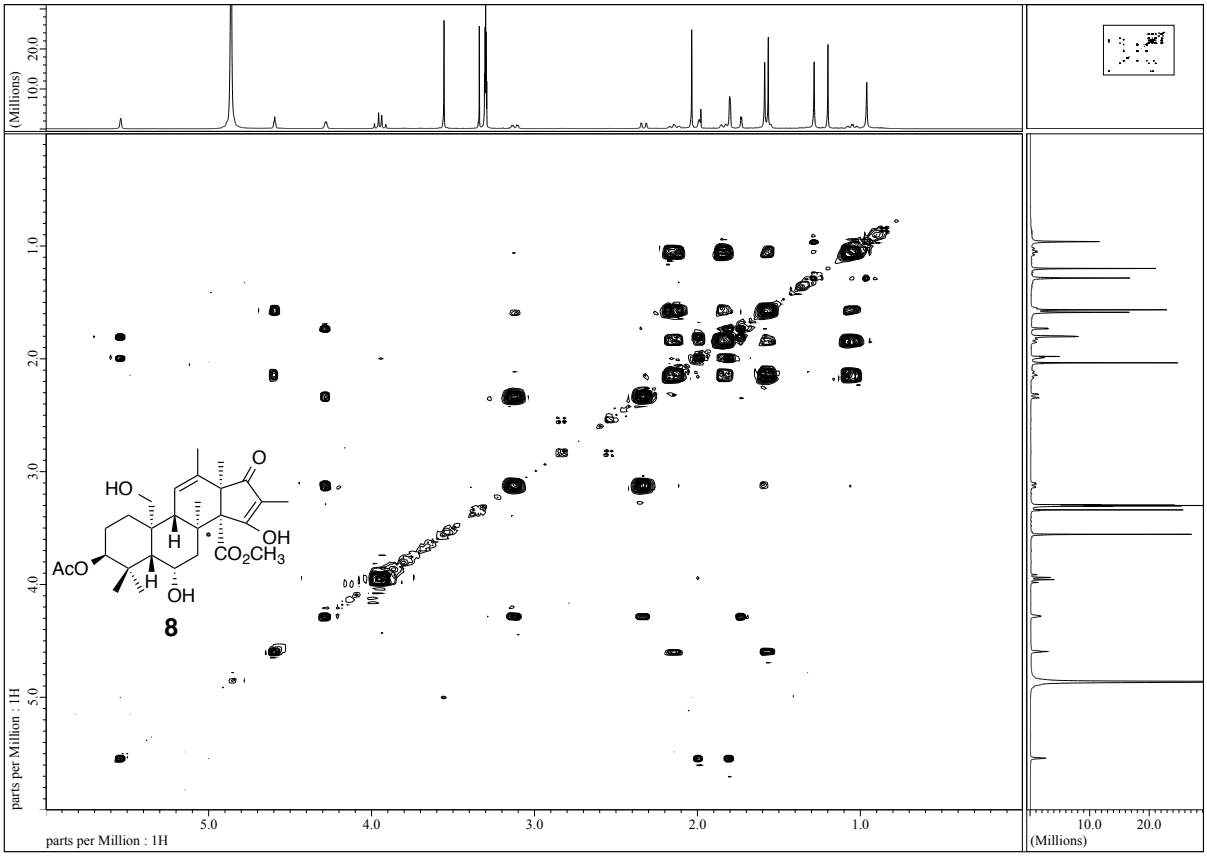

Figure 7-41. ^{1}H-^{1}H COSY spectrum of 6α-hydroxyandrastin B.

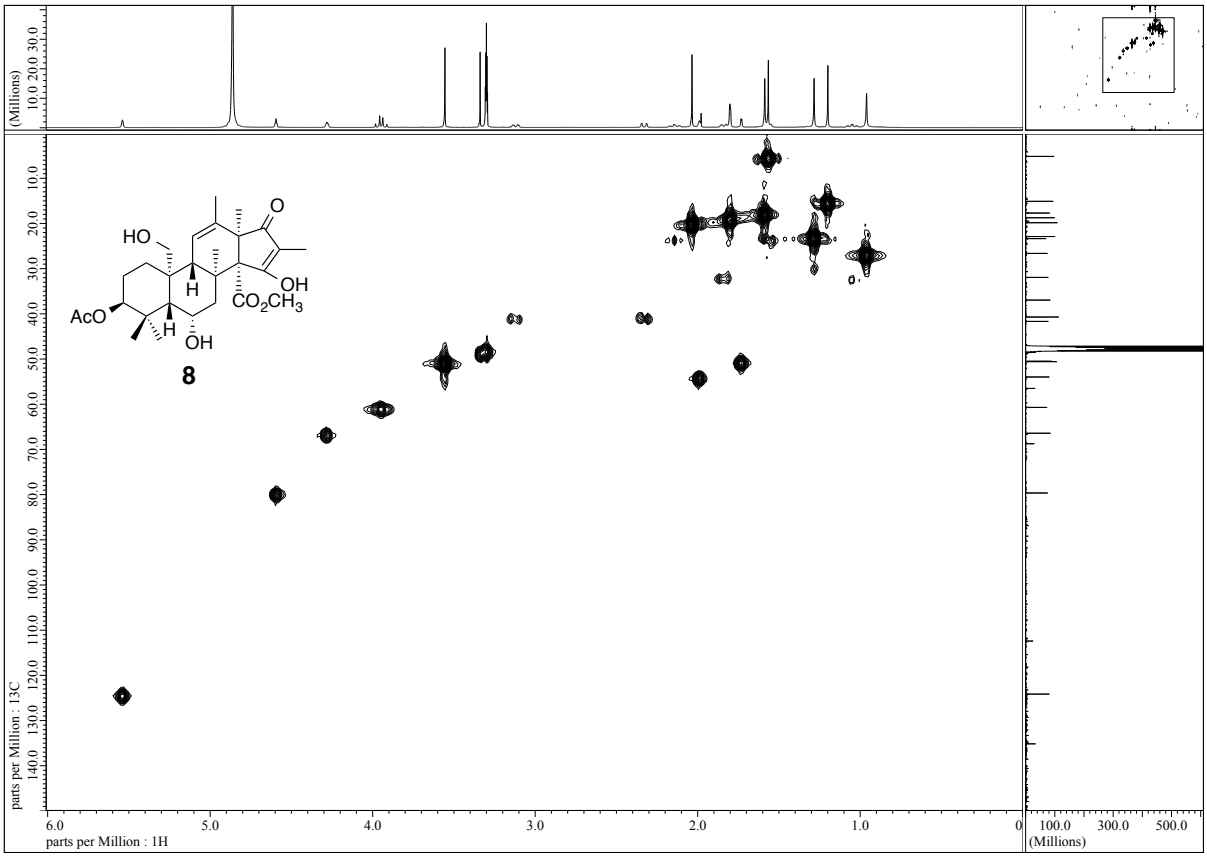

Figure 7-42. HMQC spectrum of 6α-hydroxyandrastin B.

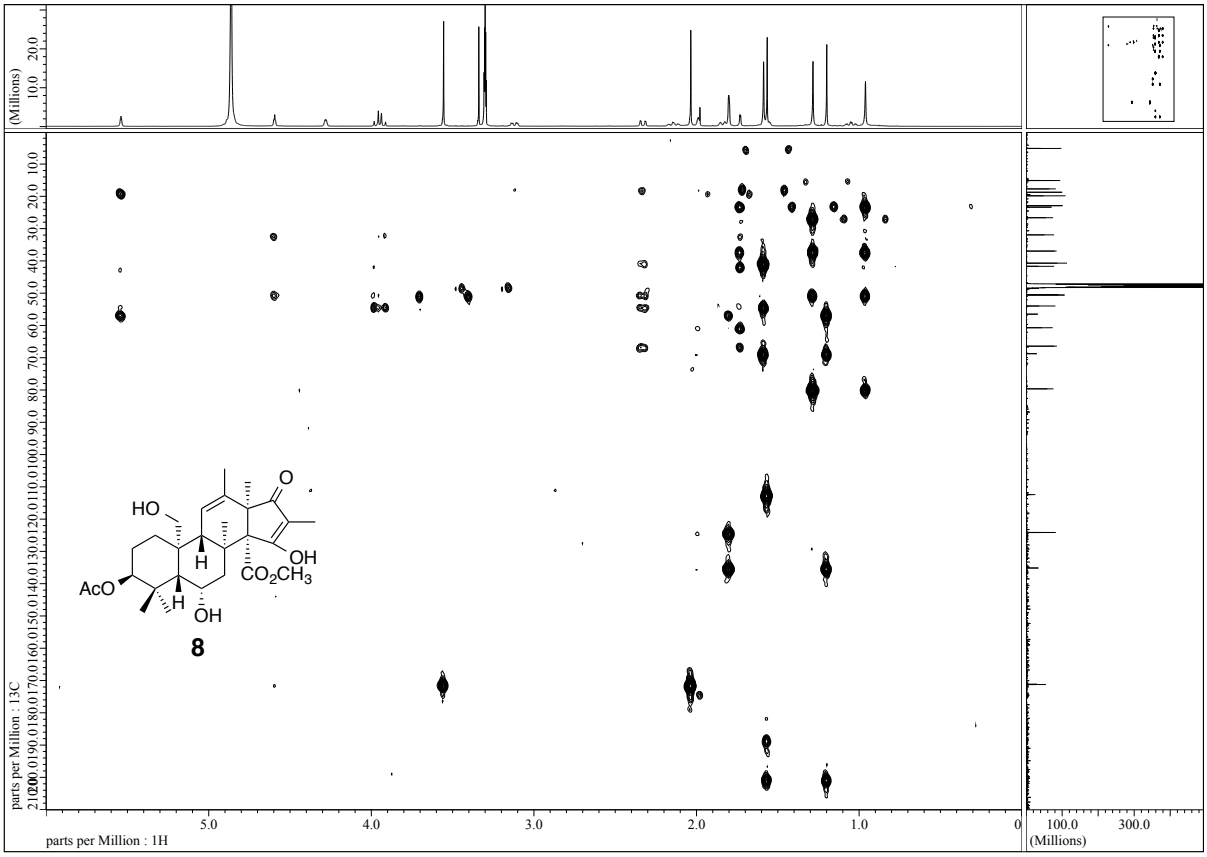

Figure 7-43. HMBC spectrum of 6α-hydroxyandrastin B.

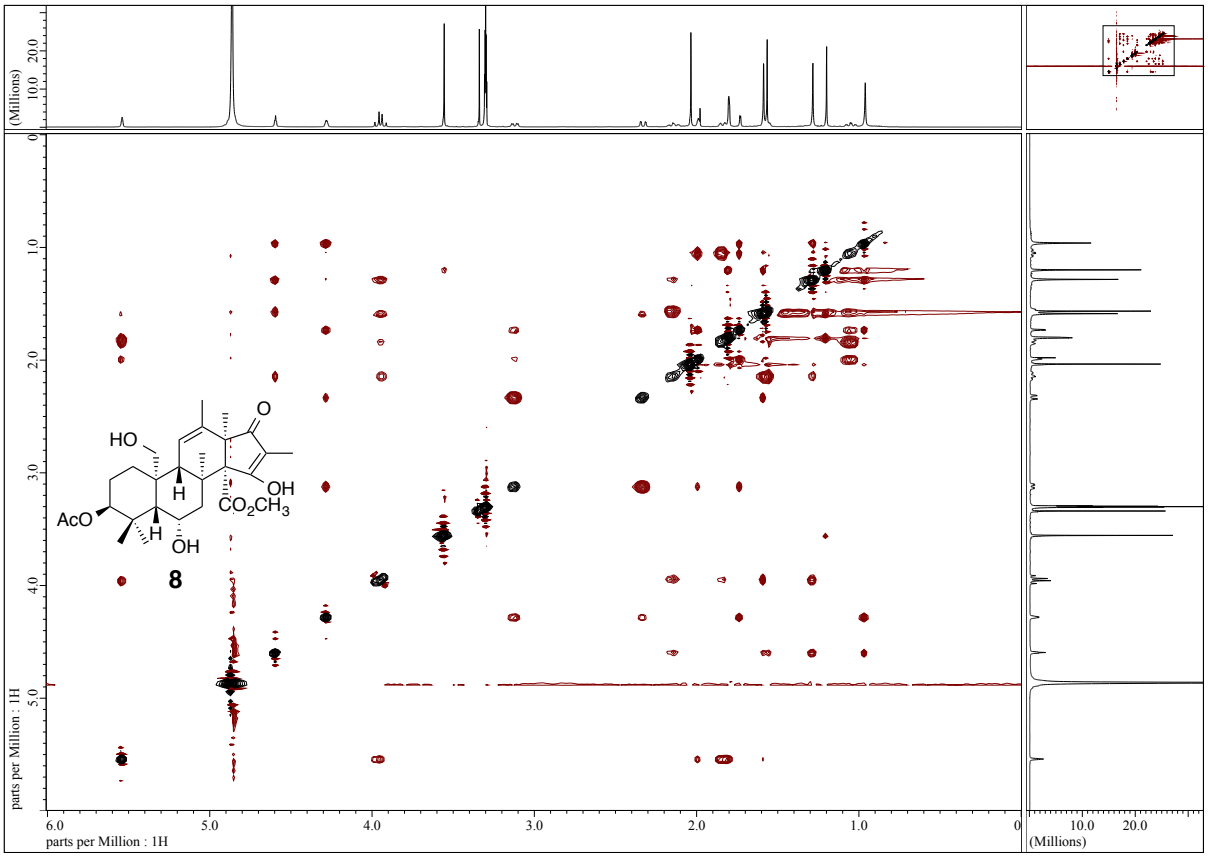

Figure 7-44. NOESY spectrum of 6α-hydroxyandrastin B.